

Aerospace Research Center

NAS 12-8
CR 86093
N68-34077

BEAM ALIGNMENT TECHNIQUES BASED ON THE CURRENT ENHANCEMENT EFFECT IN PHOTOCONDUCTORS

FINAL TECHNICAL REPORT

31 August 1968

This document was prepared under the sponsorship of the National Aeronautics & Space Administration. Neither the United States Government nor any person acting on behalf of the United States Government assumes any liability resulting from the use of information contained in this document, or warrants that such use will be free from privately-owned rights.

Prepared under Contract NAS 12-8 by
GENERAL PRECISION SYSTEMS INC.
Aerospace Research Center
Little Falls, New Jersey

for National Aeronautics and Space Administration
Electronics Research Center
Cambridge, Massachusetts

Mr. Janis Bebris
Technical Minitor
EO/Space Optics Laboratory
Electronics Research Center
575 Technology Square
Cambridge, Massachusetts
02139

Requests for copies of this report should be referred to: NASA Scientific and Technical
Information Facility, P.O. Box 33, College Park, Maryland 20740

BEAM ALIGNMENT TECHNIQUES BASED ON THE CURRENT
ENHANCEMENT EFFECT IN PHOTOCONDUCTORS

Work Performed By:

Frank V. Allan
Raymond P. Borkowski
William M. Block
Alfred Brauer
Robert Carvalho
Cecil B. Ellis
Robert Flower
Jesse C. Kaufman
Aryeh H. Samuel
Joseph C. Scanlon

Written By: Cecil B. Ellis

Approved: 

Dr. Daniel Grafstein
Principal Staff Scientist
Manager, Materials Department

31 August 1968

FINAL TECHNICAL REPORT

Prepared under Contract NAS 12-8 by
GENERAL PRECISION SYSTEMS INC.

Aerospace Research Center
Little Falls, New Jersey

for the

Electronics Research Center
National Aeronautics and Space Administration

TABLE OF CONTENTS

	<u>Page</u>
TABLE OF CONTENTS	iii
LIST OF FIGURES	vi
LIST OF TABLES	viii
SUMMARY	1
I. INTRODUCTION	2
II. BRIEF DESCRIPTION OF THE CHARACTERISTICS OF THE ENHANCEMENT EFFECTS	5
III. PHOTOCONDUCTIVE ENHANCEMENT RESEARCH ON FIVE DIFFERENT TYPES OF CELLS	14
A. Studies on A-Type Polycrystalline CdS Cells	14
1. Choice of the best parameters for minimum signal detection.	15
2. Measurement of the "minimum usable signal".	22
3. Increased areas of illuminated spots.	27
4. A moving-spot experiment.	29
5. Effect of circuit constants on time responses.	31
6. Chopping of 90 cycles/sec .	36
7. Exploration of enhancement in the infrared.	37
B. Properties of the B-Type Polycrystalline CdS Cells	41
C. Research with General Precision Polycrystalline CdS Cells	44
D. Single Crystal CdS Enhancement	46
E. Tests with Single Crystal Germanium	47

TABLE OF CONTENTS (CONT'D.)

	<u>Page</u>
IV. THE NEW PHOTOVOLTAIC ENHANCEMENT EFFECT	49
A. Research with A-Type CdS Cells	49
1. First photovoltaic enhancement experiments.	49
2. Chopper wheel experiments on A-Type CdS cells.	54
3. Fast-shutter photovoltaic experiments.	56
4. Effect of chopping frequency on photovoltaic response.	58
B. Photovoltaic Enhancement with B-Type CdS Cells.	61
C. Photovoltaic Tests with Ge.	61
V. A NEW PHENOMENON IN GERMANIUM: "DE-ENHANCEMENT"	62
VI. EXPERIMENTS RELATING TO APPLICATIONS	71
A. Photoconductive Enhancement TV Camera Breadboard	71
B. Beam Tracker Breadboard Assembly	77
C. A Voice-Modulated Photovoltaic Enhancement Experiment	78
D. The Present Position on Applications	79
VII. CONCLUDING SECTION	82

Appendixes:

A. INITIAL WORK WITH A-TYPE POLYCRYSTALLINE CdS CELLS	84
1. Variation of M with beam wavelengths	84

TABLE OF CONTENTS (CONT'D)

	<u>Page</u>
2. Effect of reversing cell polarity	90
3. Effect of changing cell voltage	93
4. Effect of changing the beam intensities	94
5. Time response to intensity modulation of the light	96
6. Variation of illuminated area at constant power density	97
7. Variations in spot positions	98
8. Multiple spot-pairs	102
B. THEORETICAL TREATMENTS	108
C. APPLICATIONS SIGNIFICANCE	109
1. Simple detectors	109
2. Communication	110
3. Navigation and tracking	112
4. Pattern recognition	114
5. Other applications	116
6. Competing sensors	117
6.1 Devices with signal gain	117
6.2 Point position indicators	120
D. NEW TECHNOLOGY	123

LIST OF FIGURES

<u>Figure</u>		<u>Page</u>
1.	Construction of A-type CdS cell	6
2.	Representation of the enhancement effect	8
3.	Typical experimental arrangement	9
4.	Apparatus for determining minimum usable signal with cell #A-D	17
5.	Rise transient at minimum signal with cell #A-D	23
6.	Decay transient at minimum signal with cell #A-D	23
7.	Initial voltage output at minimum signal — rise	25
8.	Initial voltage output at minimum signal — decay	25
9.	Repeat of Figure 5 with four times the illuminated spot area	28
10.	Effect of slow scanning with the minimum signal	30
11.	Schematic arrangement for circuit variation experiments	33
12.	Effect of load resistance on time responses - green light	34
13.	Effect of load resistance on time responses - red light	35
14.	Enhancement in the infrared - beams of equal intensity	38
15.	Enhancement in the infrared - beams of unequal intensity	40
16.	Aperture pattern for masks used in photovoltaic studies	50
17.	Photovoltaic outputs from cell #A-C; non-coincident	51
18.	Photovoltaic outputs from cell #A-C; coincident	53
19.	Chopper wheel photovoltaic experiments	55
20.	Photoresponse of cell #A-D to fast shutter beam chopping.	57
21.	Photoresponse at various chopping frequencies	59
22.	Demonstration of TV camera application	72
23.	Optical parts for the camera breadboard	74
24.	Block diagram of the electrical system for the camera breadboard	75
A-1.	Wavelength dependence of single-sided response from cell #A-J702	87
A-2.	Enhancement effect of red light added to a beam of variable wavelength	88

LIST OF FIGURES (CONT'D.)

<u>Figure</u>		<u>Page</u>
A-3.	Variation of M with beam wavelength, for red beam opposite	89
A-4.	Variation of M with beam wavelength, for green or blue beam opposite	91
A-5.	Effect of linear displacement on M	99
A-6.	Output current as a function of position on cell #A-D	101
A-7.	I and M as a function of position on cell #A-C	104

LIST OF TABLES

<u>Table</u>		<u>Page</u>
I.	Typical Output Data for A-Type Cells	7
II.	Photoconductive Enhancement Data for B-Type Cell	43
III.	De-enhancement in Ge with Two Chopped Beams	67
IV.	Deteriorating Ge De-enhancement with Large Spots	69
A-I.	Parameters Explored for A-type Cells	85
A-II.	I and M with Multiple Illuminated Spot-Pairs	105
A-III.	Response from Multiple Spot Pairs with Additional Single Spots.	107

BEAM ALIGNMENT TECHNIQUES BASED ON THE CURRENT ENHANCEMENT EFFECT IN PHOTOCONDUCTORS

Report Written by: Cecil B. Ellis

General Precision Systems Inc.
Little Falls, New Jersey

SUMMARY

The photoconductive enhancement effect is an increase in photocurrent when two illuminated spots are brought into coincidence on opposite sides of a thin photoconductor having translucent electrodes. Initially discovered by General Precision in one type of polycrystalline CdS cell, the effect has now been found with three other types of CdS cell designs, including a single crystal of CdS pressed between conducting glass electrodes. An analogous photovoltaic enhancement effect has also been found in two kinds of CdS cells, which has a frequency-response bandwidth for modulated light of at least 5000 cps. In addition, a reverse effect is found in single crystal Ge cells, where collinearity of the opposing beams causes a decrease in the photocurrent. Many static and dynamic features of the behavior of all of these cells have now been measured.

The sensitivity of the first CdS effect is sufficient to detect a light signal of 10^{-12} watts, and to locate the position of its spot on the cell face to at least 50 microns accuracy. This should suffice for tracking a laser beacon on a vehicle at interplanetary distances carrying a 25 watt laser. Numerous other applications of these various effects are discussed, including a very low light level TV camera, voice communication over a long range light beam while tracking, and several kinds of pattern matching uses. Breadboard models of three assemblies for applying the CdS cells were tested.

The detection and position-indicating properties of some of these photocells are available for any wavelength of light from the violet to the near infrared. Some of them also have spectral discrimination capability over bandwidths as narrow as 100\AA .

I. INTRODUCTION

This is the final report under Contract NAS 12-8 on the photoconductive enhancement effect. This effect is the substantial rise in photocurrent which occurs whenever narrow light beams of certain wavelengths impinge on opposite spots of some photoconductive sandwich structures. Generally, the sandwich structures are composed of photoconductive materials placed between transparent electrodes and the illumination is directed through the electrodes at opposing sides of the cell. Such a spatial effect in a photoconductive material was discovered by General Precision in 1963, with polycrystalline thin doped cadmium sulfide layers, using visible light.

Included in this report are observations on the newly discovered analogous spatial phenomena of rapid photovoltaic enhancement in doped polycrystalline thin cadmium sulfide layers, and of photoconductive "de-enhancement" in a single crystal disks of pure germanium, with infrared light. Some applications surveys and some preliminary apparatus testing concerning possible applications of these phenomena are also described.

The work under contract NAS 12-8 previous to 15 October 1967 has been discussed in three Summary Technical Progress Reports having the same title as the present report. They are available from the Clearinghouse for Federal Scientific and Technical Information, Springfield, Virginia 22151, under the following identification numbers.

<u>Issue Date</u>	<u>Report Numbers</u>	<u>NASA Accession Number</u>
April 1966	NASA-CR-431	N66-22359
November 1966	NASA-CR-80004	N67-16054
November 15, 1967	NASA-CR-86035	N68-19129

I. Introduction

Reference to these earlier reports will be made by the symbols Ref. I, Ref. II, and Ref. III, in order of their issue dates. The material therein will not be repeated here in detail. However, Appendix A and a few other short sections summarize a fraction of this work, and recapitulate it from a unified viewpoint in the light of the more recent studies.

Most of the present report will describe the work done from 15 October 1967 to 15 June 1968. The contract effort during this period was carried out by Dr. Frank Allan, Dr. Cecil B. Ellis, Dr. Robert Carvalho, Mr. Joseph Scanlon, Mr. Jesse Kaufman, and Mr. Alfred Brauer. During earlier periods Dr. Raymond P. Borkowski, Dr. Aryeh H. Samuel, Mr. William M. Block, and Mr. Robert Flower were also engaged in the work at various times. Principal Investigators in the current period were first Dr. Allan, and subsequently Dr. Ellis. The contract throughout was under the over-all supervision of Dr. Daniel Grafstein, Manager, Materials Department, Aerospace Research Center.

The Contract Technical Director for NASA Electronics Research Center, EO/Space Optics Laboratory, throughout the duration of the contract was Mr. Janis Bebris.

The current program has had five principal aims:

1. to extend our knowledge of the commercial polycrystalline CdS cells previously studied,
2. to develop a new commercial source of polycrystalline CdS cells and to study these cells,
3. to study the newly discovered photovoltaic enhancement effect in CdS,
4. to study the newly discovered "de-enhancement" behavior in single crystal germanium, and

I. Introduction

5. to survey possible applications for the enhancement effects.

These subjects are taken up in the report to follow, after a brief summary of characteristics of the enhancement phenomena in general.

II. BRIEF DESCRIPTION OF THE CHARACTERISTICS OF THE ENHANCEMENT EFFECTS

Much of the early research was done on a set of cadmium sulfide photoconductive cells obtained some years ago from Pioneer Electric and Research Co., Forest Park, Illinois 60130. These will be designated in this report as "A-type cells", and individual specimens will be referred to by cell identifications beginning with A, as cell #A-J702 or cell # A-D.*

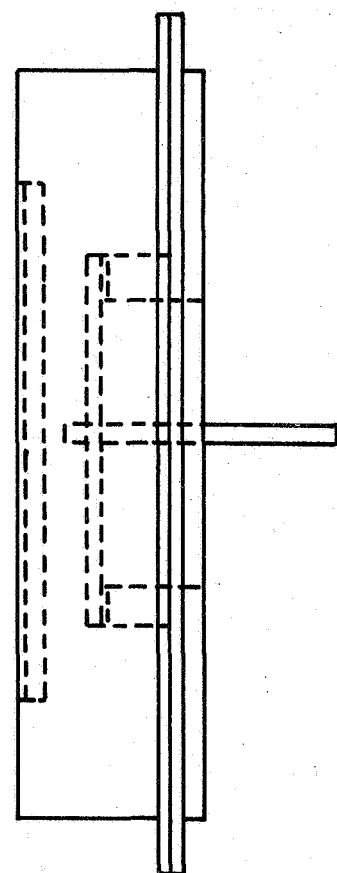
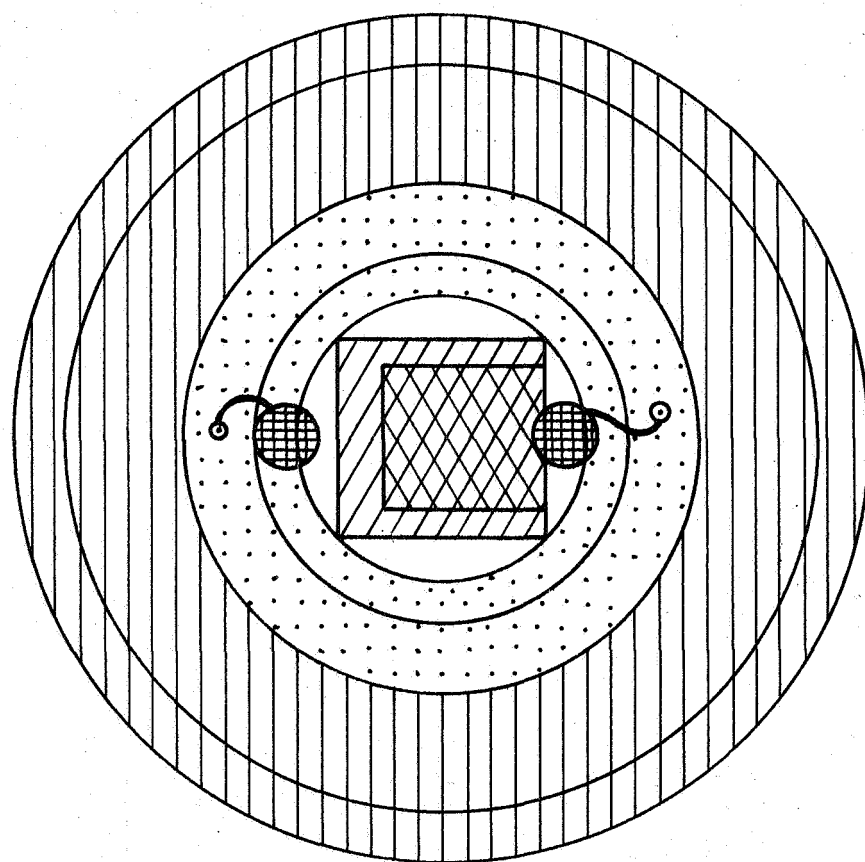
As indicated in Figure 1, each of these consists of a layer of doped polycrystalline CdS, in the shape of a circular disk of about 1 cm diameter and 50-70 μ thickness, having translucent electrodes contacting the whole area of each side of the layer. The electrode on one side is conducting glass (a type of glass covered with a tin oxide layer). The electrode on the other side of each cell is a thin translucent film of either gold or indium metal, protected by a transparent sealing material. Such an arrangement is often called a "sandwich type" photoconductive cell.

When potentials of the order of 1 volt are applied to these cells, the very small current which flows in the absence of illumination corresponds to a dark resistance for the cell of around 100 megohms. Illumination of part or all of the surface, of either one or the other side of the CdS layer, with the same applied voltage, causes an additional photocurrent whose magnitude depends on the wavelength and intensity of the light as well as on a number of other factors. When a pair of light beams is used, so as to illuminate the two sides of the CdS layer simultaneously, the separate effects of the two beams remain closely additive whenever (a) the entire surface areas are illuminated, or (b) illuminated areas on the two sides of the CdS layer are not opposite each other at any point.

However, if a fairly small spot is illuminated on each side of the CdS and if these two spots are located just opposite one another, a new phenomenon of "current enhancement"

* The "A" designations were not used in Ref. I - III, since only one type of cell was under discussion there.

Bottom View



Bottom casing



Metal film electrode



CdS layer



Solder



Glass



Top casing



Lead-in posts



Inner connection wires

FIGURE 1. Construction of A-Type CdS Cell

II. Description

appears for a few of these cells. Then, the resulting photocurrent can become much greater than the sum of the currents caused by the two illuminated spots separately. Figure 2 is a simple pictorial description of the phenomenon. Figure 3 shows one way of arranging experimental apparatus. A typical set of data is the following.

TABLE ITYPICAL OUTPUT DATA FOR A-TYPE CELLS

Cell # A-1

Applied voltage = 1.0 v.

Gold film electrode is positive.

Opposite illuminated spots, 1.58 mm diam., in center of cell faces.

White light onto gold electrode.

Light onto glass electrode passed by interference filter of central $\lambda = 4340\text{\AA}$ and 100 \AA bandpass.

Gold side only illuminated, $I = 56.8\mu\text{ amp}$

Glass side only illuminated, $I = 6.8 "$

Both sides illuminated, $I = 366. "$

Two operational cases may be distinguished, which give rise to two different classes of applications of the enhancement phenomenon. In the "static mode" of measurement, as illustrated by the data of Table I, one illuminates a spot on one side of the CdS layer only, recording a net photocurrent $I_{(\text{side 1 only})}$. A spot exactly opposite on the other

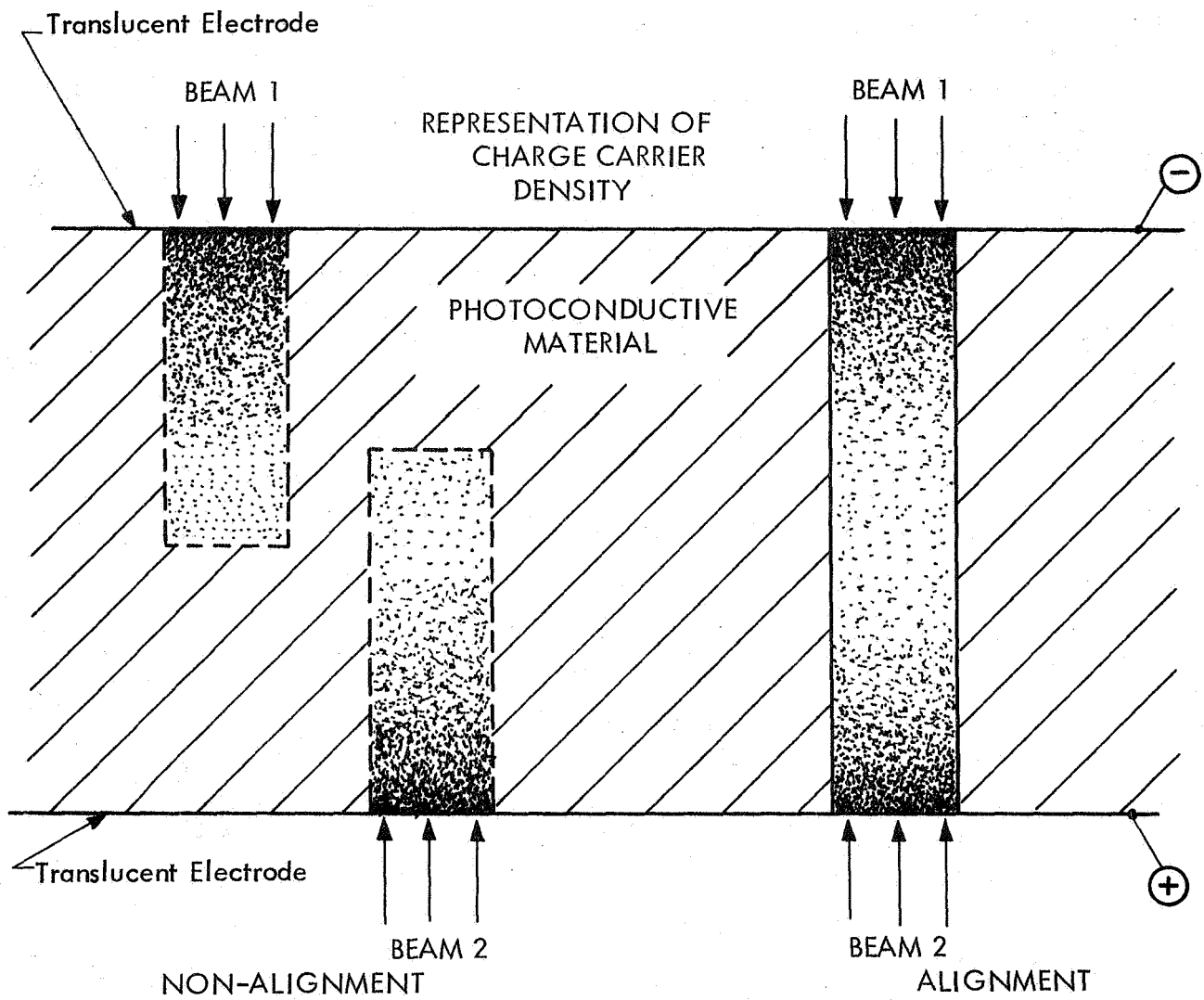
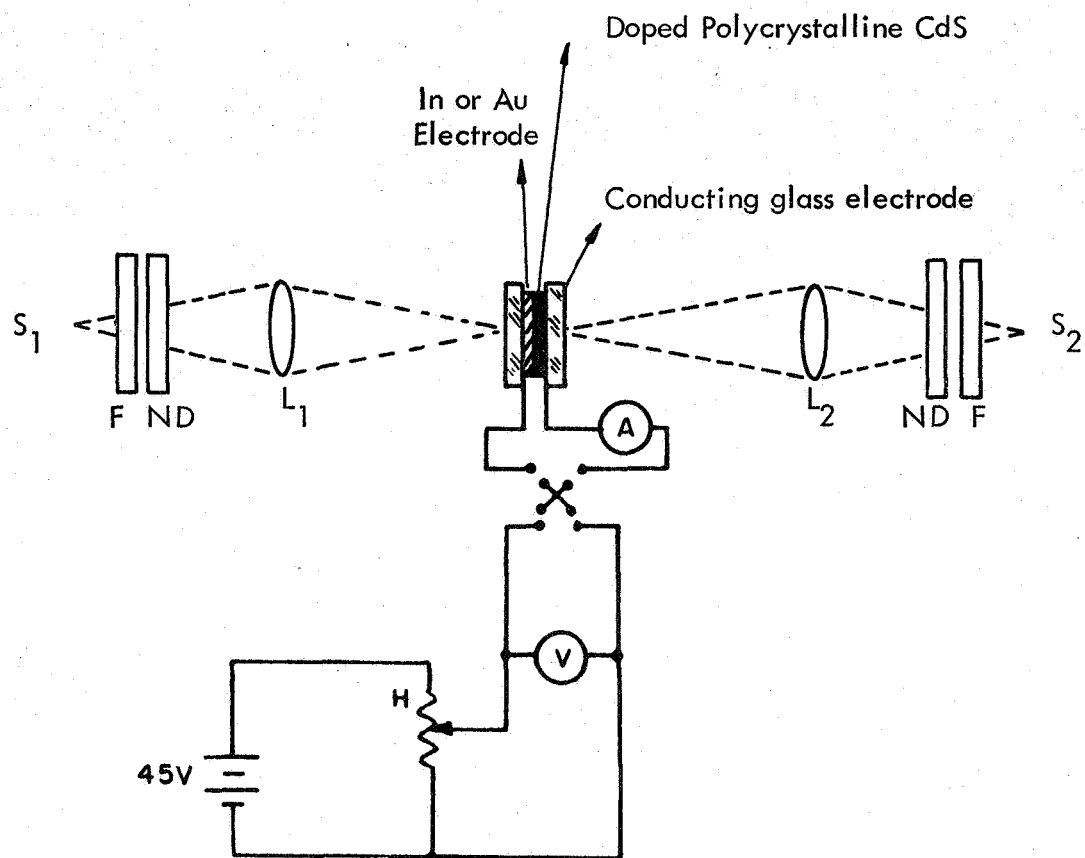


FIGURE 2 - Representation of the Enhancement Effect



S_1 and S_2 = tungsten filament lamps
 L_1 and L_2 = condensing lenses
 F = interference filter
 ND = neutral density filter
 A = Keithley # 150A electrometer
 V = voltmeter
 H = helipot, 10^5 ohms

FIGURE 3 - Schematic Diagram of a Typical Experimental Arrangement

II. Description

side of the layer is then illuminated alone, producing a net photocurrent $I_{(\text{side 2 only})}$.

If the enhancement phenomenon is present, simultaneous illumination of both these opposite spots will produce a net photocurrent $I_{(\text{both sides})}$ which is larger than the sum of the two separate currents. This is true for the data in Table I. In the present research an "enhancement factor" for this case using static spots of illumination in opposite positions has been defined as

$$M_{\text{static}} = \frac{I_{(\text{both sides})}}{I_{(\text{side 1 only})} + I_{(\text{side 2 only})}}$$

For the data in Table I, $M_{\text{static}} = 5.6$. Operation in this fashion with static light spots (of variable intensity) would be appropriate for receiving optical telemetered information from a distant small source surrounded by a bright noisy background.

In a "dynamic" mode of measurement, one may illuminate non-opposite spots on the two sides of the cell and record the resulting photocurrent $I_{(\text{non-opposite})}$. Then, without any other change, one of the light beams may be deflected so as to bring the two illuminated spots opposite one another. If the enhancement phenomenon occurs, the photocurrent $I_{(\text{opposite})}$ will then be larger than before. An "enhancement factor" for this case of photoconduction explored by movable light beams has been defined as

II. Description

$$M_{\text{dynamic}} = \frac{I_{(\text{opposite})}}{I_{(\text{non-opposite})}}$$

Operation in this fashion (but with one beam moving continuously) would be appropriate for various optical beam tracking applications.

If all the cell materials displayed perfectly uniform properties across the full area of the disk aperture, measured values of M_{dynamic} and M_{static} would doubtless be equal, and would be the same for any illuminated spot locations on the two surfaces of the CdS layer — provided the moving beam scanned very slowly. However, research described in the earlier reports has disclosed considerable non-uniformity from point to point in these CdS cells. Also, for low beam intensities the response time of the CdS is so slow that the output does not reach a steady state unless the dwell time on any one pair of illuminated spots is fairly long. Therefore, values of M to be found with a given pair of beams illuminating a given cell will always depend, at least to some extent, on the method and the locations of measurement.

II. Description

The photoconductive enhancement effect just described has now been observed in four classes of CdS materials. One is the A-type cell of Figure 1. Another is what will be called a B-type cell, obtained from the G.T. Schjeldahl Co., Northfield, Minnesota 55057. This is also a thin polycrystalline CdS layer cell of sandwich type, which is described in Section III B. The third, GP-type, cell is a thick sintered-powder CdS cell made at General Precision. The fourth, and simplest, arrangement is a 0.1 mm thick slab of single crystal CdS pressure-contacted on each side by a piece of conducting glass.

The wavelength region over which M values can be found appreciably greater than unity stretches from the violet to the near infrared. Useful current transients involving time intervals of a few milliseconds can be produced with quite weak light. Important circumstances occur in which no cell noise at all is detected. For the A-type cells sensitivity is very high; recognition of beam intensity and location can be made down to 10^{-12} watts* of radiant power and a few microns of displacement at the cell surface.

The amount of evidence now on hand points to the phenomenon being a general property of sandwich arrangements of CdS, rather than possibly arising from some peculiarity of the first A-type cells studied. It is not yet certain what degree of uniformity of materials over a large cell area can eventually be achieved. It seems likely that close uniformity in the electrode interface properties is just as important for producing constant M as is uniformity in the volume of the photoconducting material, if not more so.

An analogous photovoltaic enhancement effect has been discovered in two classes of materials so far: the A-type CdS cells and the B-type CdS cells. The experimental arrangement is the same except that no battery is needed. This phenomenon is most pro-

* Conversion to photometric units may be made by the relation: 621 lumens corresponds to 1 watt of green light at 5540Å.

II. Description

nounced in the green region of the spectrum, and it requires more light intensity than the photoconductive effect to stand out above general system noise. However, photovoltaic transients as short as about 0.1 ms seem definitely available; the effect is more or less 20 times as fast as the photoconductive mode.

A somewhat similar phenomenon, photoconductive "de-enhancement", has been found in single crystals of Ge with near infrared light. It is also spatially dependent but less sharply so than the two enhancement effects. In this case the photocurrent with opposite spots is less than the sum of the currents from illuminating the two sides separately. The phenomenon only appears at considerably higher beam intensities than are necessary for enhancement in CdS. It has the appearance of being a type of quenching phenomenon. It is not yet known whether de-enhancement in Ge partakes of the fast time-response feature of normal photoconductivity in Ge, which lies in the microsecond range.

An allied effect is seen in single crystal CdS when one of the beams lies in the infrared, around 8000\AA , and the other is in the green near 5300\AA . Illumination of opposite spots produces much less current than the sum of the two currents from single-sided illumination. However, the response time of this phenomenon is very slow.

Section III will now describe photoconductive enhancement research with the various types of cells. The photovoltaic phenomena, and de-enhancement in Ge, will be discussed later.

III. PHOTOCONDUCTIVE ENHANCEMENT RESEARCH ON FIVE DIFFERENT TYPES OF CELLS

A. Studies on A-Type Polycrystalline CdS Cells

The major piece of research on the A-type polycrystalline CdS cells during the current period has been a project to vary all the adjustable parameters to establish quantitatively the smallest light signal which could be detected in a "usable" manner.

The best interpretation of the term "usable" will be discussed in Subsection 1 immediately below. Subsection 2 follows with a description of the experimental results. The answer came out to be 10^{-12} watts, as the smallest signal which it would probably be practical to detect and apply to a servo system.

Subsection 3 will show that the detector output at this low signal level really responds to watts of incident radiation, rather than to watts/cm² as might possibly have been the case.

Subsection 4 demonstrates that these cells will define the position of an illuminated spot at least as closely as 50 μ under these conditions of minimum usable signal.

Subsection 5 describes the dependence of observed cell rise and decay times on the constants of the measuring circuit used. It would probably be best to use a special circuit rearrangement which kept a constant voltage applied to the cell, despite cell resistance changes during illumination transients. However, using only a simple battery circuit, a series load resistor of 940,000 ohms gave equal (and shortest) rise and decay times with green-green illumination of the cell used, while 100,000 ohms was best with red-red illumination.

Subsection 6 concerns an experiment in square-wave chopping the light incident on the cell at 90 cps. No enhancement could be seen, possibly because too high a light intensity had driven $M \rightarrow 1$. (Earlier experiments described in Appendix A.5 had produced enhancement with a light continuously sine-wave modulated at 400 cps.)

III A. A-Type

Subsection 7 explores the photoconductive enhancement phenomenon in the A-type CdS cells for illumination in the near infrared region. Values of M somewhat greater than unity were found as far out as 2.0μ .

All of the following material may perhaps be made more clear by reference to Appendix A, which summarizes related experiments described in the previous reports. In particular, Table A-1 gives a quick survey of the response of A-type cells to a number of major parameter variations.

1. Choice of the best parameters for minimum signal detection

This experiment was intended to provide an approximation to some of the basic data which would be needed for design of a beamtracker, to follow either the weakest possible star image or the weakest possible CW laser signal from a space vehicle at interplanetary distances. For such an application, a collector mirror or lens would form a very weak pinpoint image on a very small spot on one side of the CdS cell. The other face of the cell would then be scanned - either over the complete area in an acquisition phase or immediately around the known image position in a tracking phase - with a small flying spot which would intermittently sweep across the coincidence position. The enhancement factor involved in forming the output current pattern would then be M_{dynamic} , and the results would surely depend upon the speed of scanning, among other factors.

The experiment reported here is a first approximation to this kind of measurement. Two beams were arranged to illuminate small opposite spots, arbitrarily chosen with 50μ diameter as defined by holes in metal masks, which were located at the centers of the cell faces. These were illuminated first separately and then simultaneously; voltage drops proportional to the photocurrents were read; and a value of M_{static} was computed. An oscilloscope trace of the transient response was photographed as the weaker beam (the "signal beam") was turned on in the presence of the collinear steady beam (the "local beam") on the other side.* The

* The employment of only single spot-pair illumination, without any background flood-lighting, precluded simulation of a tracker operating against a bright daytime sky or a pattern of many sources.

III A. A-Type

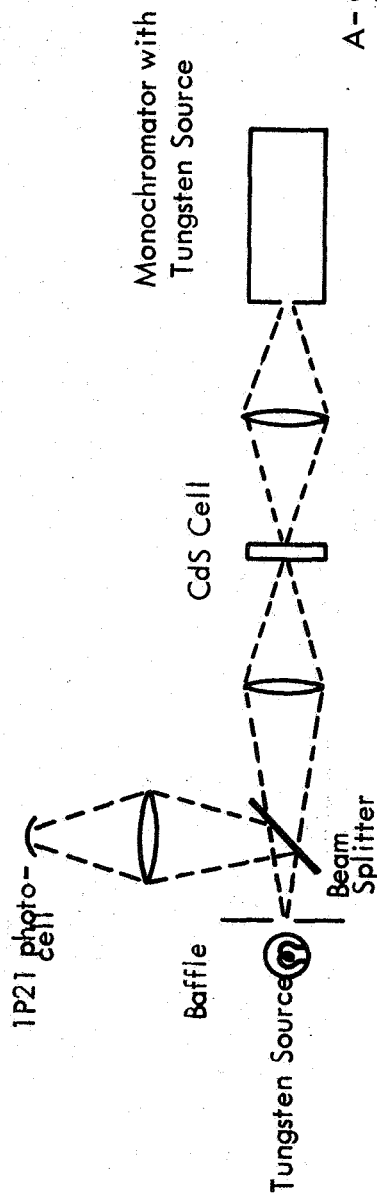
particular cell used was # A-D. The arrangement of the apparatus is shown schematically in Figure 4.

A "usable" signal would clearly have to have the following properties:

- a. the photocurrent transient resulting from turning on the signal beam must be detectable with good probability against the background of any existing noise; that is, a good S/N ratio is needed;
- b. the value of M must be large enough to suggest that a scanning mode would operate as favorably as the static mode here tested; and
- c. the photocurrent rise time must be acceptably short, with a similarly short decay time.

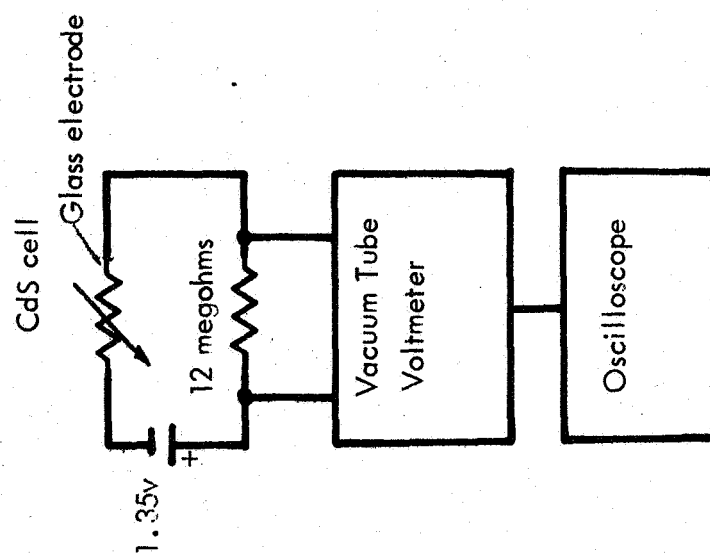
None of these requirements is precise, in advance of engineering design of an actual tracking system, and so the problem was sharpened up in the light of experience as the experiment proceeded.

Most importantly, it was found that the system as defined above could be considered as time-response-limited and M-limited, rather than noise-limited. The earlier work, summarized in Appendix A, had shown that low intensities with CdS lead to longer response and decay times. As the light signal intensity was decreased in this experiment, a reasonable rise-time limitation was reached at a point when the current transient was still large enough to be seen clearly, for a level of amplification which showed no noise whatever with the equipment being used - as will be discussed below. In this circumstance, it was not considered useful to measure a S/N ratio or to determine the D^* parameter customarily used for describing performance of a detector.



A - Optical Equipment

Bausch and Lomb
#33-86-03 Monochromator
Cell #A-D



B - Electronic Equipment

Hewlett-Packard
#425A voltmeter
Tektronix #536
oscilloscope

FIGURE 4 - Apparatus for Determining Minimum Usable Signal

III A. A-Type

A definition of rise time can be approached from several points of view. The customary mathematical definition as the time to reach $(1-1/e) = 63\%$ of the final steady-state value of the current might either be a useful one, or might sometimes constitute an impracticably long parameter. This will depend to some extent on the magnitude of the final current. The current (or usually, the voltage drop across a load impedance) at any instant is used to activate a servo system or other practical output device. If the final current is quite small, then 63% of that current is indeed a suitable number for describing the rise time. However, if circumstances can be arranged to make the final current quite large, then an instantaneous current of perhaps $1/50$ of 63% of the steady-state value would suffice to operate the servo. If a current of 1 milliamperes, or corresponding V millivolts across a load, is required to operate a device, then the important parameter is the time required to reach that current I or voltage V . In general, decay times should be no longer than rise times.

Of course, what is being done by this approach is attempting to choose a time interval for the current measurement which should give a reasonable approximation to the way the system might behave if actually M_{dynamic} was being found, with a scanning beam which crossed the coincidence position at a reasonable rate. The breadboard beam tracker assembly built earlier (as will be described in Section VI) had operated best with this same cell, although at considerably greater light intensity, when the tracking servo swept back and forth across the coincidence position with a frequency of 2 cps. Therefore, we make the arbitrary decision that several millivolts of transient output voltage must appear within 0.5 sec, in order for the incoming signal to be strong enough to be called "usable."

At this point, reconsideration of the equipment as shown in Figure 4 shows it to be adequate. The limiting frequency bandpass of the electronic circuits occurs in the DC amplifier within the Hewlett-Packard #425A voltmeter. This amplifier passes from 0 cps to approximately 1 cps (the half-maximum sensitivity points).

III A. A-Type

When the various parameters were adjusted to yield a few mv output within 0.5 sec for weaker and weaker signal light inputs, this chosen rise rate could be maintained by using stronger and stronger local beams on the other side of the cell. The earlier work noted in Appendix A had already shown that greater total light power for the two faces of the cell added together led to faster rise rates. However, this process must be stopped before the enhancement feature disappears ($M \rightarrow 1.0$).

As some of the experiments in Appendix A showed, too great a disparity between the beam intensities on the two sides of the cell tends to decrease M . This raises the question of what is the smallest values of M_{static} which will lead to a "usable" M_{dynamic} in an actual tracker. Such a correlation involves the desired scanning rate, the noise level, and the desired image resolution or angular tracking accuracy. Resolution in the present experiment was governed by the illuminated spot size, which was arbitrarily chosen in advance as 50μ , and by the fact (determined in a

separate experiment to be described in a later subsection) that the value of M fell to unity outside a width not greatly larger than the spot diameter. It should be recognized that a choice of smaller illuminated spots would have led to somewhat different results, and that certain long-range tracking applications might require resolution much finer than 50μ . Due to the close of the contract period there was no time available to repeat this experiment, and allied experiments, with 5μ spots for example.

As to the effect of noise level, with the choices of rise rate and desired voltage mode above, no noise at all was observed to pass through the 1 cps filter in the Hewlett-Packard voltmeter. Because of this great steadiness of the signal, the quite low value of $M_{\text{static}} \geq 1.2$ was chosen as being a reasonable limit for this experiment.

IIIA. A-Type

In an application involving small signals to be seen against large background noise, a value of $M > 10$ or more would probably always be necessary. However, where it appeared that millivolts of output would be available for a very weak input signal, in a situation from which noise could be practically excluded, values of M very close to 1.0 are quite acceptable.

The basic features of the experiment having then been set by the above arbitrary choices, the following parameters were available for adjustment.

1. direction of the electric field applied to the cell;
2. which face of the cell is exposed to the signal beam;
3. cell voltage
4. load resistance in the photocell output circuit;
5. dominant wavelength and spectral composition of the weak light, called the signal beam;
6. dominant wavelength and spectral composition of the light on the other side of the cell, called the local beam; and
7. intensity of the local beam.

First, a rough exploration was made of the general effect of each of these parameters, guided by all the experiments previously carried out. Having made an approximate adjustment of each of the parameters, the set of apparent best choices was arranged as a first standard experiment. Then, small changes in chosen parameters were made, to sharpen up the exact values for this unified system. In view of the complex interactions of these parameters, one cannot be positive that the very best arrangement was found in the end.

IIIA. A-Type

For example, a change in the wavelength of one of the light beams might conceivably throw the system into an area for which different parameters could lead to a greater sensitivity. However, the method of gradually zeroing in on a combination which appeared jointly to lead to greatest sensitivity for the system under the chosen conditions seems to offer a good likelihood of success.

The result of these tests was the choice of the following set of circumstances for measurement of the "minimum usable signal" for photoconductive CdS cell #A-D with one pair of opposite 50μ illuminated spots, with $M \geq 1.2$, and with several millivolts of output voltage drop across a 12 megohm load resistor within 0.5 sec after the signal beam is turned on:

1. The In electrode was negative.
2. The signal beam fell on the glass-electrode face of the cell.
3. The voltage applied to the cell was 1.35v.
4. The load resistance in series with the cell was 12 megohms.
5. The central wavelength of the signal beam was 6330\AA , obtained with a narrow-band interference filter whose bandpass was approximately 100\AA . The light source for this beam was a 110v quartz-bromine incandescent tungsten lamp bulb. This lamp was run on only 8v DC, at a corresponding low output level. The beam was attenuated by the interference filter, by a 30% transmission neutral density filter, and by a beam splitter whose function will be described below. Adjustment of this beam intensity constituted the final independent variable of the experiment.

IIIA. A-Type

6. The local beam had a central wavelength of 5300\AA , obtained with a Bausch and Lomb monochromator whose slit width was adjusted to pass about 320\AA . The source of light for the signal beam was also a tungsten filament lamp run at reduced voltage.
7. The local beam intensity was adjusted to a value whose measurement is described below.

2. Measurement of the "minimum usable signal"

Some outputs from this system are shown in Figures 5 and 6. These traces show the rise and decay signals obtained with a Tektronix No. 536 oscilloscope, under the final conditions of "minimum usable signal", when the signal beam was turned on and off abruptly with a manual shutter. The horizontal time scale of these pictures is two seconds per large division of the grid. The vertical scale displayed in these pictures is arbitrary, (determined by an unmeasured amplification factor in the oscilloscope). The actual output data of the experiment were the readings of a Hewlett Packard No. 425A DC millivoltmeter, connected across the 12 megohm load resistor, which was in series with the cell and the potentiometer voltage supply. The final steady-state voltage reading was 230 millivolts, at the time shown in Figure 5 occurring near the center of the picture on the second sweep of the oscilloscope. This means that one large grid division vertically on Figure 5 represents about 40 mv. Although at the very low signal beam intensity being used (whose measurement will be described below), τ_{rise} defined as 63% of the final value is about 6 sec, it is apparent from Figure 5 that in 0.5 sec the output voltage transient has risen to approximately 15 mv.

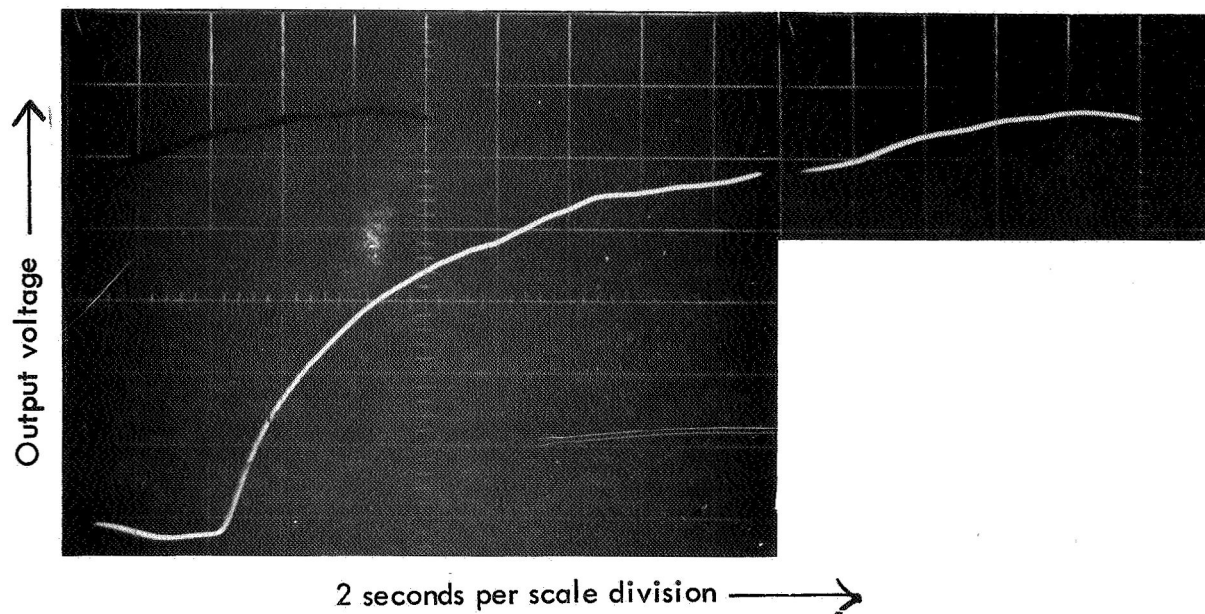


FIGURE 5. Rise Transient at Minimum Signal With Cell #A-D.

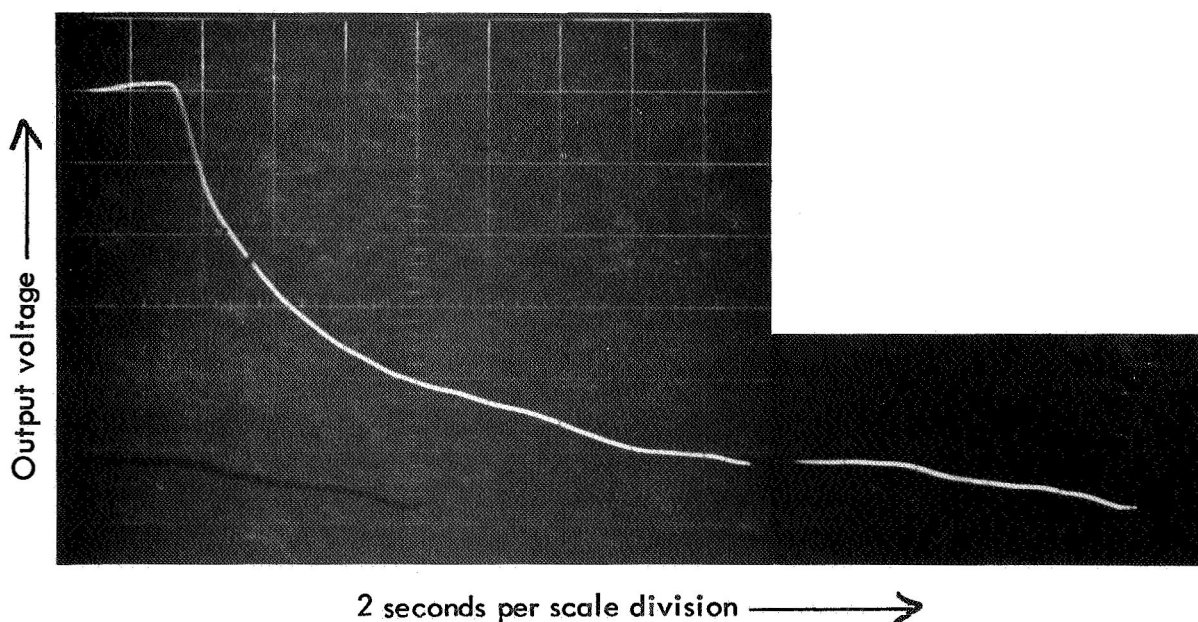


FIGURE 6. Decay Transient At Minimum Signal With Cell #A-D.

(Figure 5 was composed by joining prints together from two parts of a picture of an oscilloscope trace consisting of two sweeps, with a flyback between which occupied a negligible time interval. Therefore, the break in the trace shown is not real, and does not represent appreciable elapsed time. Figure 6 is of the same type.)

IIIA. A-Type

Figure 7 is taken at a higher vertical amplification on the scope, but with all conditions otherwise the same. Figures 6 and 8, the latter being to the same enlarged vertical scale as Figure 7, indicate that the decay time pattern is practically the same as the rise time pattern.

The value of M_{static} under the conditions of Figures 5-8 was calculated from the following readings of the millivoltmeter across the 12 megohm series resistor, after the transients had reached equilibrium: signal beam alone = 0.3 mv, local beam alone = 178 mv, both beams = 230 mv. This yields $M = 1.3$.

Having thus determined the probable best assemblage of parameters for finding the minimum signal yielding an acceptable response, the final part of the experiment was to measure the intensities of the local beam and the signal beam — at the minimum signal setting illustrated by Figures 5-8.

The basis of the calibration was the Barnes Engineering Co. Infrared Reference Source, Model 11-200T which was run at 1000° C. Light from this approximately black body was sent to an Eppley thermopile, Model 5053. The number of microwatts of radiation falling upon the thermopile was known from the geometry of the arrangement, and from the calibration constants of the Infrared Reference Source. The output of the thermopile was read by a Keithley No. 150A microvoltmeter. In this fashion, the calibration factor of the thermopile-voltmeter assembly was determined as $1 \mu v = 3.5 \mu \text{ watts of radiation}$.

When this calibrated thermopile was placed in the signal light beam at the position previously occupied by the CdS cell, with the same 50μ diameter aperture in front of it, the amount of signal light which had been falling on the cell was too weak to give measurable readings. Therefore, a proportionality arrangement was devised.

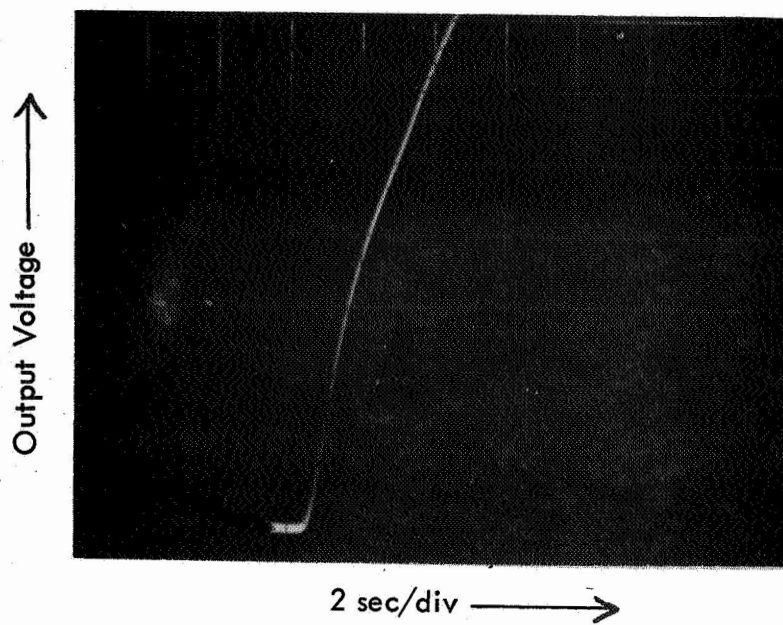


FIGURE 7. Initial Voltage Output At Minimum Signal; Rise.

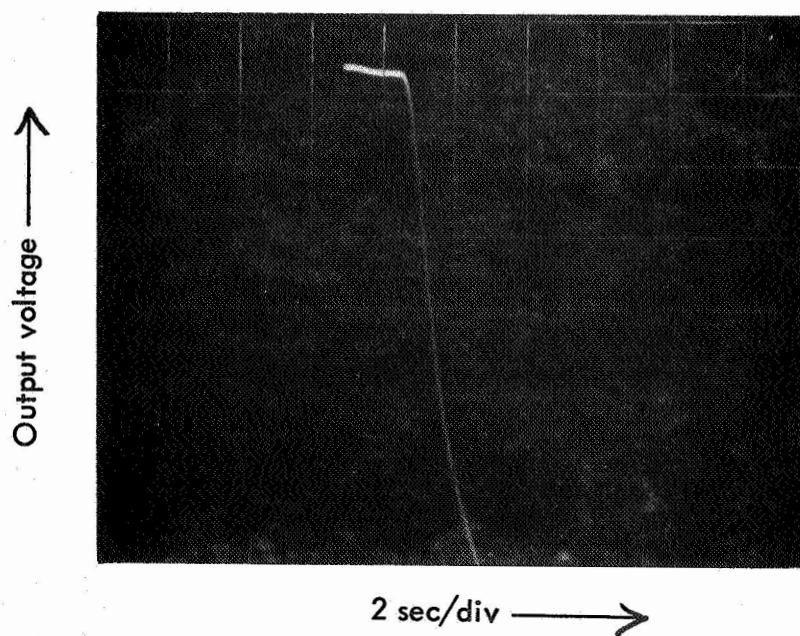


FIGURE 8. Initial Voltage Output at Minimum Signal; Decay.

IIIA. A-Type

The intensity of the signal light was monitored by taking a fraction of its beam to one side through a beam splitter, to an RCA photoemissive cell Model 1P21, which led to a Photovolt Corp. amplifier. The reading of the 1P21 photocell amplifier was recorded at actual minimum-signal beam intensity. The voltage on the lamp providing the signal beam was then greatly increased, to give a strong beam whose intensity was measured with the thermopile. The signal beam was then reduced to back its original intensity, as monitored by the 1P21 photocell and amplifier, by means of calibrated neutral-density absorbing glass filters placed in the beam. The known reduction factors of the neutral-density filters were applied to the thermopile reading, to determine the micro-watts of radiation which had been passing through the 50μ spot onto the CdS cell at the minimum signal intensity.

By this method of calibration it was found that the signal power incident on the 50μ spot on the glass-electrode face of the CdS cell under the conditions of Figures 5-8 was 1×10^{-12} watts. The local beam power used at that time was measured in the same fashion to be 2×10^{-9} watts, onto the 50μ spot on the indium-electrode face of the cell.

These measurements completed the planned experiment for determining a "minimum usable signal". The arbitrariness of the choices is recognized. However, the results should be useful for at least an approximation to the behavior to be anticipated from such a cell as a tracker of weak point sources.

The next subsection describes a slight extension of the same experiment to see if the cell was responding to received power, or really to received power per unit area.

IIIA. A-Type3. Increased areas of illuminated spots

The following question seems pertinent: If one wishes to get the greatest possible photo-current response from a very weak signal beam arriving from a distant source, does the focal length of the collector mirror or lens matter? That is, aside from image resolving power requirements or training accuracy requirements, is it important to focus the available radiation down to as small a spot as possible on the face of the cell, in order to have large incident power per unit area?

Although this exact point was not tested, a related experiment was performed which showed that power per unit area is not a unique determining factor for the magnitude of the enhanced photocurrent. A cell was given the same incident power per unit area over two opposite-spot-pairs of different diameters. The two outputs were not the same, even though the power per unit area was the same in the two cases. Total received light power, rather than power per unit area, is the parameter that counts. The spot-pair of larger size showed larger currents, a greater M , and a shorter τ_{rise} than the other.

The experiment actually consisted of making only one change in the final circumstances of the "minimum usable signal" case described above. The two 50μ apertures over the faces of cell #A-D were replaced by two 100μ diameter apertures in the same positions. The measured output voltages then became: signal beam alone = 4mv, local beam alone = 240 mv, both beams = 590 mv. The latter is much larger than the 230 mv recorded with the 50μ apertures. These values correspond to $M_{\text{static}} = 2.4$ instead of the previous $M=1.3$ at the same incident power per unit area.

Figure 9 shows that the (63%) time constant has correspondingly dropped from the previous 6 sec to about 2 sec.*

* Caution is needed about inferring any really quantitative relationship here, since the load resistor was not re-optimized for the new light power input, as Subsection 5 below shows may often be important. Note also that the output current tests corroborate an earlier experiment reported in Appendix A.6 for a different cell and greater light intensities.

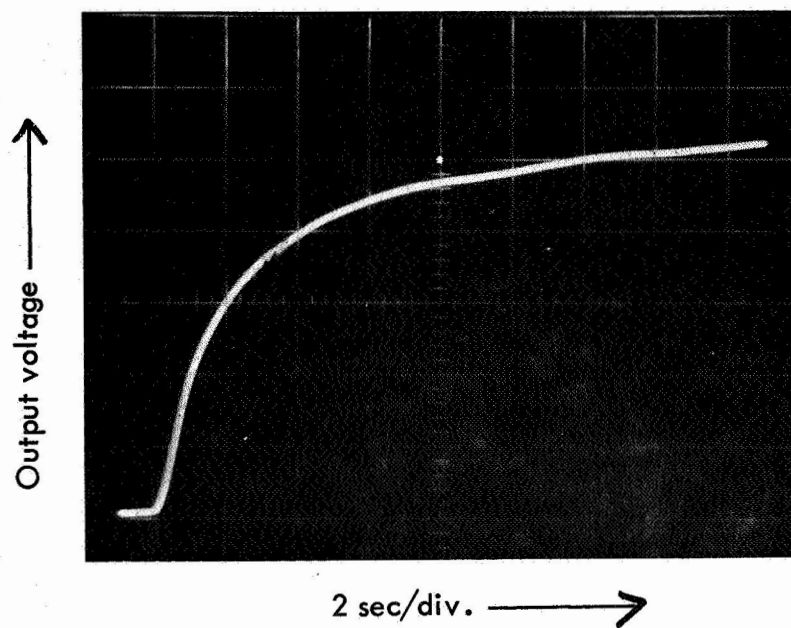


FIGURE 9. Repeat of Figure 5. with Four Times the Illuminated Spot Area.

III A. A-Type4. A moving-spot experiment

Among remaining questions about the experiment described in Subsection 2, three important related ones would be: Is $M=1.3$ really large enough for practical uses? Is there noise arising from material nonuniformity which would appear in a scanning experiment, even though no noise was seen in the static experiment? With the local light much brighter than the signal light, will the resolving power as a tracker still be comparable to the spot diameter, or will the effect of the local beam spread out sideways too much? A subsidiary experiment was performed to contribute a little more information on these matters, although there was not sufficient time for thorough research in such areas.

The equipment and all adjustments remained the same as in the basic experiment, except that the mask containing the $50\ \mu$ hole was removed from the "local" side of the optical setup. The local beam was now focussed onto the exposed indium-electrode face of the CdS cell through a slit having approximately $50\ \mu$ width. By moving one of the lenses in the optical train by hand, the $50\ \mu$ slit image was slowly swept across the surface of the cell behind the $50\ \mu$ spot illuminated by the signal beam on the other face.

The output response for this procedure is shown in Figure 10. The intensity of the signal beam in this experiment remained the same as before; that is, 10^{-12} watts were incident on the $50\ \mu$ spot on the signal side of the cell.

The linear displacement of the slit image across the face of the CdS between the two positions which showed half-maximum response in Figure 10 was very close to $50\ \mu$ distance. This showed that the effect of the signal spot and of the local beam slit on the surface of the CdS layers at these intensities did not spread out very much beyond the geometrical edges of the exposed area.

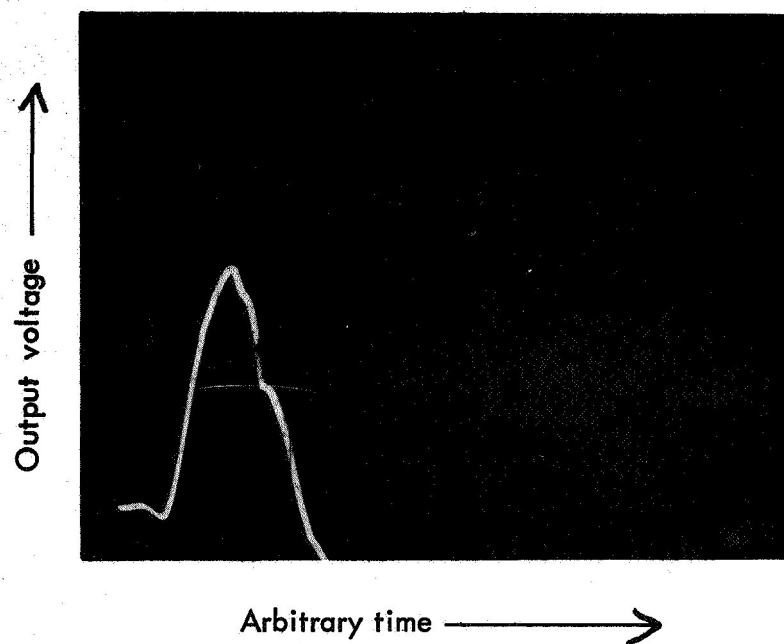


FIGURE 10. Effect of Slow Scanning With The Minimum Signal.

IIIA. A-Type

Figure 10 also gives a preliminary indication that noise* and false coincidence signals arising from nonuniformities in the cell properties may not be extreme, when averaged over $50\ \mu$ spot areas at least — although this test only covered a small fraction of the cell face area, and there are obviously anomalies in the trace shown in Figure 10. Repetitions of the hand scanning procedure gave a number of pictures which were all quite similar to Figure 10. Such results indicate that random noise was no more prominent in these circumstances than would be deduced from Figure 10.

This completes the experiments done with cell # A-D and the minimum-signal arrangement illustrated in Figure 4. The next subsection describes a separate set of experiments to explore the effect of the electrical circuit constants on the measured rise and decay times.

5. Effect of circuit constants on time responses

It was mentioned in Subsection 1 that the value of the load resistance in the cell output circuit was an important parameter, which had to be adjusted to obtain the shortest rise and decay times. This circumstance can be well illustrated by a set of data taken at a different time with different apparatus, using cell # A-C, illuminated with opposite $50\ \mu$ diameter spots.

The most straightforward measuring arrangement would consist of only three components — the cell, the battery, and a sensitive ammeter, in a single series loop. Even though the cell resistance dropped by a considerable factor upon illumination, it will always remain large compared to the resistance of any ammeter. Therefore, with this circuit, the electric field applied to the CdS layer would stay the same during both dark and light conditions.

* Within the 0-1 cps passband at the slow scanning rate used here.

IIIA. A-Type

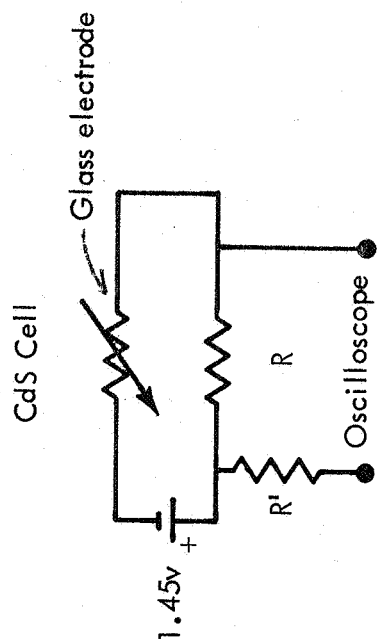
However, photocurrents are often too small to be read by a meter directly and so their effect requires amplification. Since voltages are more easily amplified than current, it is then simplest to use a series loop consisting of the cell, the battery, and a fairly large load resistor — with suitable equipment applied to amplify and measure the voltage drop across the load resistor, which is proportional to the photocurrent.

Figure 11 shows the circuit of this type actually used for this experiment.

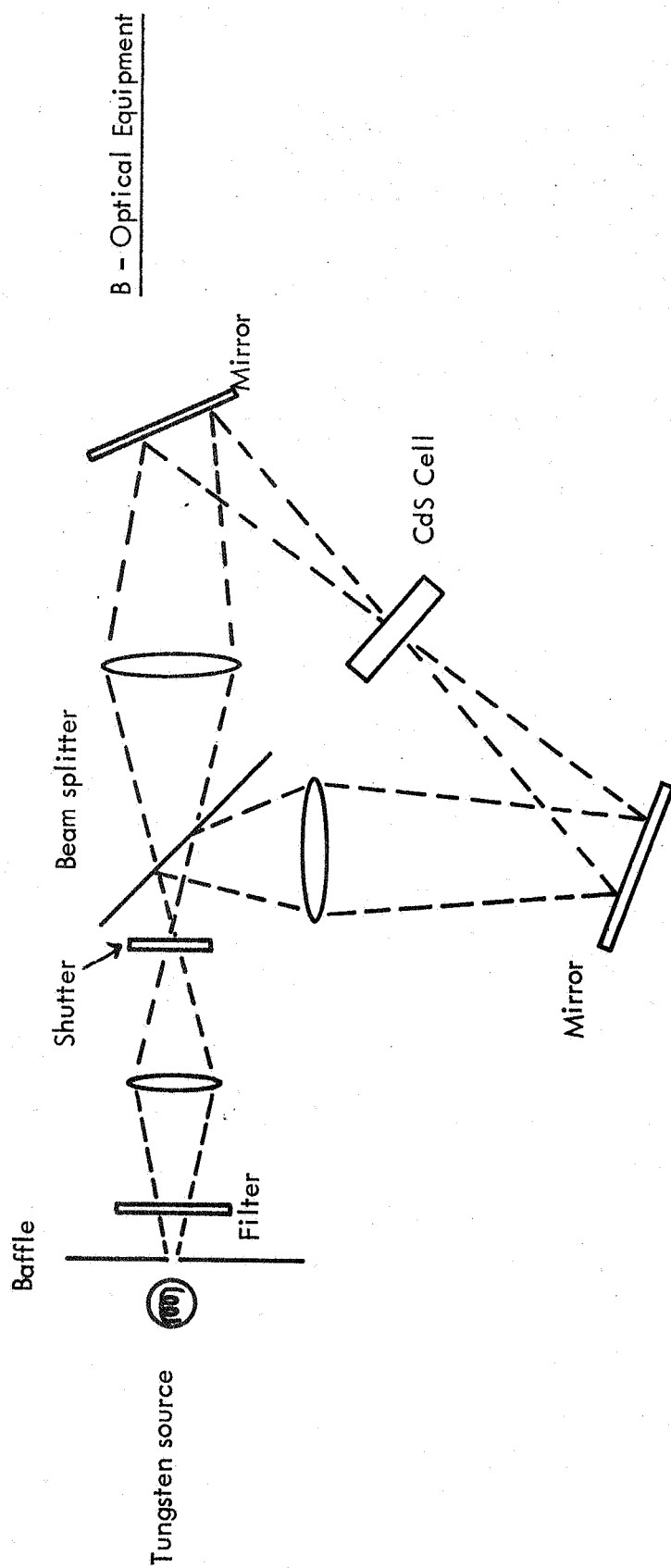
But with any such circuit, the fixed battery voltage is connected across the cell and the load resistor in series, and when the cell resistance decreases by a factor of as much as 10^5 under strong illumination, that fraction of the battery voltage which appears across the cell becomes less. The electric field acting on the CdS material then decreases automatically as soon as the light appears. This can have an effect on the photocurrent, and so sometimes cause M values and time responses to be sensitive to the particular load resistance employed. Figure 12 shows the output voltage rise and decay times actually found upon opening and closing the shutter with green-green dual illumination,* for different values of the load resistor. One large horizontal grid division represents 2 sec in this Figure. The time required for the shutter to open or to close was less than 0.01 sec. Figure 13 shows the corresponding results with red-red illumination.

It was not felt practical in the time available to either explore this phenomenon with care, for its scientific value, or to devise a power supply system which would maintain a constant electric field at the CdS at all times. For this reason, in the minimum-signal experiment the value of the load resistor was simply adjusted empirically to give the smallest, and equal, values of rise and decay times for the beam wavelengths used.

* This terminology describes the colors of the two light beams being used, which are both green in this case. As shown in Appendix A.1, it is often advantageous to use a green beam on one side of the cell and a red beam on the other side. This would be termed green-red illumination.

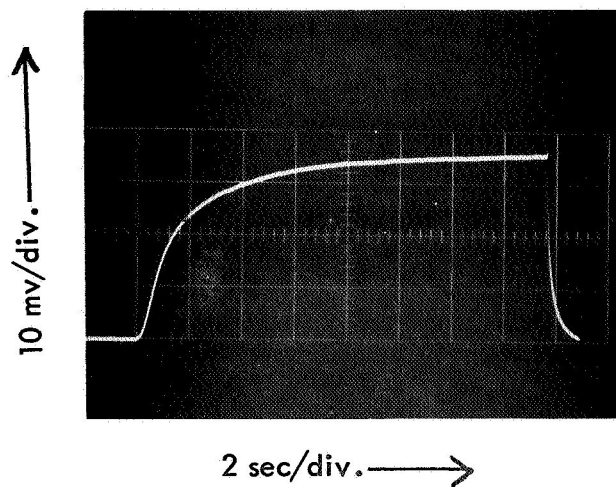


A - Electronic Equipment

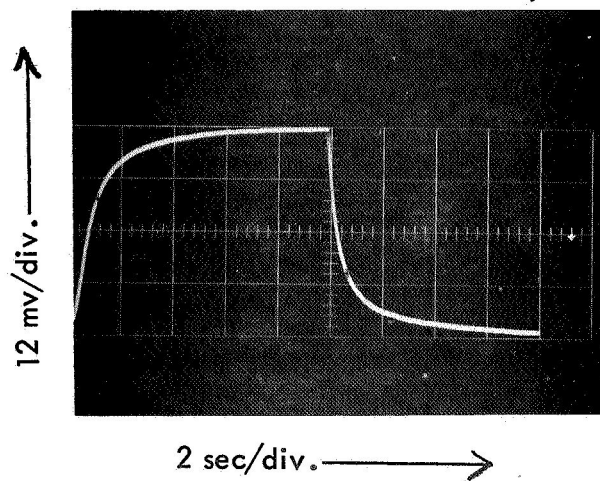


B - Optical Equipment

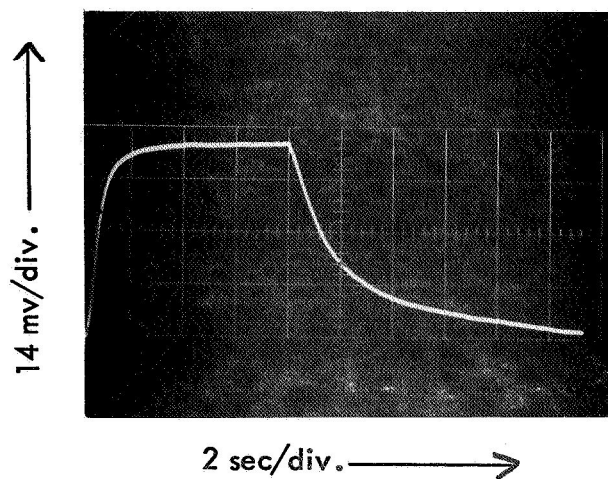
FIGURE 11. Schematic Arrangement for Circuit Variation Experiments



(A) $R = 200,000$ ohms
 $R' = 20$ megohms

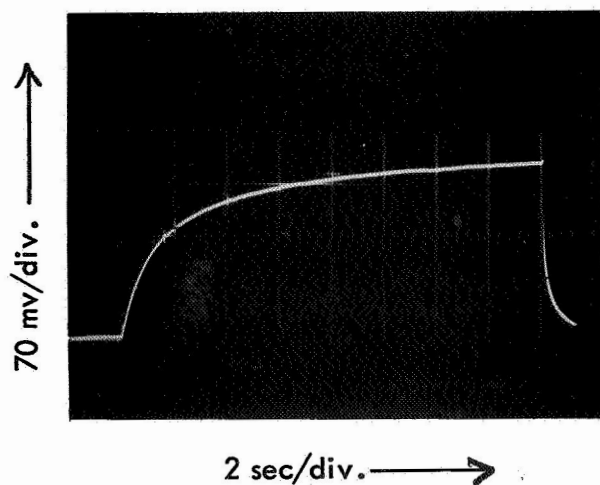


(B) $R = 940,000$ ohms
 $R' = 20$ megohms

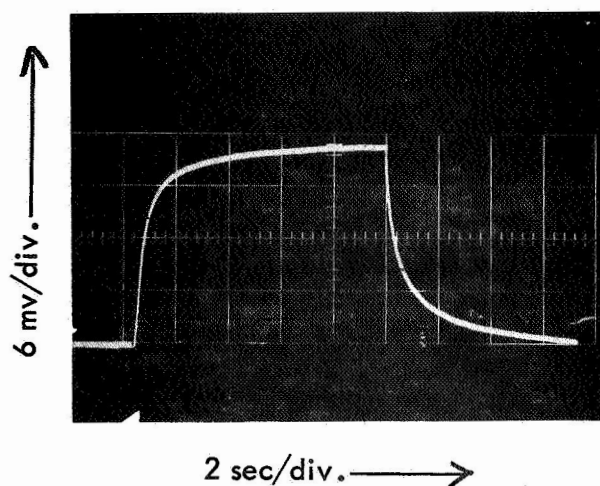


(C) $R = 10$ megohms
 $R' = 20$ megohms

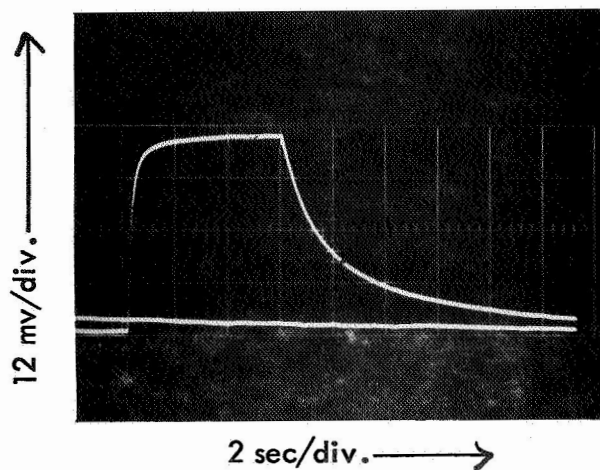
FIGURE 12. Effect of Load Resistance On Time Responses; Green-Green Light (5000\AA)



(A) $R=5000$ ohms
 $R'=0$



(B) $R=100,000$ ohms
 $R'=20$ megohms



(C) $R=940,000$ ohms
 $R'=20$ megohms

FIGURE 13. Effect of Load Resistance on Time Responses; Red-Red Light (6330\AA)

IIIA. A-Type6. Chopping at 90 cycles/sec

Most of the work on A-type CdS cells described in this report dealt with either steady light beams, or with the transient responses from abruptly starting or stopping the illumination. However, one short set of experiments on cell # A-D was performed with both beams continuously chopped in-phase at 90 cycles/sec by rotating slotted wheels.

As a typical measurement, a 90 cps chopped beam at 6330 \AA illuminated a 50μ diameter spot in the center of the In electrode face of the cell, to produce 6 mv across the 1000 ohm load resistor. This voltage was being read by an Infrared Industries Model No. 600 Tunable Microvoltmeter which was set for maximum sensitivity to 90 cps voltages, with its sensitivity dropping by 50 % at ± 4 cps away from the maximum point. This means that the output was being measured with a highly resonant system which detected only the response of the cell at the chopping frequency and almost ignored any other components which might have been in the response. Using 7340 \AA light chopped at 90 cps on an opposite spot gave 100 mv alone. Combined illumination (with both choppers in phase) gave only 100 mv also. This means that M differed very little from unity.

Attempts to make similar measurements with blue or green light failed for lack of output near 90 cps large enough to be registered by this narrow bandpass meter.

It was not practical in the time available to pursue this matter further. The experiment must be viewed as rather fragmentary, since there was not time to vary the load resistor, the beam intensities, the beam wavelengths, the bandwidth of the output meter, or the chopping frequency. It is possible that the beam intensities were so high as to drive $M \rightarrow 1$, in the manner described in Appendix A.4. Certainly, in the experiments

IIIA. A-Type

described in Appendix A.5, enhancement was observed in some of these A-type cells with light beams sinusoidally modulated at 400 cps.

Possibly this experiment is best viewed as a warning that all the interlocked parameters must varied before one can be sure of what is happening with these cells— even on the macroscopic level.

The remaining photoconductive research on A-type CdS cells was of a different character from that discussed so far in this section. It was an exploration to see what degree of enhancement could be found in the near infrared part of the spectrum, as will be described next.

7. Exploration of enhancement in the infrared

A detailed search was made for evidence of any major degree of enhancement with light beams at numerous wavelengths between the visible and 2.7μ . For the set of measurements of M displayed in Figure 14 the two sides of cell # A-D₁ were illuminated with rather closely equal optical systems. Two Barnes Engineering black body emitters at 1000°C irradiated the opposite surfaces through two $f/1$ lenses and two interference filters which had about 100\AA passband in every case. For all the points on the diagonal of the graph, where $\lambda_{\text{left}} = \lambda_{\text{right}}$, the two filters used passed the same wavelength bands. With two filters whose passbands centered at 1.0μ , the systems were delivering about 2.5×10^{-4} watts to each side of the CdS cell. Opposing central spots with 3.6 mm diameter were illuminated on the CdS faces. At these high light levels the recovery time of the CdS is very long. The cell was allowed to rest in darkness after every measurement until it returned to its normal dark current condition, typically about 5 minutes. The reason for the use of relatively great intensities is the low photoconductive response of these cells in the infrared.

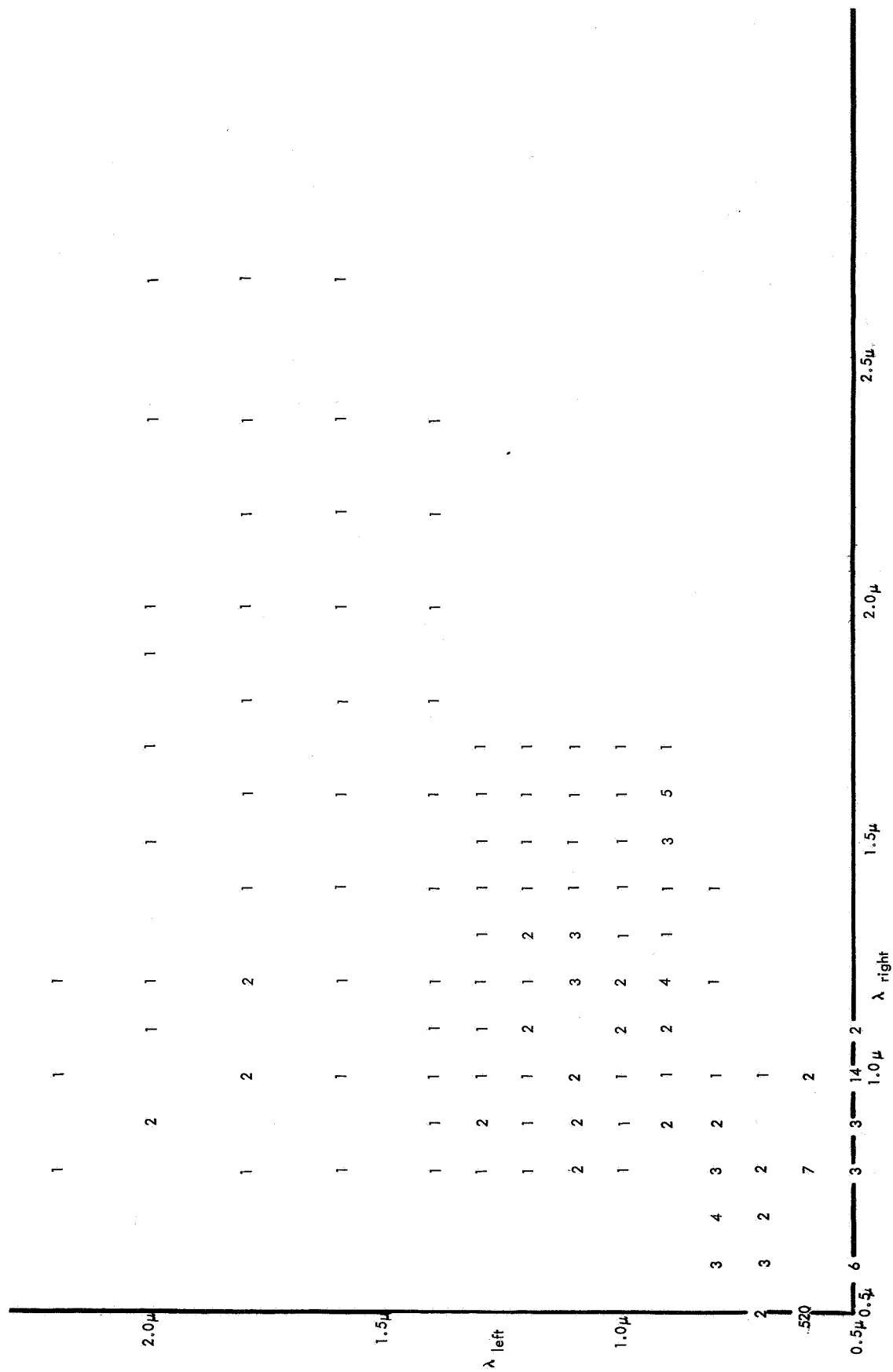


FIGURE 14. M as a Function of Wavelengths of Beams
On the Two Sides of the CdS.

IIIA. A-Type

For points off the diagonal in Figure 14, the filters on the two sides of the cell had different pass-bands, as listed. For the measurements displayed in Figure 15, an additional neutral-density filter was added on the right hand, or conducting glass, side of the cell which transmitted approximately 10% throughout the wavelength range being studied. Comparison of some of the numbers shows the same kind of variability of M with beam intensities which is discussed in Appendix A.4 for the visible region. From the information given, the standard black body tables will permit calculation of the energy flux density on each side of the cell at each measurement point, if needed.

The conclusion from the exploration seems to be that this CdS cell shows no new type of phenomenon in the near infrared. The small values of M found appear to merely constitute the "tail" of the phenomenon already explored in the visible part of the spectrum. However, M values of 2-3 can be used in important applications if the photocurrents are large enough for relatively noise-free amplification. As a typical example, in Figure 14 for $\lambda_{\text{left}} = 0.9\mu$ and $\lambda_{\text{right}} = 1.5\mu$ the observed current values were $I_{\text{left}} = 43$ nanoamp, $I_{\text{right}} = 5$ nanoamp, $I_{\text{both sides}} = 160$ nanoamp, which yields $M_{\text{static}} = 3.3$. It would appear that A-type CdS cells might be used successfully in the infrared for some applications.

FIGURE 15. M as a Function of Wavelengths of Beams On the Two Sides of the CdS with 10% Transmission Neutral Density Filter in the Right Beam.

III B. Properties of the B-Type Polycrystalline CdS Cells

Cells of the A-type are no longer available from the original supplier in research quantities. In order to develop an alternate source, and also to check on the existence of enhancement in cells from another manufacturer, an extensive search was made for another supplier of research quantities of a sandwich type of thin polycrystalline CdS cell. Finally, the G.T. Schjeldahl Co., Northfield, Minnesota 55057, agreed to try to fabricate a few cells of this type, for the first time in their laboratory, to a very short delivery schedule (because the present contract was nearing its end). Very likely, much better cells could have been made by this Company with more development time.

Of several sandwich-type samples submitted, only cell # B-376-50 showed good photoconductivity and that only at one small spot near one edge. But this spot did show the photoconductive enhancement effect.

The following information about the cell was provided by the supplier: "1.0 mil CdS thickness deposited in an organic binder, between cover plates of 1mm thick Pyrex. Semitransparent electrodes of BiO and Au (5 ohms/square, approximately 60% transmission) are bonded to both sides. The doping and treatment schedule... involves chlorine doping". Note that this cell had only half the thickness or less (25μ), of the A-type cells.

A mask with a 1mm hole was placed over one cell face, to define the spot which a rough survey showed to be most responsive. A beam from a tungsten lamp, passed through an interference filter, was sent to one side of this spot and a beam from a monochromator was sent to the opposite location on the other face of the cell. Photoconductive enhancement factors as large as $M = 7$ were measured for various beam wavelength combinations over the ranges 5140-7360 Å on one side and 5000-7700 Å on the other side. .

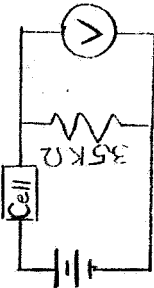
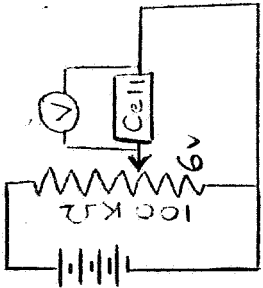
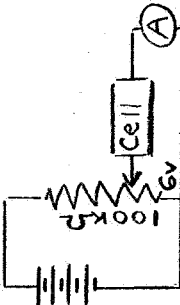
III B. B-Type

The measurements are presented in Table II.

Although this cell was nominally symmetric, reversal of battery polarity did make a difference. Presumably this is an indication that in the B-type cell also, the exact nature of the interface between electrode material and CdS has an effect on the enhancement factor.

TABLE II
PHOTOCONDUCTIVE ENHANCEMENT DATA FOR B-TYPE CELL

Cell #B-376-50
 Mask with 1mm hole
 Keithley Microvoltmeter

Circuit	Beam Wavelength, Side 1	Beam Wavelength, Side 2	Battery Voltage	Output, Side 1, only	Output, Side 2, only	Output, Both sides	M _{static}
	7360Å	6930Å	6v	1.8mv	1.6mv	15, mv	4.4
	6330	"	"	0.5	1.2	10.5	6.2
	5140	"	"	0.3	1.3	6.3	4.0
	6330Å	6930Å	3v	0.1mv	0.4mv	2.1mv	4.2
	"	"	6	0.3	1.3	11.0	6.9
	"	"	6*	< 0.05	3.2	10.0	3.2
			*(reversed polarity)				
	5140	5000	6	0.2	0.6	2.2	2.8
	"	7250	"	0.1	1.8	8.0	4.2
	6330	7250	"	1.0	2.0	11.0	3.7
	5140	5000	6v	9ma	18ma	67ma	2.5
	6330	"	"	27	25	123	2.4
	"	6930	"	30	60	360	4.0
	7340	7700	"	40	150	600	3.2

III C. Research with General Precision Polycrystalline CdS Cells

Ref. II describes research on photocells made by General Precision from a brand of doped-CdS powder sold by Sylvania Electric Products especially for photoconductive applications. This powder was pressed at 20,000 psi and sintered, to form about 40 disks with 1.3 cm diameter and thicknesses between 0.2 mm and 5 mm. Six of these cells were found to be photoconductive. Electric fields were applied to the cells through pressure contacts to conducting glass electrodes on each side of the disks, for four of the cells. Two of the cells had translucent evaporated In electrodes on one side and conducting glass on the other.

Photocurrent enhancement was found in all six of the cells. For all but the thickest one, the enhancement showed the usual spatial discrimination feature. The results show that the photocurrent enhancement phenomenon is not peculiar to very thin cells alone. So long as the cell thickness is less than perhaps 2.0 mm, just the same enhancement phenomenon is also present in the sintered GP cells, using simple pressure-contacted electrodes in most cases. The values of M are quite large enough for many applications.

Cell #GP-2, with thickness about 1.0 mm, was illuminated on small opposing spots with red-red, red-green, or white-red wavelength combinations. At intensities which yield nanoamperes of current with from 4.5 to 40 volts across the cell, the values of M_{static} obtained lay between 4.5 and 11.8.

Cell #GP-3A, which was 0.47 mm thick with an In electrode, gave $M = 2.5$ under white-red illumination. Cell #GP-4A, which was 1.58 mm thick with an In electrode, gave $M = 9.7$ with white light falling on the In (+) face and green light on the glass face, at 40 volts. It showed $M = 15.1$ with white light on the In (-) face and red light on the glass face, at the same voltage.

III.C GP-Type

Cell #GP-16, whose thickness was 2.40 mm, showed $M_{\text{static}} \approx 2$ under white-red or white-green illumination of opposing small spots, with 40 volts cell bias. However, the spatial discriminating characteristics of the enhancement phenomenon are apparently lost at this cell thickness. That is, values of $M_{\text{static}} \approx 2$ were also measured when the two spots were not opposite, but had their projected areas separated by several spot diameters of dark CdS. As an additional phenomenon, values of $M_{\text{static}} \approx 2$ were also found for full-area illumination of the complete cell width—a circumstance not found with any of the thinner cells which were checked for this point, either of A or GP types.

The dark resistance of the GP cells was typically about 1000 megohms. Under the illumination levels used, the resistance of the best cells decreased to about 5×10^5 ohms. Part of these resistances were contributed by the electrode contacts. The cells were found to be definitely non-ohmic.

III D. Single Crystal CdS Enhancement

The same kind of photocurrent enhancement effect has been found with 0.5mm thick single crystals of slightly doped CdS pressed between conducting glass electrodes. The phenomena investigated seem about the same as with the A-type cells, except that photocurrents are quite small. Values of M_{static} as high as 4 were measured.

A single crystal of CdS, purchased from Semi-Elements, Inc., Saxonburg, Pennsylvania, was cut and polished to form a thin square plate with 0.5 mm thickness and 5 mm sides. When using dual green-green illumination (5225Å in opposing spots) the observed value of M_{static} was about 1.6. As mentioned in Ref. I, the τ_{rise} with this dual illumination was 1.2 sec, as compared to ≈ 2.1 sec for single-sided illumination. The phenomenon of faster rise time in the presence of $M > 1$ which was found for the A-type cells is thus also present for single crystal material.

Some results on similar single crystal CdS cells carried out in 1964, which were not covered in Refs. I-III, are also of interest. Using a crystal 1.0 mm thick, with red-green illumination (6640Å, 5200Å) on small opposite spots, an enhancement factor of $M=2.66$ was found. This involved currents in the nanoampere range with 15 v across the cell. With constant red light on one side of the crystal and a beam of roughly constant intensity but variable wavelength on the other, the shape of the curve of M_{static} vs. λ was very similar to the curve in Appendix A.1 found with the A-type cells. In a test with green-green illumination (5200 Å on each side), $M = 4.0$ was reached.

In another very interesting experiment with the same cell, a steady near-infrared beam at 8000Å was kept on one side, while the wavelength of the other side was varied. No enhancements $M > 1$ were found, but for shorter wavelengths of the variable beam than 5850Å a type of quenching appeared. This became most pronounced for the combination (8000Å, 5300Å), where $M_{\text{static}} = 0.1$ was measured. The time response for this phenomenon was extremely slow.

III E. Tests with Single-Crystal Germanium

Ref. III detailed a considerable amount of research with 1 cm diameter and 1 mm thick pure single crystal germanium disks, obtained from Semi-Elements, Inc. Saxonburg, Pa. No positive evidence was found for an enhancement factor M_{static} greater than unity. Subsequent to 15 October 1967 more work was done of the same character as described in Ref. III, with the same negative result.

Much effort was put into the attempt to apply low resistance, translucent, uniform, stable metal film electrodes to the Ge disks. With the CdS cells made at General Precision this matter did not seem so important. The CdS cell dark resistances were usually around 100 megohms and the resistances were still many ohms under illumination. However, because of the lower resistivity of germanium, the Ge disks used had a computed front-to-back resistance of only 0.5 to 5 ohms. It seemed unreasonable to try to look for changes in these small resistances as a result of illumination when using electrodes such that the measured total cell resistance was several hundred ohms. Pressure-contacted conducting glass electrodes also seemed too variable to trust for investigating changes of a fraction of an ohm.

However, to make evaporated metal films which are both semi-transparent and of low electrical resistance parallel to the film face is a difficult task. (The electrode resistance was also a severe problem with most samples of the B-type CdS cells). To reduce electrical resistance from center to edge of the 1 cm diameter circular films, they were pressure contacted with a 400-mesh flat gold screen. But still, the problem was not really solved satisfactorily in the time available. The measurements leading to the above statement of negative results were made under fairly stable conditions with over-all cell resistances of about 70 ohms.

This concludes the description of photoconductive current enhancement research.

Section IV will turn to the newly discovered photovoltaic enhancement phenomenon.

IV. THE NEW PHOTOVOLTAIC ENHANCEMENT EFFECT

A. Research with A-Type CdS Cells

During the course of the quantitative studies described in preceding sections, a routine check was made to see if voltages arising from the well known photovoltaic effect could be of sufficient magnitude to perturb the measurements of voltage drop across a load resistor carrying the currents generated photoconductively. In most of the circumstances being studied, the photovoltaic effect was found to involve microvolts, whereas the photoconductive measurements involved millivolts, so that corrections were negligible.

However, it was discovered that particularly with cell # A-C the small photovoltaic outputs had low noise, and displayed the same kind of spatial enhancement phenomenon being studied through photoconductivity, but with about 20 times faster time responses. The effect was most prominent for green-green spot illumination. Some of the initial experiments will now be described. It seems that bandwidths of around 5000 cps can probably be used.

1. First photovoltaic enhancement experiments

In this experiment, the spatial discrimination property of photovoltaic enhancement was demonstrated. A pair of masks was placed over the two sides of cell # A-C having four holes in opposite positions in each mask. The pattern of holes is shown to scale in Figure 16. A blue-green beam of radiation could be focussed onto one hole in each side of the cell, using either opposite or non-opposite holes. The hole diameter was 0.36 mm.

First, Figure 17 shows that the photovoltaic outputs with non-opposite holes are merely additive, with no enhancement. Figure 17A shows the changing photovoltaic output, from light off to light on, when the cell is irradiated on one side only — through the top hole in the mask over the Indium electrode face. Figure 17B is the same thing with the radiation coming through the center hole on the glass electrode side of the

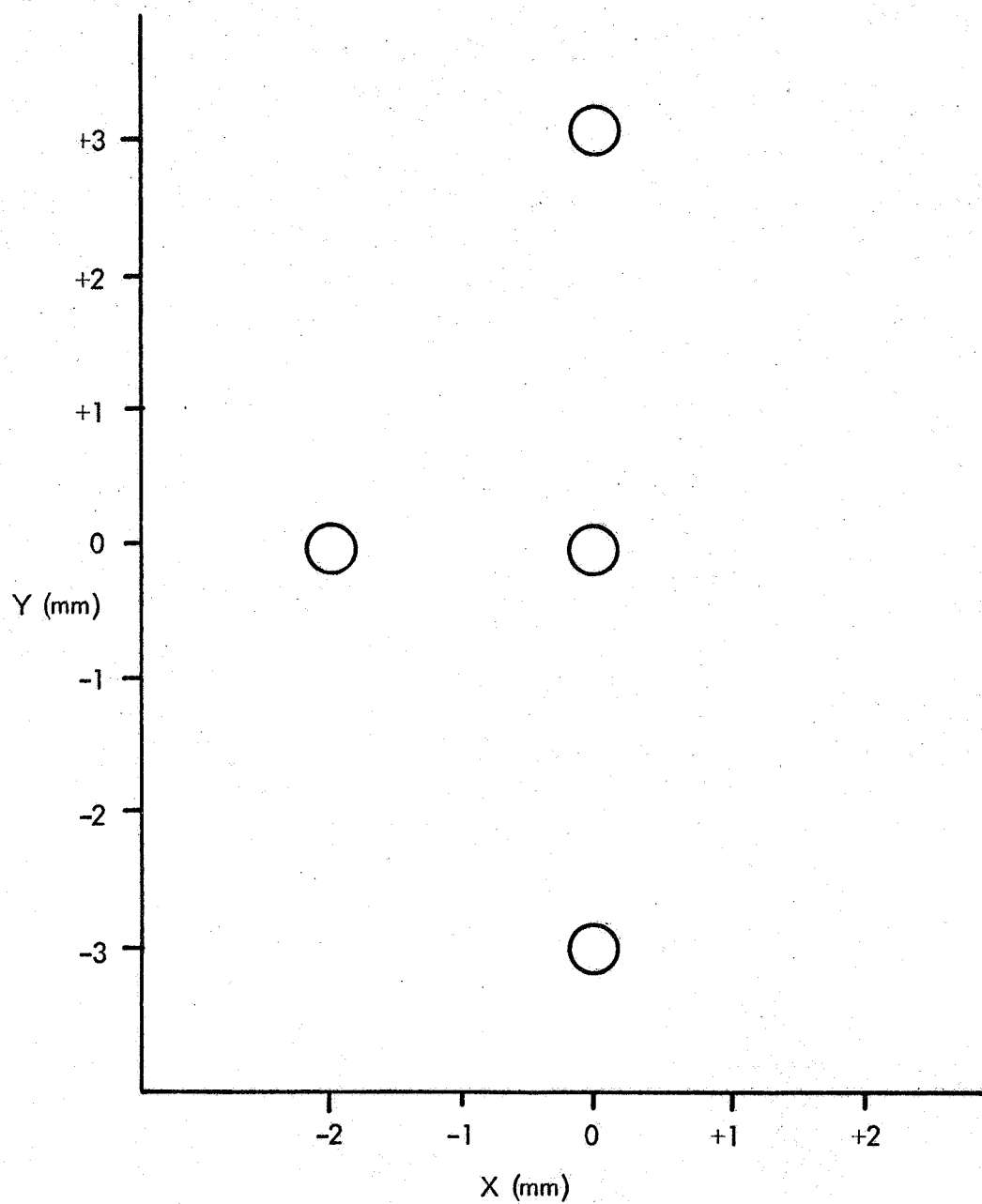
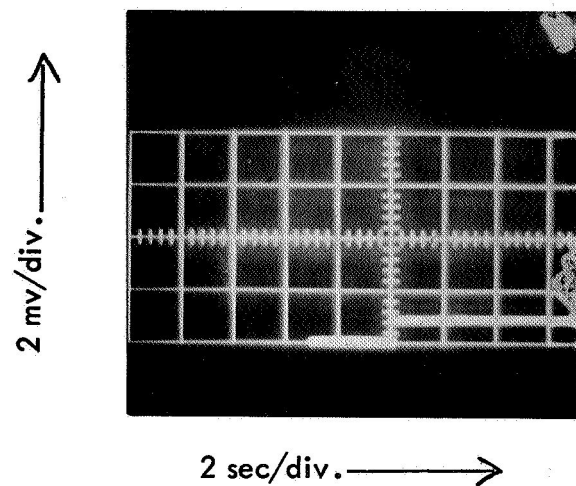
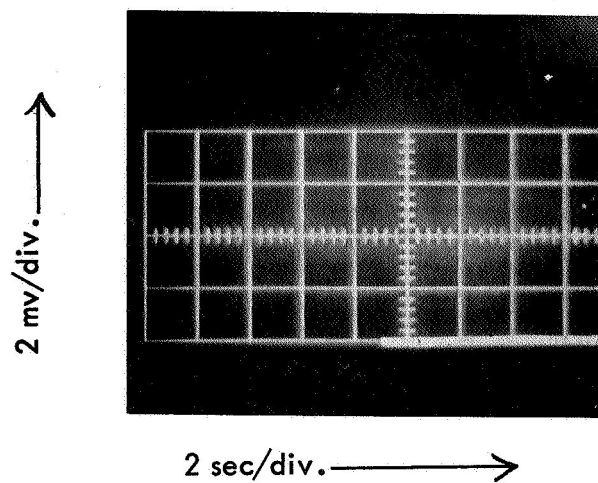


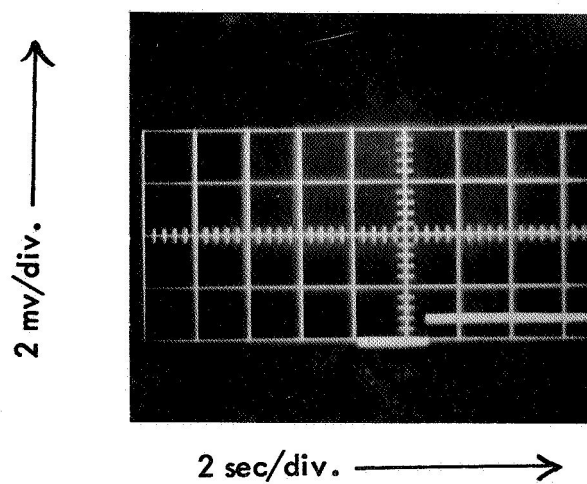
FIGURE 16. Aperture Pattern for Masks Used in Photovoltaic Studies.



(A)



(B)



(C)

FIGURE 17. Photovoltaic Outputs from Cell #A-C; Illumination of Non-Opposite Spots.

IV. Voltaic

cell (the difference between off and on being not observable in this photograph; that is, the signal is too weak to be seen). Figure 17C results from simultaneous irradiation of both sides, with these two beams. With non-coincident radiation the photovoltaic effect is merely additive. The change between off and on in Figure 17C is roughly the same as the sum of the changes in Cases A and B.

Figures 18A, 18B, and 18C are a similar set, except that the two beams were opposite each other, through the middle hole. Presence of an enhancement effect when the beams are in coincidence is obvious. Figure 18A is for irradiation through the middle hole on the indium side. Figure 18B is for irradiation through the middle hole on the glass side. Figure 18C results from radiation passing through both holes together. The respective photovoltaic outputs measured with only the megohm internal resistance from a Tektronix No. 536 oscilloscope placed directly across the CdS cell, with no battery or other circuit components, were $\approx 400 \mu v$ for the In electrode side, $\approx 100 \mu v$ for the glass electrode side, and $3200 \mu v$ for dual coincident illumination. This yields $M_{\text{static}} \approx 8$. It may be noted that at this degree of amplification no noise is observable in the photographs, with the broad band amplifier being used.

The next sections explore the time constants of the new effect more closely.

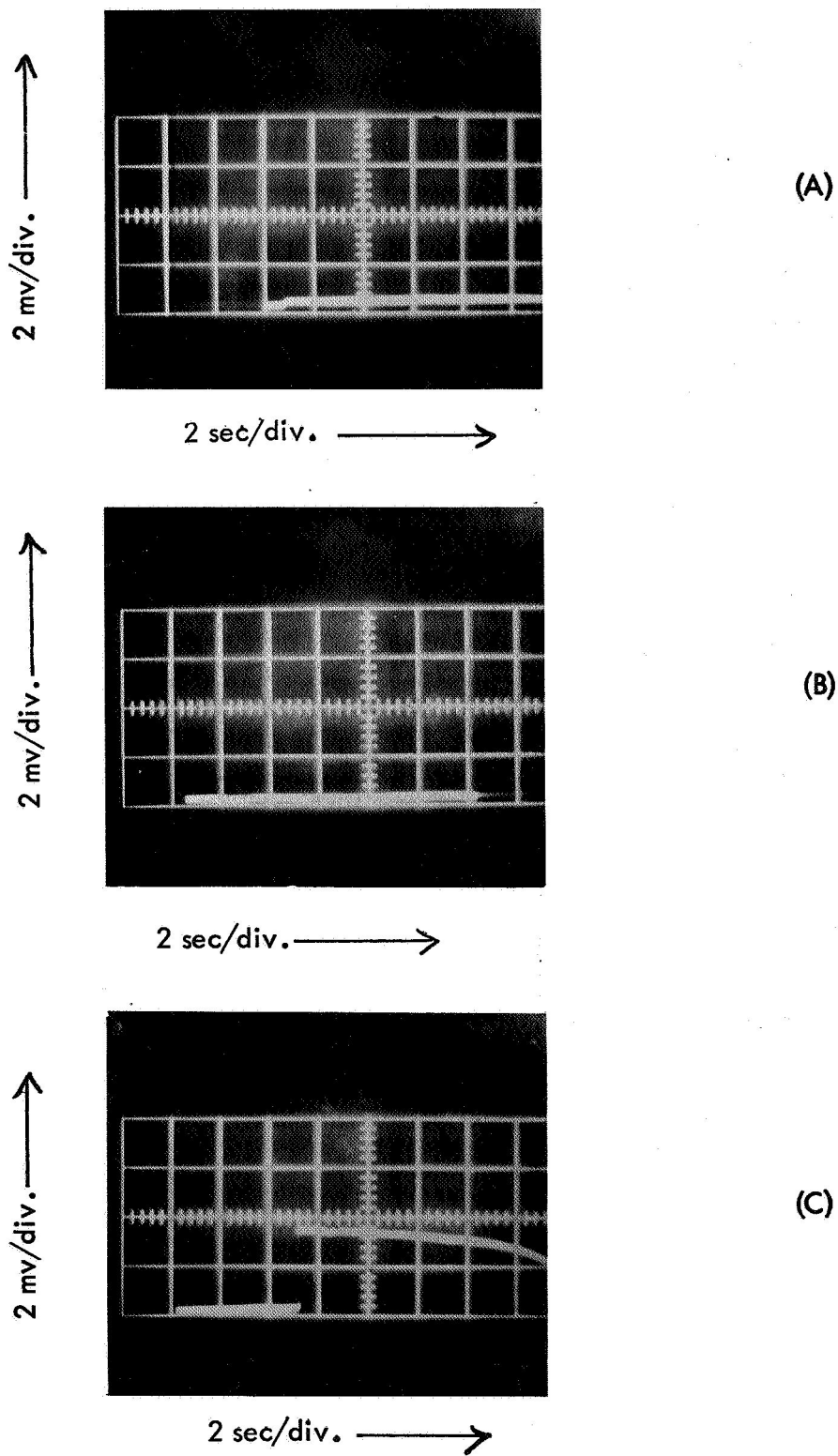


FIGURE 18. Photovoltaic Outputs From Cell #A-D; Illumination of Opposite Spots.

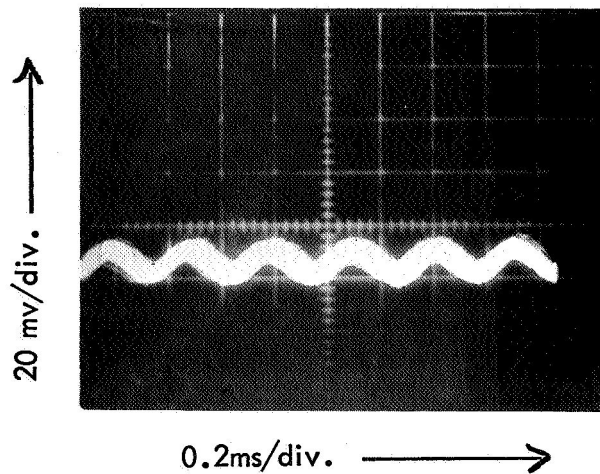
IV. Voltaic2. Chopper wheel experiments on A-type CdS cells

A dual wheel chopper was installed, so that the beam on each side of the cell was interrupted at 3240 cycles/sec in a more or less square wave pattern. The purpose of this preliminary test was simply to show that enhancement in a circuit without a battery could actually be observed at this chopping speed. No $M > 1$ had ever been seen in the photoconductive mode with fast chopping.

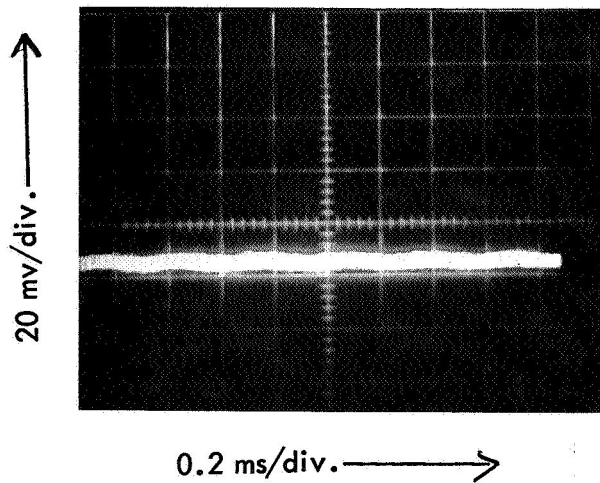
Figure 19A shows the result of 3240 cps chopping of a blue-green beam falling on one side of the cell alone. Figure 19B shows the result of a similar green beam falling on the other side of the cell alone. Combined illumination on opposite spots of the cell produced the result displayed in Figure 19C where the presence of an M value greater than unity is very evident.

The cell used for this experiment was cell # A-C. The illuminated holes on each face were of 0.4 mm diameter. The cell was enclosed in an aluminum housing, except for the exposed holes, in order to shield against local electronic noise picked up in the laboratory room. The Type D very broad-band amplifier plug-in unit was used in the Tektronix No. 536 oscilloscope chassis. Noise from the cell is again negligible at this amplification.

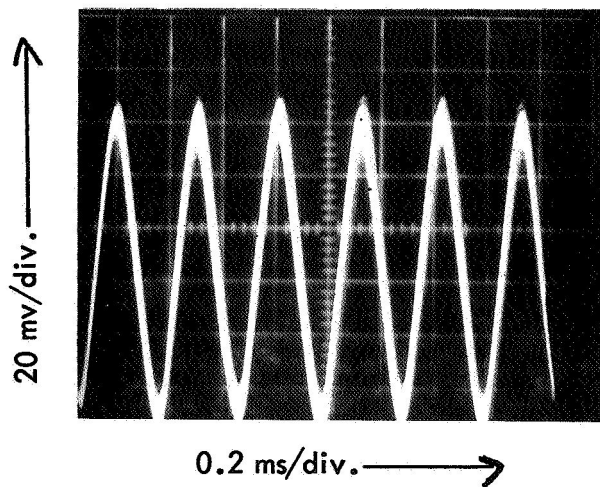
One cannot really calculate a meaningful value of M from these experiments, since the shapes of the curves at this fairly high speed of 3240 cps do not exactly follow the shape of the time intensity pattern for the light passing the two chopping wheels. Subsequent experiments will indicate that at this chopping speed the cell surely cannot reach



(A) Side 1 Illuminated



(B) Side 2 Illuminated



(C) Both Sides Illuminated

FIGURE 19. Chopper Wheel Photovoltaic Experiments; 3240 cps

IV. Voltaic

steady state during each exposure interval. The somewhat sawtooth, or somewhat sinusoidal, curves shown in these pictures probably represent only the first segments of approximately exponential rise and decay curves.

Somewhat faster effects are investigated in the next section, with the aid of a high speed camera shutter.

3. Fast-shutter photovoltaic experiments

In this experiment with cell # A-D, a "Graflex 1000" shutter was used to turn on a 5050Å beam to a 50μ spot on the glass electrode face, very abruptly. An opposite spot had steady illumination with green light. It was not practical under the circumstances to calibrate the shutter precisely, since the clover leaf pattern of the blades of the shutter opened in such a fashion that the rise time for the light intensity passing through depended very sensitively on the exact point within the shutter aperture at which the beam was focussed. However, it is probable that the rise time of the light pattern put on the cell was in the neighborhood of 20μsec.

Figure 20 shows very dramatically that there are two phases to the photovoltaic enhancement effect with green-green illumination of 50μ spots on cell # A-D. A fast initial phase, whose rise time as shown in Figure 20 is of the order of 0.1 ms, is followed by a relatively slow retreat (the shutter still being open) which appears to require several milliseconds before it would reach steady-state under constant illumination. In Figure 20 the shutter, which was only open for about 1 ms, closed before the photovoltage reached

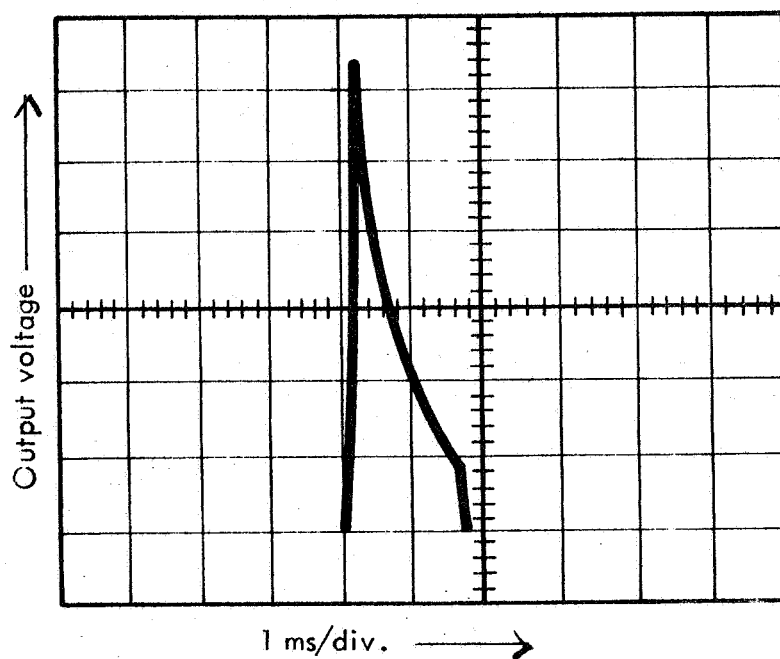


FIGURE 20. Tracing from Photograph of Oscilloscope Face, Showing Photo-response of Cell #A-D for Fast Shutter Beam Chopping.

IV. Voltaic

its steady-state value for constant illumination.* It is apparent that the phenomena of Figure 18 had been demonstrating an enhancement factor $M > 1$ for the slow or equilibrium photovoltaic effect. Whereas, the chopping at 3240 cps displayed in Figure 19 was demonstrating $M > 1$ in the fast photovoltaic effect.

Exploration into the nature of these two new phenomenon has not yet been undertaken. However, in the next section a few chopper wheel experiments at varying speeds are mentioned, which trace the transition from the slow to the fast phenomenon.

4. Effect of chopping frequency on photovoltaic response

A chopper wheel capable of interrupting the beam to a 0.4 mm diameter central spot on the indium electrode face of the cell at any of three frequencies was installed. The intensity pattern passed by this chopper was approximately square wave. Cell #A-D was used for this experiment.

Figure 21A shows the result of chopping at 90 cycles per second, Figure 21B at 560 cycles per second, and Figure 21C at 3240 cps. The chopped beam was light at 4890Å obtained from a monochromator, and the steady beam on an opposite spot of the conducting glass electrode face of the cell was white light. Measurements with the calibrated thermopile discussed in Section IIIA.2 gave 3×10^{-9} watts delivered to the illuminated spot by the chopped beam, and 2.4×10^{-5} watts delivered similarly by the steady beam. Both the

* Figure 18C seems to show yet another feature of the time behavior of photovoltaic enhancement with A-type cells - a slow fall off stretching over at least 10 sec. This matter has not yet been pursued further.

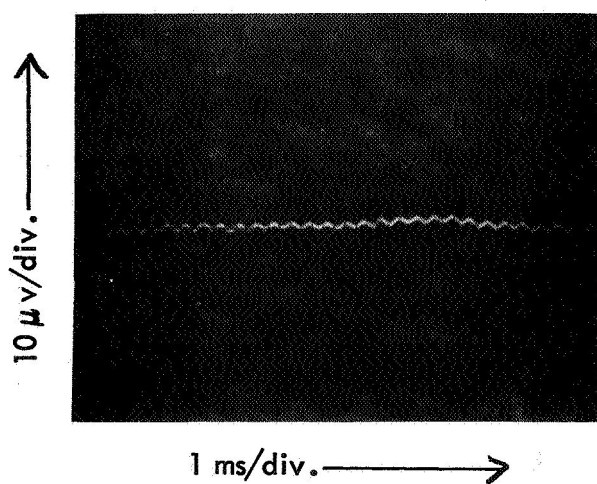
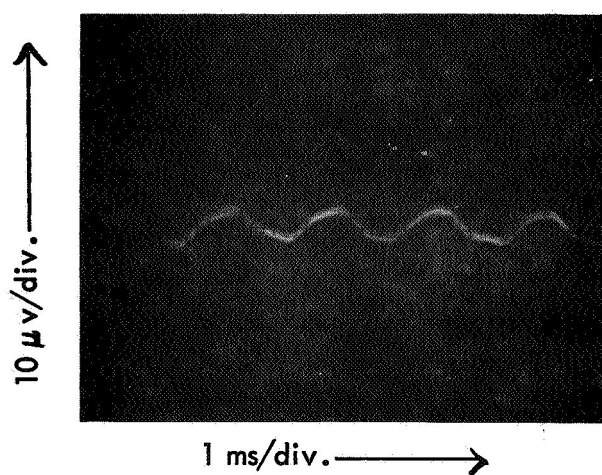
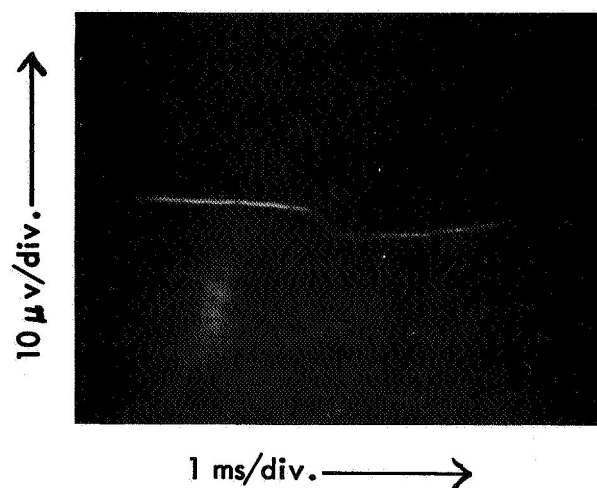


FIGURE 21. Photoresponse at Various Chopping Frequencies.

IV. Voltaic

the beam intensity and the circuit amplification are the same for the three curves in Figure 21. The relative amplitudes are thus a measure of the variation of cell response with chopping frequency, under these conditions. The sensitivity holds about constant as high as 560 cps but has begun to fall off by 3240 cps.

From the foregoing experiments, it seems probable that these three photographs illustrate the transition between the slow and the fast photovoltaic enhancement phenomena. The 90 cps picture doubtless shows mostly the slow phenomenon, the 560 cps must be a mixture, and the 3240 cps must be largely concerned with the fast photovoltaic effect.

The Type 1A7A plug-in solid-state amplifying circuit was used with the Tektronix No. 536 oscilloscope for the production of these records. This amplifier contained a bandpass feature, which limited the frequencies displayed on the scope to the range between approximately 100 cps and 3000 cps. This means that in Figure 21C the high frequency components greatly above 3000 cps which might have shown spikes at the beginning of each wave crest (in the manner of Figure 20) would not have been recorded.

Although Figures 21A to C thus probably represent a mixture of two phenomena occurring within the CdS, they would illustrate in a composite way the practical response of the photovoltaic enhancement effect to irradiation with a light beam of complex time-intensity patterns. A later experiment, to be described in Section VI.C, showed by a voice modulation arrangement that the response to a complex pattern does stretch over a frequency band of several thousand cps.

Similar photovoltaic research was also carried out on the same cell of the B-type which had shown photoconductive enhancement, as will be described in the next section.

IV B. Photovoltaic Enhancement with B-Type CdS Cells

The photovoltaic output at the good spot on cell # B-376-50 was not as large as with the A-type cells. However, using white light on one side and blue (4590\AA) light on the other side, enhancement factors of $M \approx 2$ were obtained.

The response with chopped light was explored at 560 and 3240 cps. The sensitivity fell off at the higher chopping frequency to a greater degree than with the A cell.

It is of interest to note that in contrast to the A-type cells, the wavelength dependence for these chopped photovoltaic experiments was quite sharp. Using white light on one side, and varying the other wavelength with a monochromator, the enhancement which was at a maximum at the 4590\AA monochromator setting fell off almost to unity at no more than 50\AA change of the setting on either side. With a narrower monochromator slit this resonance might have been even sharper.

It therefore seems possible that the B-type cell might be developed for various special applications which depend on close wavelength discrimination, as well as on the spatial feature of the enhancement phenomenon.

IV C. Photovoltaic Tests with Ge

Results were negative in a search for photovoltaic enhancement in the infrared with the Ge disks.

V. A NEW PHENOMENON IN GERMANIUM: "DE-ENHANCEMENT"

As has now been discussed, the efforts to find a photoconductive or photovoltaic enhancement phenomenon in single crystal disks of germanium gave negative results. Efforts to prepare translucent electrodes such that the over-all cell resistance would be comparable to the known volume resistance of the Ge itself, also were not very successful.

However, it turned out that low-resistance translucent electrodes do not have to be achieved in order to have a useful infrared enhancement phenomenon with Ge. The so-called "de-enhancement" effect was discovered. This involved resistance changes of hundreds of ohms under fairly strong illumination, and it could be observed satisfactorily with high resistance electrodes. The phenomenon must involve the electrode - Ge interface, rather than being mainly a volume effect characteristic of pure Ge. For lack of understanding at this date of the physical processes involved, the new behavior in Ge has been provisionally labelled "de-enhancement." It consists of the occurrence of M values markedly less than unity, for opposite illuminated spots.

This has some of the aspects of a saturation or quenching phenomenon. It is most pronounced at quite high light intensities. Since the effect was recognized late in the course of the contract, experiments so far have been of a rather preliminary character.

V. Germanium

The first series of tests is most easily described in terms of a set of numbered cases, as follows.

Case 1:

Continuous-spectrum, unfiltered radiation from a 1000° C blackbody source, chopped at 90 cycles/sec, was applied to a 3 mm diameter spot on a 1 cm diameter Ge disk 1 mm thick. The Ge surfaces were in as-received condition (doubtless more or less oxide coated), and were pressed against conducting glass electrodes. The resulting photoconductive current, as measured in terms of the voltage drop across a load by an amplifying AC microvoltmeter tuned to 90 cycles/sec, could then be made to decrease as much as 15 % by shining a similar beam, but unchopped, on an opposing spot on the other side of the Ge disk.

Case 2:

A similar experiment was carried out with a nominally 0.1 mm Ge disk (identified as # Ge 41, which had its 100 crystal face parallel to the disk face). The surfaces of the disk were cleaned with an etchant solution consisting of hydrofluoric, nitric, and acetic acids, and were pressed against gold screen electrodes. The gold screen, of 200 holes per linear inch and 36 % quoted transparency, was obtained from Ladd Industries, Burlington, Vermont. After the etching, the Ge thickness was probably closeto 50 μ .

V. Germanium

Both light beams were obtained from quartz-bromine tungsten filament lamps, illuminating spots on the Ge of about 2 mm diameter. The beam chopped at 90 cycles/sec was transmitted through an interference filter with about 100 Å bandpass centered at 1.4 μ . The steady beam was unfiltered white light. The apparent resistance of the cell, although somewhat fluctuating, was always about 1000 ohms; the series load resistance was maintained at about the same value as the cell; and the battery voltage in the circuit was 1 volt. With no illumination, the noise reading of the tuned microvoltmeter across the load was 5 μ v. With the steady white light beam turned on alone, the reading was approximately the same since the tuned microvoltmeter records principally AC signals.

The 1.4 μ chopped beam alone produced a reading of 1500 μ v, but the output signal dropped to 650 μ v when the collinear white beam was added on the opposite side.* This 850 μ v change constitutes a decrease of 57 %.

Case 3:

Conditions as in Case 2, but with the beam intensities reduced so that the chopped 1.4 μ light alone gave a 110 μ v signal, still well above the 5 μ v noise. Turning

* A similar phenomenon, but of much less magnitude, was observed when the steady collinear beam also contained a 100 Å bandpass filter centered at any one of a number of wavelengths between 1.0 μ and 2.0 μ .

V. Germanium

on the collinear white light beam dropped the output signal to $10\mu\text{v}$. The $100\mu\text{v}$ change constitutes a decrease of 90%.

Case 4:

To check that the phenomenon was a spatially sensitive effect in the same sense as with CdS, light spots of only about 0.3 mm diameter were used. One side of the 0.1 mm Ge disk (with all other conditions as in Case 2) was covered with a mask having a hole in the middle of the disk. The mask on the other side of the Ge had one hole in the middle and also one offset hole, with 4 mm between the hole centers.

With dark currents giving 5 - $10\mu\text{v}$ readings, the 1.4μ chopped beam reading of $800\mu\text{v}$ dropped to $500\mu\text{v}$ when the steady white beam was incident on the Ge in the collinear configuration, this being a 37% decrease. The corresponding readings were $1400\mu\text{v}$ and $1300\mu\text{v}$ when the two beams were offset; which is only a 7% decrease. The spatial dependence is therefore clear, though not so sharp as found with the smallest spots on CdS.

Case 5:

The cell assembly as in Case 4, with its battery connections intact, was rotated on the optical bench through 180° about an axis normal to the light beams. Both the collinear de-enhancement effect itself, and the spatial sensitivity of the phenomenon,

V.. Germanium

were now found to be very much less pronounced. The investigation did not determine whether this is due to the sides of the Ge which receive the chopped infrared light and the steady white light, respectively, having been reversed in battery polarity or their having been reversed in regard to some feature of the Ge surfaces.

Case 6:

It is not really necessary to have a steady light on one side of the Ge disk. Possibly, the only real requirement may be that at least one of the beams be rather bright, so as to be able to produce appreciable quenching or saturation. Table III presents data with an etched, but not In-plated, 1 mm Ge disk pressure-contacted by copper screen electrodes (160 holes per linear inch, 15 % transmission), which was illuminated with narrow-band 90 cycles/sec chopped collinear light beams of equal intensity from both sides. The dark current noise signal was about $0.8 \mu\text{v}$. It is apparent that the de-enhancement phenomenon can thus be observed when two in-phase chopped infrared beams are used.

Case 7:

It does not seem that this apparently surface-controlled phenomenon is necessarily favored by using low-resistance contacts to the Ge. All the data listed so far were taken with high resistance electrode contacts. But experiments were also done with carefully In-plated 1 mm thick disk Ge-2 (crystal face 100 parallel to the disk face), whose apparent resistance was only about 100 ohms. Tests were

TABLE III
 "DE-ENHANCEMENT" IN GERMANIUM WITH TWO CHOPPED BEAMS

Mean λ of Each Beam	Signal Due to Left Beam Alone	Signal Due to Right Beam Alone	Signal Due to Both Beams Together	M
1.9 μ	48 μ v	25 μ v	64 μ v	0.88
1.8"	135"	70"	175"	0.85
1.7"	157"	92"	187"	0.75
1.6"	190"	126"	210"	0.66
1.5"	200"	135"	215"	0.64
1.4"	220"	182"	225"	0.56

V. Germanium

carried out at numerous different light levels and wavelength combinations, using either 90 or 3240 cycles/sec chopping of one or both collinear beams, and with varying pressures against the gold screen electrodes. Rather qualitative measurements produced the general impression that conditions can sometimes make M as small as about 0.85, but that values very close to unity are more usual with these low resistance electrodes.

Subsequent experiments were chiefly aimed at more careful delineation of the spatial dependence of the "de-enhancement" effect. Disk #Ge-41, nominally 0.1 mm thick, had surfaces cleaned and etched and pressure-contacted with gold screen electrodes. One side was illuminated with white light, and the other with infrared at 1.4μ which passed through an interference filter having about 100Å bandpass. Both beams were chopped at 540 cycles/sec. A selectively amplifying microvoltmeter tuned to the chopping frequency read the drops across a load of about 1000 ohms. The dark-current noise seen by the tuned microvoltmeter was always less than $1\mu\text{v}$.

The two faces of the Ge were covered with Al masks having opposing central holes of 0.79 mm diameter. In addition, one of the masks had an offset hole of the same size with 3.18 mm between hole centers; i.e., with three hole-diameters between the edges of the holes.

Table IV shows the voltage drops across the load due to photocurrents when first opposite spots and then non-opposite spots were illuminated at various light levels.

TABLE IV
DETERIORATING "DE-ENHANCEMENT" IN Ge WITH LARGE (0.79mm) SPOTS

Illuminating Opposite Spots		Illuminating Non-Opposite Spots**		
1.4 μ on Side 1 alone	Both Sides Illum.	Decrease due to Illum. Side 2	1.4 μ on Side 1 alone	Both Sides Illum. Decrease due to Illum. Side 2
34 μ v	14 μ v	59%	105 μ v	78 μ v 26%
140 μ v	80 μ v	43%	270 μ v	200 μ v 26%*
160 μ v	155 μ v	3%*	500 μ v	420 μ v 16%*

** Spots 3 diameters apart; disk #Ge-41, 0.1mm thick with pressure contacted gold screen electrodes.

* High apparent cell resistance measured after these readings

V.. Germanium

Although "de-enhancement" was observed in every case, the spatial coincidence effect is much less pronounced with these large 0.79 mm illuminated spots than with the 0.3 mm spots reported as Case 4 above, with the same 0.1 mm thick Ge cell.

The probable requirement that the illuminated spots be quite small in order to produce strong spatial discrimination, as has also been found in the CdS work, is not necessarily a disadvantage for most practical applications. The usual need for high resolving power will lead to the employment of very small spots in most types of apparatus.

The last readings made on this cell showed much less "de-enhancement" than previously. Perhaps this may be due to variable electrode contact pressure, or to oxidation of the Ge surfaces, since the cell was found to have developed a high apparent resistance at the end of these runs.

Only a beginning has yet been made in studying these phenomena, but it would seem that application of Ge de-enhancement in the near infrared could be just as practical as applications of CdS enhancement in the visible -- although at generally higher light intensities.

Time response measurements have not yet been made on the Ge behavior. However, much faster response than is possible with CdS should become available, if the de-enhancement phenomenon has the same fast response as the usual photoconductive effect in Ge, which lies in the microsecond range.

VI. EXPERIMENTS RELATING TO APPLICATIONS

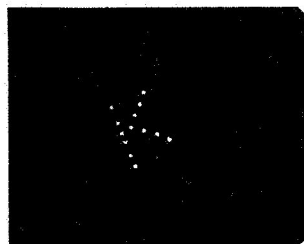
The preceding sections have dealt with research on the various physical properties and macroscopic parameters involved in the behavior of the different types of cells. Short descriptions will now be given of the operational behavior of some A-type cells in three simple breadboard arrangements, to illustrate some of the possible applications. These are a low light level TV camera, an automatic beam tracker, and a voice-modulated communications beam. Following these, a short summary is presented as to the degree of evaluation of applications which is now possible as a result of all the experiments to date. Further discussion on many potential applications for the various enhancement effects may be found in Appendix C.

A. Photoconductive Enhancement TV Camera Breadboard

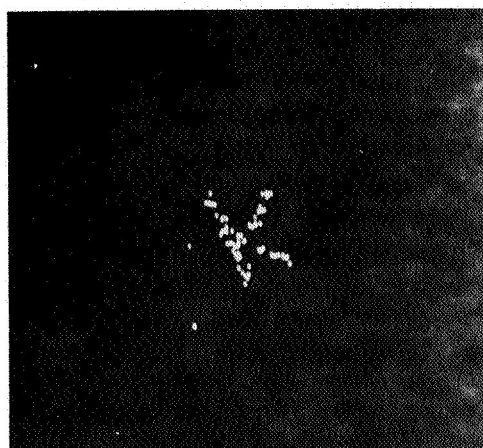
A low light level TV camera breadboard arrangement was constructed, using the image sensor capability of an A-type photoconductive cell. Scanning (readout) is accomplished with a light beam on the other side of the cell, instead of the electron beam used in ordinary TV cameras.

The object to be viewed was a piece of black paper containing needle-pricked holes in the pattern of the letter K (for Kearfott Group of General Precision Systems Inc), as shown in Figure 22A. A field lens formed an image of this object (backlighting with green light) on one face of one of cell # A-D, covering an area of about 1 cm². The image on the CdS of the K pattern was receiving a total of about 1 μ watt of green light.

A small spot of green light was swept repeatedly, but rather slowly, over the other face of the CdS layer in a raster pattern. Whenever the illuminated spots on the two sides of the CdS were opposite one another, an electrical pulse significantly exceeding the noise level was produced in the output leads. Each vertical line of the raster pattern was traversed in 0.2 sec, and the entire pattern was covered in 4 sec.



(A)



(B)

FIGURE 22. First demonstration of the use of the CdS enhancement effect as a low light level TV camera. (A) is the object pattern being viewed; (B) is the televised image as displayed on an oscilloscope.

VI A. Camera

The output from the CdS was amplified and caused to modulate the electron beam and so to vary the brightness of the phosphor spot on an oscilloscope screen — when this spot was being made to execute the same raster pattern which had been used to scan the CdS. Figure 22B is a Polaroid photograph of the face of the output CRT which shows the clearly visible K pattern. Other types of output display devices, such as an electroluminescent panel array, could have been used if desired. Alternatively, the electrical output from the CdS could be stored on tape if immediate viewing was not needed.

Various types of light beam scanning arrangements could have been used to cause a spot to execute the read-out raster pattern on the second face of the CdS layer. The one found most convenient for this crude breadboard assembly was to use an oscilloscope, to cause the phosphor spot on its screen to execute the desired raster pattern, and then to image this moving green spot on the second face of the CdS with a lens. Figure 23 is a schematic of the optical parts of the camera breadboard, showing this method of scanning the read-out beam.

Figure 24 is a block diagram of the electronic equipment used. The rectangular electrical scanning raster pattern was generated by combining the internal horizontal sweep of the Tektronix No. 536 with a vertical sweep obtained from a Hewlett-Packard No. 202-A sine wave generator. Since real-time viewing was desired, these same raster voltages were fed synchronously to the output image CRT.

Figure 22B is actually a time exposure of repeated scans with the equipment used in this manner, which shows the repeatability, uniformity, and low degree of electronic and optical noise obtainable with cell # A-D and off-the-shelf components. The area being scanned was approximately 1 cm^2 . This evidence reinforces the tentative conclusion mentioned previously, that noise arising from nonuniformity of cell properties over the face area would not be excessive for at least some kinds of applications.

Phosphor Spot on Face of Scanning
CRT, Executing a Raster Pattern

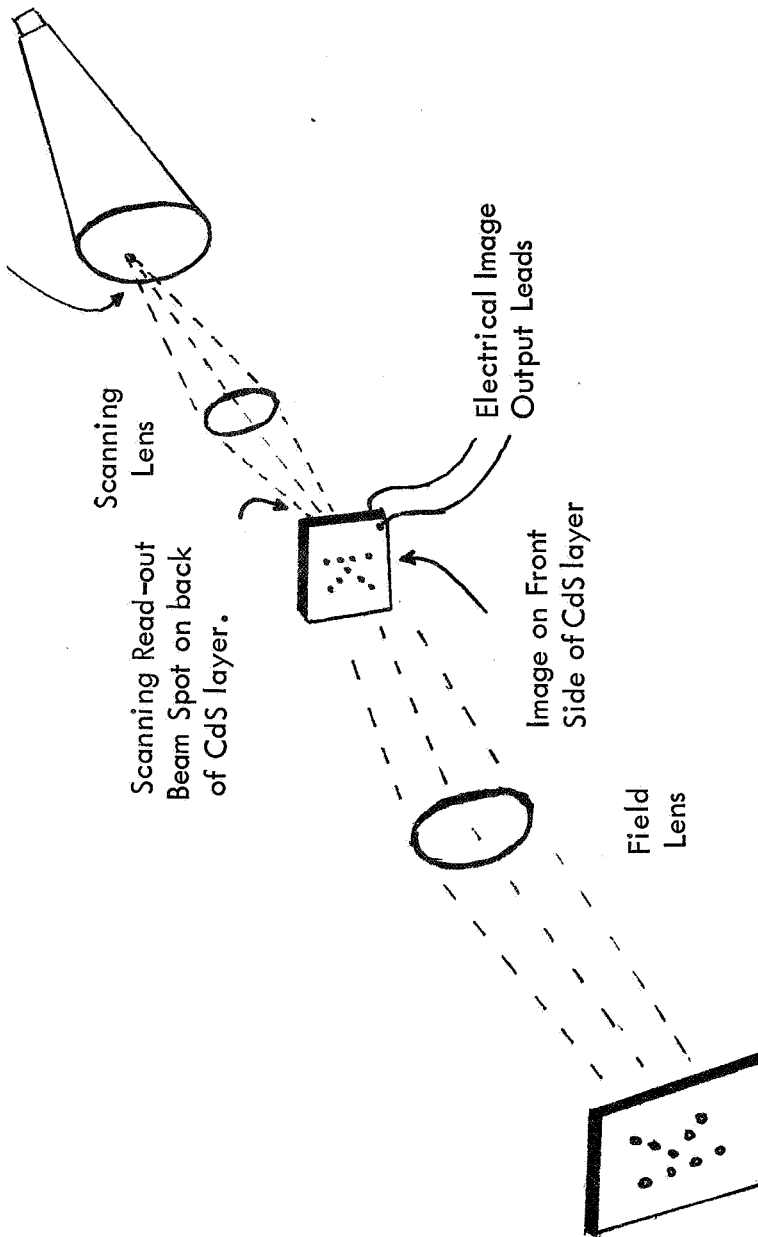


FIGURE 23 --- Schematic of Optical Parts for a Low Light Level
Camera Based on the Photoenhancement Phenomenon in a CdS
Layer, Using a CRT for Read-out Beam Scanning

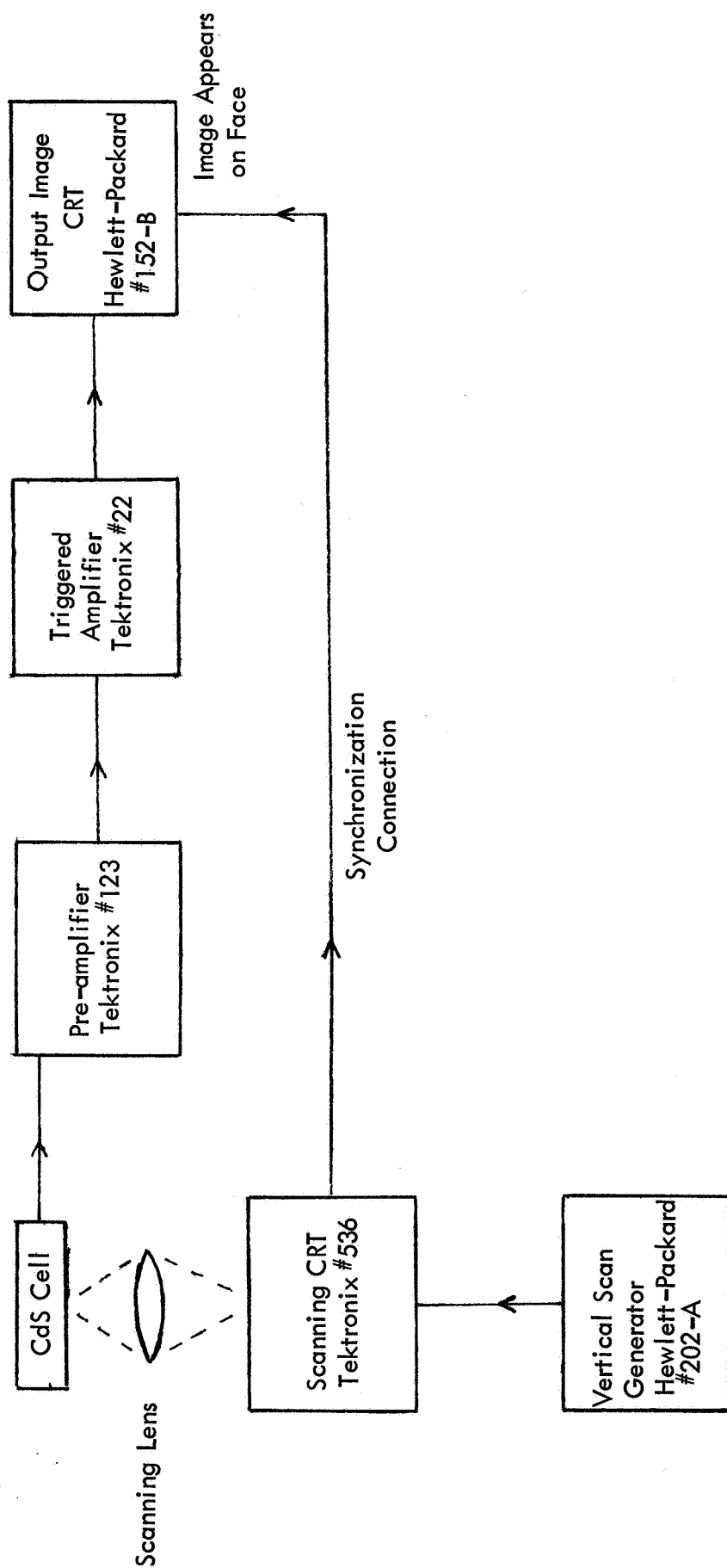


FIGURE 24 -- Block Diagram of Electrical System for Low Light Level Photoenhancement Camera

VI A. Camera

It would have been very interesting to have used this arrangement with infrared light instead of green light, in view of the present strong need for improvement in TV camera IR technology. However, no infrared flying spot scanner system was immediately available at this laboratory.

Although such a simple breadboard arrangement successfully illustrates the desired principle, actual use of this principle would be limited to "slow television" applications. Discovery of the new and much faster photovoltaic enhancement phenomenon should permit applications to TV camera situations at much higher scanning speeds, although not quite as low light levels.

In the next subsection the construction and tests of a beam tracker assembly will be mentioned only briefly, since it was described at some length in Ref. 11.

VI B. Beam Tracker Breadboard Assembly

The breadboard beam tracker device demonstrated the capability to align automatically two light beams which illuminated opposite sides of the photoconductor cell.

Full details of the construction are to be found in Ref. II. Cell # A-D was used. The signal beam source was mounted on a carriage driven by a manually operated screw, permitting translation in the direction perpendicular to the beam axis. The local beam source and the photocell were mounted on a similar carriage to which a servo drive was applied. The photoconductor provided an error signal, enabling its servo to drive to a null position as it tracked the signal beam.

After a number of tests it was concluded that at the maximum tracking speed feasible with the equipment as built, the maximum allowable velocity of the signal beam image on the cell face was 0.02 cm/sec. Since the focal length of the imaging lens was 10 cm, this would correspond to an angular rate of 0.002 radians/sec if the signal source was moving across the sky. The signal beam intensity used with this assembly was measured with the calibrated thermopile as 4.5×10^{-9} watts. From a considerable number of test runs, the standard deviation of the null position of the follower for a given position of the master was found to be 0.07 mm, which would correspond to 0.7 milliradians. This is less than a usually practical angle for the divergence of a laser beam. It would therefore be possible to use this device, even as roughly assembled, to train or track a laser beacon.

VI C. A Voice-Modulated Photovoltaic Enhancement Experiment

One reason for interest in the photovoltaic enhancement effect is that its faster time response should give a considerably greater bandwidth for communications applications than the photoconductive arrangement. As a first exploration of the possibilities, a simple voice communication system was set up.

The experiment consisted of transmission of the human voice over a blue-green light beam, with the CdS photovoltaic enhancement phenomenon serving as the detector. One light beam was of constant intensity; the other was modulated by a piece of black paper (extending partially across the beam) which was fastened to the vibrating cone of a small loudspeaker driven by a microphone circuit. Partial interruptions of the beam produced a light intensity modulation pattern which more or less reproduced the sound waves.

With the two light spots in line on opposite sides of the cell, and each delivering about 5×10^{-8} watts to the CdS surface, the photovoltaic output was fed to a second loudspeaker through a broad-band amplifier. A person speaking into the microphone was clearly intelligible from the second loudspeaker, although the output tones seemed to be somewhat lacking in the higher harmonics. This could have been due to either a drop in sensitivity of the CdS cell at the higher frequencies, as implied by the previous chopper wheel experiments, or to a sluggishness in the simple paper arrangement for modulating the light beam.

Of course, if the enhancement phenomenon can thus be used in connection with voice transmission at near 10^{-8} watts of signal power, it probably follows that the simple waveforms of digital telemetering signals could be read at reasonable speed down to much lower signal/noise levels.

VI D. The Present Position On Applications

One of the major important features of the enhancement detector is its ability to cover a broad field of view without the use of any moving parts. However, this implies a successful scanning system for illuminating spots in sequence on the back side of the sensitive layer, without using any moving parts for this process. To date, such a scanning system has not been applied with any precision to the enhancement detector problem.

The pre-contract work mentioned in Appendix A.5 included some experimentation with an electroluminescent panel array as the source of a moving spot of light which could be focussed on the back of the CdS for scanning purposes. The TV camera breadboard assembly used the moving spot of the face of a cathode ray oscilloscope as a scanning device. Both of these systems certainly need improvement in resolution and reliability, beyond the preliminary arrangements tested so far. It would probably be highly desirable to paint a cathodoluminescent phosphor layer over one of the cell electrodes and then use this layer as the target inside a cathode ray tube. Presumably this would lead to scanning spots of the smallest possible size and highest intensity.

Insufficient data are available for deciding on the exact properties of an enhancement detector system as it might be used in any of the scanning-type applications. The degree of correlation which can be obtained between M_{static} and M_{dynamic} has not been explored, and the amount of material nonuniformity noise which can be expected over the extended area of a cell face has not been adequately studied. At the present time, therefore, any quantitative comparisons between enhancement detectors and conventional detectors for the same purpose must be confined to the non-scanning applications.

VI D. Applications

Today, we know that good resolution with an A-type cell can be obtained down to dimensions of 50μ , but we do not know how much smaller one can go without running into new noise problems. We know that the A-type CdS cells can be used with photoconductive arrangements in situations involving time responses in the milliseconds, and with photovoltaic arrangements for time responses around a tenth of a millisecond.

From the multiple spot experiments described in Appendix A.8 we know that today's A-type cells used in the photoconductive mode would give a considerable false alarm rate for pattern recognition applications involving two or three spots. We cannot be sure that the false alarm rate would be acceptably low with more complex patterns, using these existing cells. However, improvements in the cell uniformity which would help this problem are surely to be expected from a reasonable development effort.

It could be expected that large areas of uniform bulk material would become available if cells were made from single crystal CdS. However, one could not be definitely sure of low noise over a large cell face area even with such material. It may well be that extreme uniformity of the transparent electrodes, and of the bonding interfaces between the electrodes and the crystal, are of great importance for producing constant values of M over the cell.

The struggles to obtain good transparent electrodes on germanium, as described in Ref. III, and the variability of the electrodes noted with the first samples of the B-type CdS cell, indicate that obtaining suitable electrode uniformity is not easy — although it should surely become possible with enough development effort.

One may hope that time responses in the microseconds range may be available from the "de-enhancement" effect with germanium, but this has not yet been tested.

VI D. Applications

It thus appears that the only type of application for which information suffices today for an evaluation of the enhancement detector in competition with existing conventional detectors is for use with relatively slow intensity fluctuations of a very weak light, or with small position variations of a single signal spot. The most important use in this class would appear to be for tracking the beam from a very remote space vehicle. The sensitivity limit indicated by the experiment in Section III of 10^{-12} watts for such an application, could indeed be matched as a mere matter of signal reception by a vacuum photoemissive cell. However, the capability of the enhancement detector for tracking this signal to a small angular accuracy cannot be matched by any other detector without the use of complicated array connections, or else the use of very precise mechanical training components.

Thus, the most important application which can be validated today seems to be for tracking laser beacons at interplanetary distances. Numerous other applications will probably be seen to be competitive after the accumulation of more data, or after materials research which develops cells with a proven high degree of uniformity over an extended surface area. Appendix C discusses such possibilities.

VII. CONCLUDING SECTION

Five different kinds of materials have now been shown to display one or more of three different types of photoenhancement phenomena. Two of these effects, photovoltaic enhancement for visible light with polycrystalline CdS, and "de-enhancement" for near infrared light with single crystal Ge, were first discovered in the course of this contract and demonstrated to depend on spatial opposition of beams striking the two cell faces.

From this variety will follow many useful applications. Quantitative measurements have now established properties of one type of thin polycrystalline CdS cell which gives it a clear advantage over previous detectors for an important space mission: precision tracking of low-power laser beacons on vehicles at distances comparable to the Earth-Mars separation. This requires a received beam intensity of only 10^{-12} watts.

It has already been demonstrated that the human voice could be received intelligibly over such a closely tracked beam when an intensity of 5×10^{-8} watts was available. This limit, established with the same cell type in the photovoltaic mode of use, could probably be decreased by at least a factor of 10, even with the existing cell, by more sophisticated electronic arrangements.

The enhancement phenomena probably involve quite subtle properties of the interface between the basic photoconductive material and the translucent electrode applied to it. Producing reliable sandwich-type cells with closely uniform properties over extended areas of the cell faces remains a difficult and delicate art.

VII. Conclusions

Considerable further materials development would be necessary, to achieve volume production of enhancement cells sufficiently uniform to be used without individual tailoring, for the numerous possible camera and pattern-recognition applications.

CBE/DG: HJF
3-1540
8/31/68

AEROSPACE RESEARCH CENTER • GENERAL PRECISION SYSTEMS INC.

APPENDICES

APPENDIX A. INITIAL WORK WITH A-TYPE POLYCRYSTALLINE CdS CELLS

In the period before 15 October 1967, which was covered in detail by Refs. I-III, the largest fraction of the photoconductive work on A-type CdS cells was concerned with the effect of numerous parameters on M_{static} . Table A-I lists the parameters studied and the major results found.

In the following subsections, summaries of various features of this work are presented which chiefly represent new viewpoints, as a result of surveying the picture as a whole. The subsections cover these topics in the same order as listed in Table A-I; the first deals with the wavelength dependence of M , with a given A-type cell.

1. Variation of M with Beam Wavelengths.

Just a quotation of M values alone does not give an adequate picture of the wavelength dependence of the phenomenon. The most striking behavior is the extremely powerful enhancement effect which a weak red beam incident on a spot of the CdS layer can have, when an opposite spot on the other side is being more strongly illuminated with any of a considerable range of wavelengths. The general tendency with such a red "signal" beam can be stated as follows:

With any green or yellow light striking a spot on one side of the CdS layer, the addition of a much weaker red light on an opposite spot tends to raise the photocurrent towards the large value it would have shown if the strong light had also been red.

TABLE A-I
PARAMETERS EXPLORED FOR A-TYPE CELLS

<u>Parameter</u>	<u>Major Photoconductive Result</u>
1. Beam wavelengths	Strongly sensitive; red-green and green-green combinations give largest M values; red-red gives largest currents.
2. Cell polarity	Some cells strongly sensitive; no fixed polarity rule.
3. Cell voltage	Increasing voltage at constant light intensity increases output current, but decreases M.
4. Beam intensities	M usually goes through a maximum at some ratio of the two beam intensities.
5. Time response to light intensity variations	Rise and decay times in tenths of seconds; fastest whenever M is large; a certain amount of output follows light modulation pattern up to at least 400 cps..
6. Variation of illuminated area at constant incident power density	Output current proportional to received radiant power, except for smallest spots with short light wavelengths.
7. Variations in spot positions	Output current roughly proportional to projected overlap area of nearly-opposite spots. Variation of sensitivity by factor of 13 across one sample cell.
8. Multiple pairs of spots.	Currents not completely additive.
9. Angle of incidence of radiation.	Not sensitive, at least up to 27° .

A. A-Type

Of course, implied in this statement is the fact that under all circumstances (single-sided or dual illumination) the A-type cells give far more photocurrent per unit incident energy for red light than for any other color.* This property of the cell is illustrated by Figure A-1 for light of various wavelengths sent onto a spot on the glass-electrode side of cell

A-J702. .

Returning to the dual illumination case, the solid line in Figure A-2 is a repetition of the curve of Figure A-1 showing the effect of a fairly strong beam of variable wavelength incident on the glass-electrode face alone. But the dotted line above it shows the drastic output current increase from simultaneously adding a weak red (6550 Å) beam on the opposite spot of the indium-electrode face of the cell.

The intensity of the red light reaching the CdS was so small that by itself it gave only 3μ amp photocurrent. From the definition of M , as $I_{\text{(both sides)}}$ divided by the sum of the currents from single-sided illuminations, Figure A-2 implies a large value of M for a red-green combination and smaller M 's for red-red or red-blue. The resulting peak (at 5200 Å) in a graph of M vs. wavelength of the strong variable beam — for a constant weak red beam (6640 Å for this particular curve) on the opposite spot — is displayed by Figure A-3.

* This is a property of the dopant added to the CdS during cell manufacture. Very pure CdS is known to be most photoconductive with green light near 5200 Å.

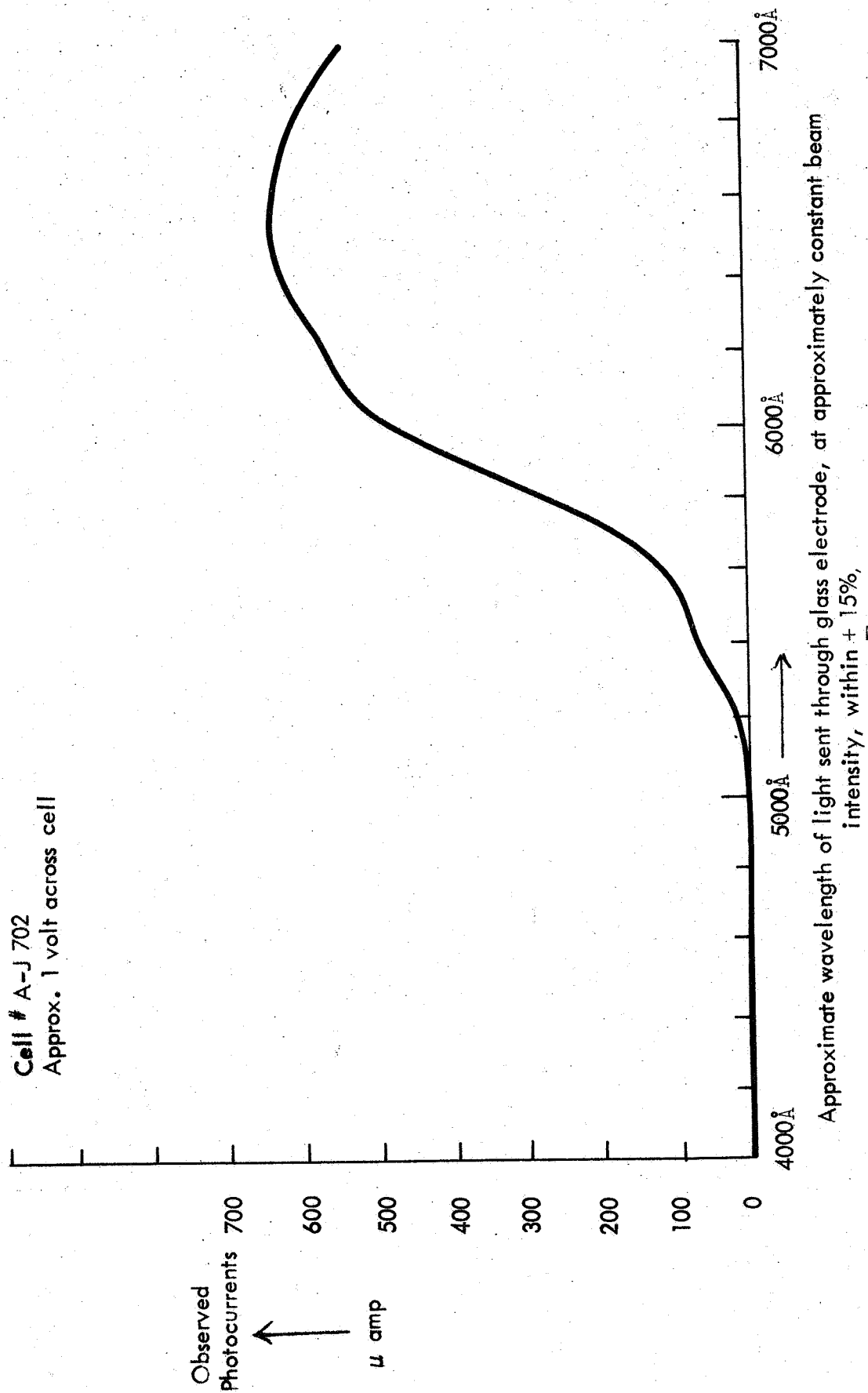


FIGURE A-1 - Wavelength Dependence of Single-Sided Response of A-Type Cell

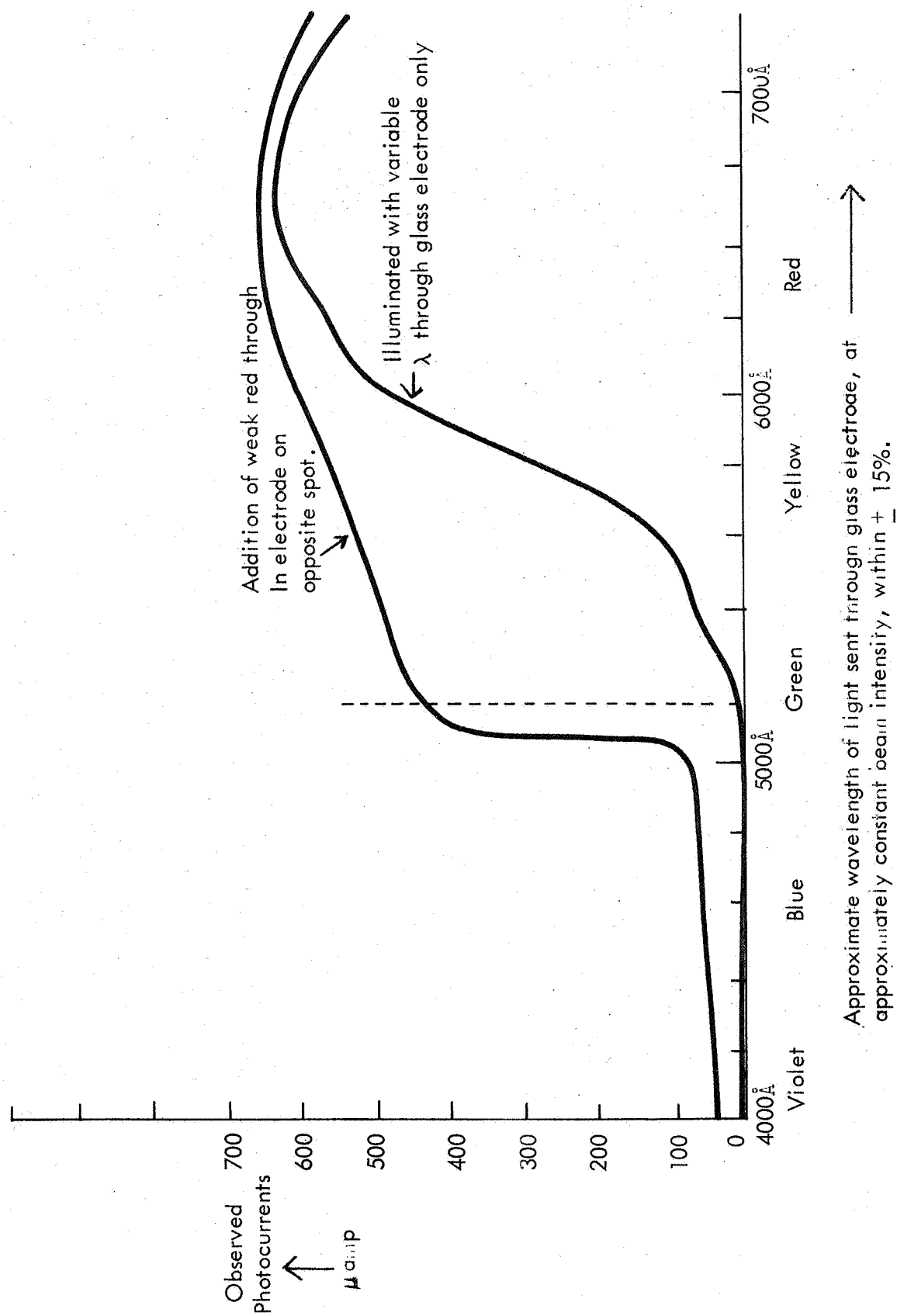
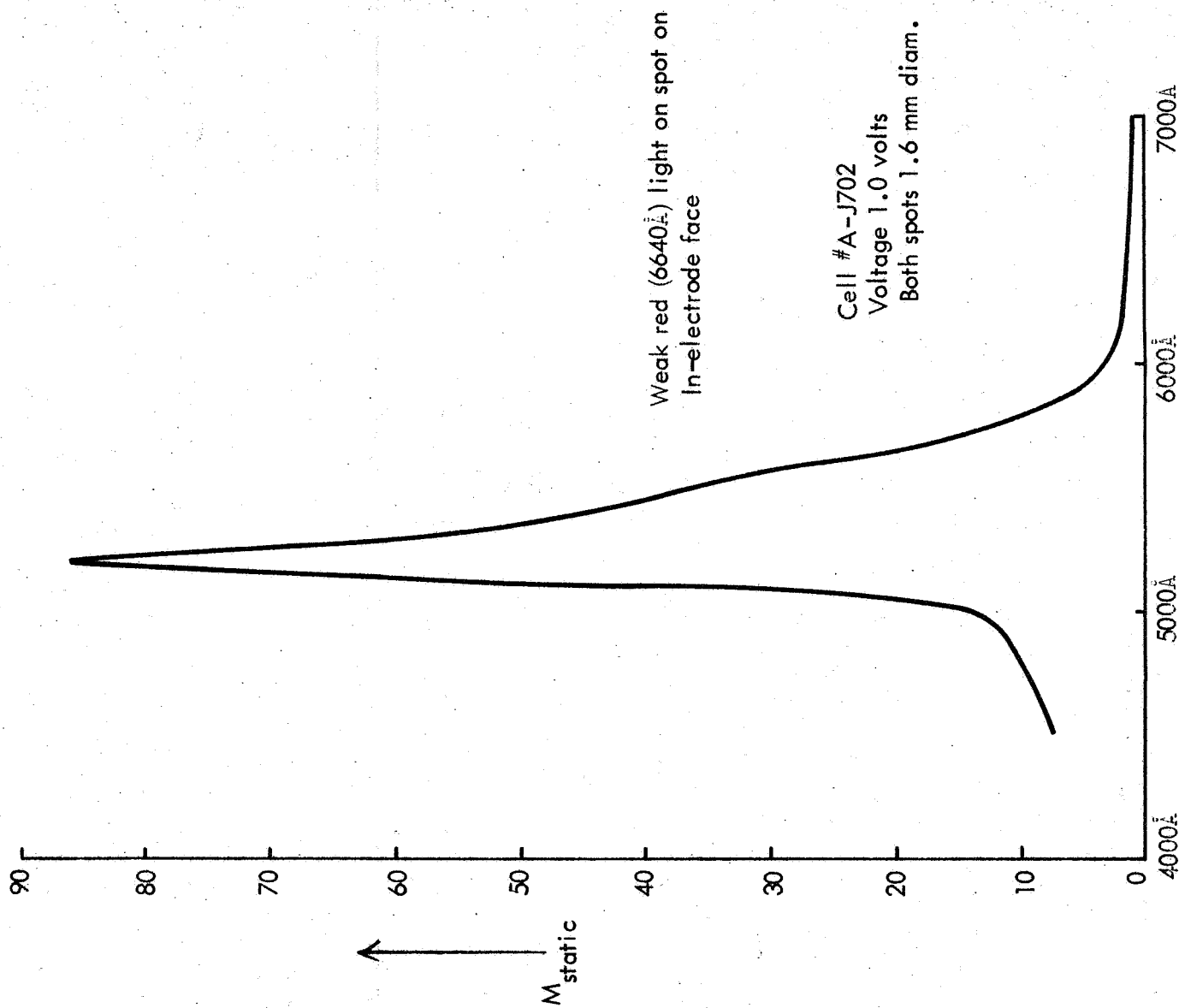


FIGURE A-2, Enhancement Effect of Weak Red Light Opposite Beam of Variable Wavelength



A. A-Type

These graphs have only illustrated the case which leads to the largest M value for the A-type cells — the red-green combination. However, if the weaker steady light on the In-electrode face was green, as the wavelength band on the glass electrode side was changed, somewhat similar curves would be found. Although the added green light does not have quite so strong an effect as the added red light, Figure A-4 shows that rather large M values can still result. This is particularly true for a green-green combination with both beams near 5200 Å.

Figure A-4 also shows the case of a blue signal light. Enhancement does result throughout the spectrum, but for such a combination as blue-violet illumination the photocurrents are small, as compared to any case involving even a small amount of red light.

Further details of these experiments are given in Ref. 1. The next subsection deals with the effect of the direction of the electric field acting upon the CdS.

2. Effect of Reversing Cell Polarity.

Reversing the battery terminals, without any other change, usually changes the photocurrent outputs and the value of M . No definite rule can be stated as to which polarity will give the best results. The cells all seem to be different in this respect.

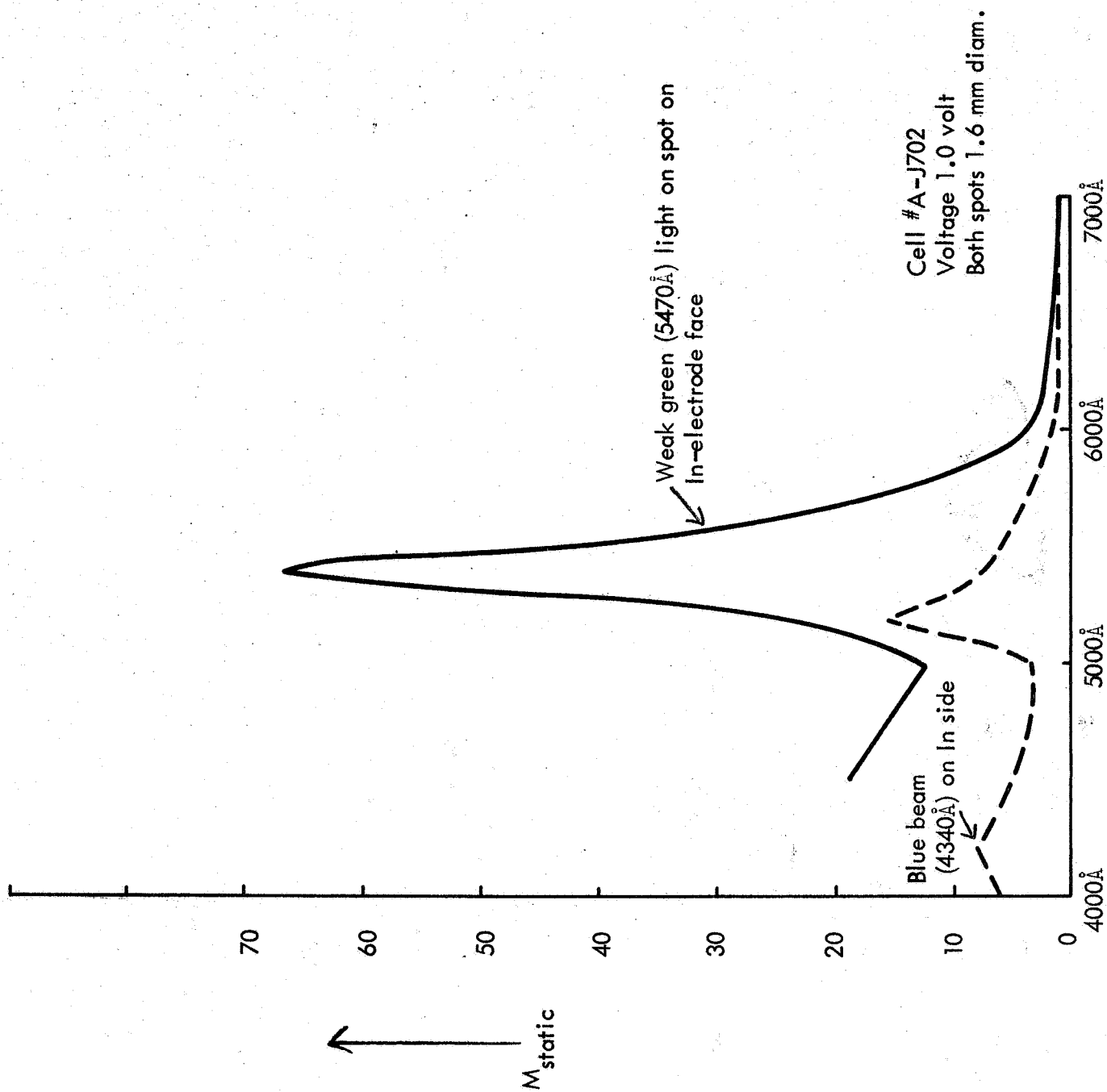


FIGURE A-4. Variation of M with Beam Wavelength, for Green or Blue Beam Opposite

A. A-Type

The most obvious assymetry in the cell construction lies in the materials at the two electrode interfaces. Although photoconductivity is normally considered to be a volume phenomenon, the battery reversal experiments indicate that the special enhancement effect must be strongly influenced by the situation very near to the surfaces of the CdS layer. This could arise from electrode interface phenomena, or perhaps sometimes from random differences in the initial layers of CdS being penetrated by very weak beams near the two sides of the cell.

Measurements of current-voltage curves for several cells under full-surface illumination showed that the electrode contacts were ohmic, but rectifying. That is, at constant illumination, the current-voltage curves were linear, but the cells showed different resistances for the two directions of the electric field.

Three examples of the effect of reversing the electric field will now be mentioned. Figure A-2 illustrated a case where the indium electrode, through which the red signal beam reached the CdS, had been made positive. In several cells where the In electrode was made negative, the curves were quite similar but M values were all smaller by a factor of two or three.

A. A-Type

On the other hand, Ref. II reports experiments with two green light beams on spots in the center of cell #A-G at very low intensities. In this case $M = 81$ was found with the In electrode negative, but very little current at all could be seen at any time with the In positive.

Again, an experiment is described in Ref. II where typical photocurrent measurements were being made under single-sided illumination of a central spot on cell #A-4 through the glass electrode only, with the glass electrode positive and the In negative. Then, with no other change but a reversal of the battery polarity, the photocurrent became too small to be measured.

The next subsection treats the allied question of the best electric field strength to apply to the cell.

3. Effect of Changing Cell Voltages.

It was found (Ref. II) that increasing the voltage across the cell raises the output current, under given illumination conditions. However, the value of M decreases at the same time.

For designing a particular application of the cell, the signal to noise ratios would have to be explored, to decide whether larger coincidence current signals or larger ratios of on-to off-coincidence currents (larger M) would be preferable. The response time properties would also be involved in such a design choice, as was discussed in Section III A.1.

A. A - Type

As a typical example, opposite spots in the center of cell # A-J686 were given yellow (5893\AA) and violet ($\sim 4340\text{\AA}$) illumination at constant intensity levels. Increasing the cell voltage from 0.5 volts to 30 volts greatly raised the coincidence photocurrent — from $30\mu\text{amp}$ to $1030\mu\text{amp}$. But M_{static} decreased from 6.7 at the minimum voltage and current to 1.8 at 20 volts, and thereafter remained the same for all higher voltages. Similar results were found for another cell with several different wavelength combinations. The possibility of long-term damage to these cells at 30 volts permanent bias, which is about 4000 volts/cm across the CdS layer, was not explored.

Let us now turn to the matter of light beam intensities.

4. Effect of Changing the Beam Intensities

For a given color combination, as the intensity ratio of the beams striking the two sides of the CdS layer is varied, M will usually go through a maximum. The practical reason for this seems to be as follows. As one of the beams becomes brighter and brighter, current caused by its single-sided illumination alone becomes very large. Addition of a weak beam on the other side then can no longer produce a very large percentage increase in the current, and so M decreases toward unity.

A. A-Type

However, just as in the high voltage case of the last subsection, a engineering balance must be made in designing for an application. The question is whether it is better to have large M or large current change due to the signal beam. Whenever one is working in the large-current realm, a small percentage increase can still constitute an easily detectable current transient.

A quantitative study of the effect of beam intensities on M_{static} was reported in Ref. II for a green-green wavelength combination, using illuminated spots of 0.4 mm diameter in the center of cell # A-G. The spectra of the two beams were defined by interference filters having a bandpass of about 100Å. A constant intensity of 3.5×10^{-9} watts, with central wavelength of 5450Å, was focussed onto the spot on the In electrode side of the cell. As usual, considerably less energy flux than the above figure must have reached the CdS itself, because of partial absorption in the metal film. On the opposite spot of the CdS layer, a beam with central wavelength 5120Å and adjustable intensity was sent through the glass electrode. This produced the following M_{static} values at the glass beam intensities listed:

<u>5120Å Intensity</u>	<u>Measured M</u>
2.8×10^{-12} watts	3.5
2.8×10^{-10} watts	46.
2.8×10^{-9} watts	23.5

The next subsection deals with the very important subject of time of response to a light signal.

A. A-Type5. Time Response to Intensity Modulation of the Light

When the intensity of the light beam is abruptly changed, in single-sided illumination of A-type cells, values of τ_{rise} near 0.2 sec were usually found. This photocurrent rise time was measured as the time required for half the change to its final value, of the voltage drop across a load resistor in the circuit.

For dual illumination, about the same values of τ_{rise} were found for coincident spot intensities or wavelength combinations where $M_{\text{static}} \leq 1.1$. However, cases of larger M value yielded rise times faster by a factor of 2-3 for dual illumination than with either side receiving the signal alone.

In general, greater total light intensity on a cell led to a faster time response to abrupt intensity changes.

Research in 1963 by Kearfott Division of General Precision, Inc., on some of the A-type polycrystalline CdS cells, employed a light beam which was intensity modulated at 400 cycles/sec, for illuminating the spot on one side of the CdS layer. In general, the results followed some of the same behavior described in the present report, although a number of inconsistencies remain.

A. A-Type

It is particularly noteworthy that even though the measurements already quoted show that the half-maximum rise times of these cells lie in the range of tenths of seconds, or longer, for the illumination intensities of interest, all the major parameter variations are easily observable with ever-changing beams whose period is only 2.5 milliseconds. This means that one can contemplate various applications which involve only the first small fraction of the time interval needed for reaching final steady-state current, and still utilize the spatial advantages of the enhancement phenomenon.

The final subsections will discuss various points concerning the areas, the positions on the cell face, and the number of the illuminated spots used.

6. Variation of Illuminated Area at Constant Power Density

Several points are demonstrated by experiments described in Ref. 1. They may be listed as follows:

1. With single-sided red beam illumination (6000\AA) at constant power per unit area through apertures of various areas the photocurrent output was proportional to the area. This means that the total cell conductance change was always proportional to the received power.
2. However, with yellow and green beams at small aperture sizes (near 50μ diameter) the current was less than would be expected from such

A. A-Type

a proportionality. It is not known if this decrease in sensitivity becomes accentuated at smaller spot sizes.

3. With constant-intensity dual beam illumination through pairs of opposite identical apertures of increasing size, more exposed area meant more received energy. This caused proportionally more output current for all beam wavelength combinations, but M always passed through a maximum just as it did in the previously described experiments on increasing beam intensity at constant hole size.

7. Variations in Spot Positions

An experiment described in Ref. 1 mapped the changes in the value of M_{static} as the illuminated spot on one cell face was traversed step by step across the position behind an illuminated spot on the other cell face. Figure A-5 shows that the influence of an illuminated spot having 0.4 mm diameter does not spread out across the cell face very far beyond the geometrical edge of the exposed area. The details of this experiment have a bearing on any application of such a cell for a scanning process.

In order to obtain the data shown in this Figure, spots on the two surfaces of cell #A-3 having dimensions as listed were illuminated with a yellow-yellow light combination from two monochromators. The spot on the surface having the In electrode (whose edge was not sharp but was surrounded by a weak halo which probably arose from multiple reflection between the In surface and the surface of the protecting glass cover), was displaced by a series of steps, with M_{static} being measured each time.

Cell #A-3

Right Spot: $\approx 400\mu$ Diameter; 5930\AA Light

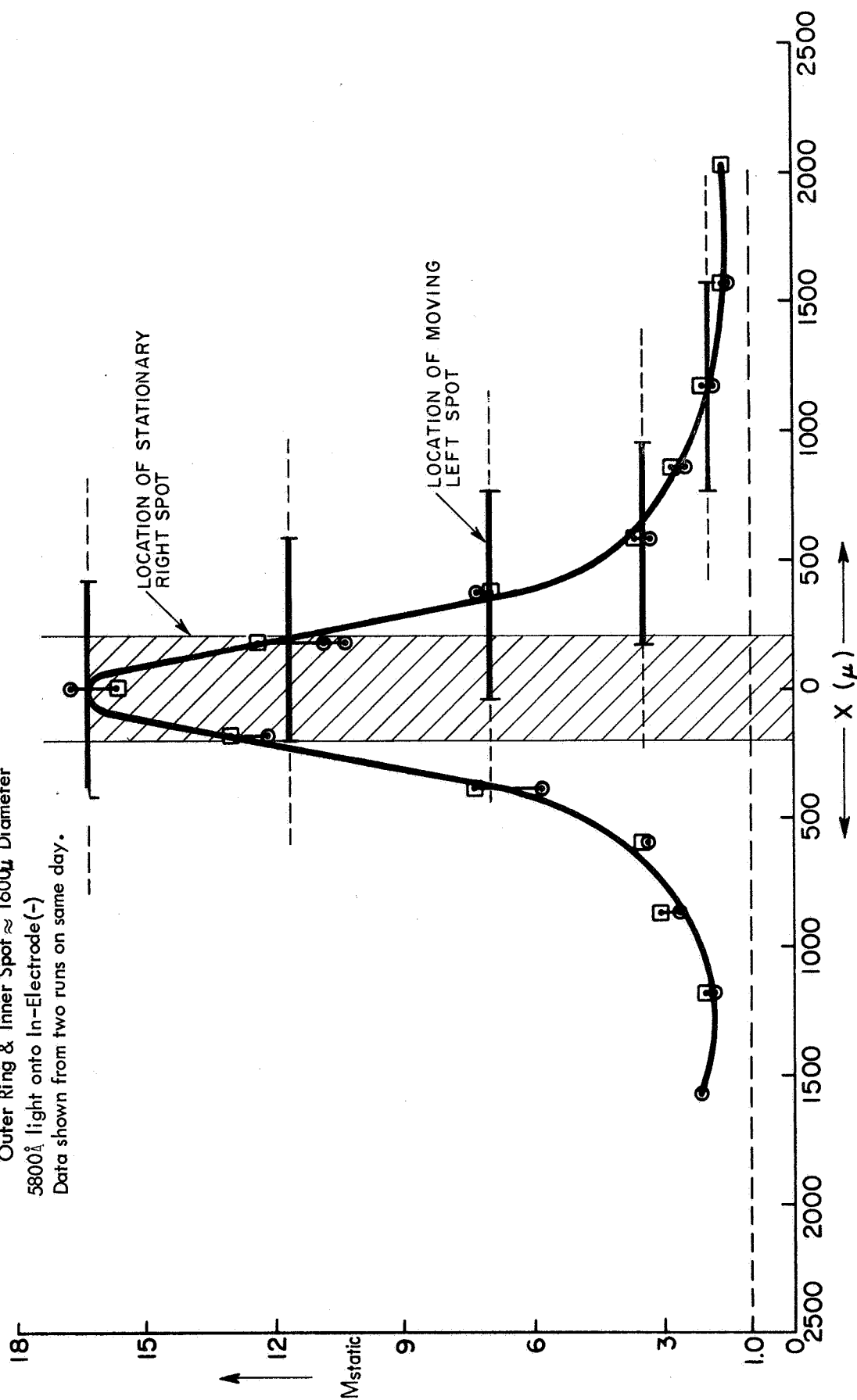
Left Spot:

Inner Spot $\approx 800\mu$ Diameter

Outer Ring & Inner Spot $\approx 1600\mu$ Diameter

5800\AA light onto In-Electrode (-)

Data shown from two runs on same day.



Displacement of left spot from coincident position

FIGURE A-5 - Effect of Linear Displacement on M .

A. A-Type

The intensities of the two beams were such as to produce photocurrents of about $3\mu\text{amp}$ and $9\mu\text{amp}$ for the left and right beams separately. The current with combined illumination varied between $15\mu\text{amp}$ and $145\mu\text{amp}$, depending on the projected overlap of the spots, which corresponded to the set of M_{static} values displayed in Figure A-5.

This Figure might suffice to justify the following generalizations: (a) the signal current decreases with decreasing projected overlap of the two illuminated spots, dropping to less than $1/5$ of its maximum as the two projected areas disengage; (b) appreciable enhancement, $M \approx 1.5$, still occurs when there is a clear un-illuminated distance of one spot diameter between the two projected areas, (since this is surely due to the complex phenomenon of charge carrier diffusion, the exact relation may be a function of spot size, cell thickness, temperature, speed of a moving spot, and other factors); (c), the cell material properties show no important variation across some 4 mm width — at least when averaged over these considerable spot areas, and when using yellow-yellow illumination which gives $M \leq 17$ with photocurrents in the microampere range.

Another experiment which explored the uniformity of the materials across the cell face was reported in Ref. II. Figure A-6 is a scale drawing showing the location of fifteen pairs of opposite illuminated spots scattered over several square millimeters of cell area. With constant dual illumination, the output currents were found to vary by a factor of 13.

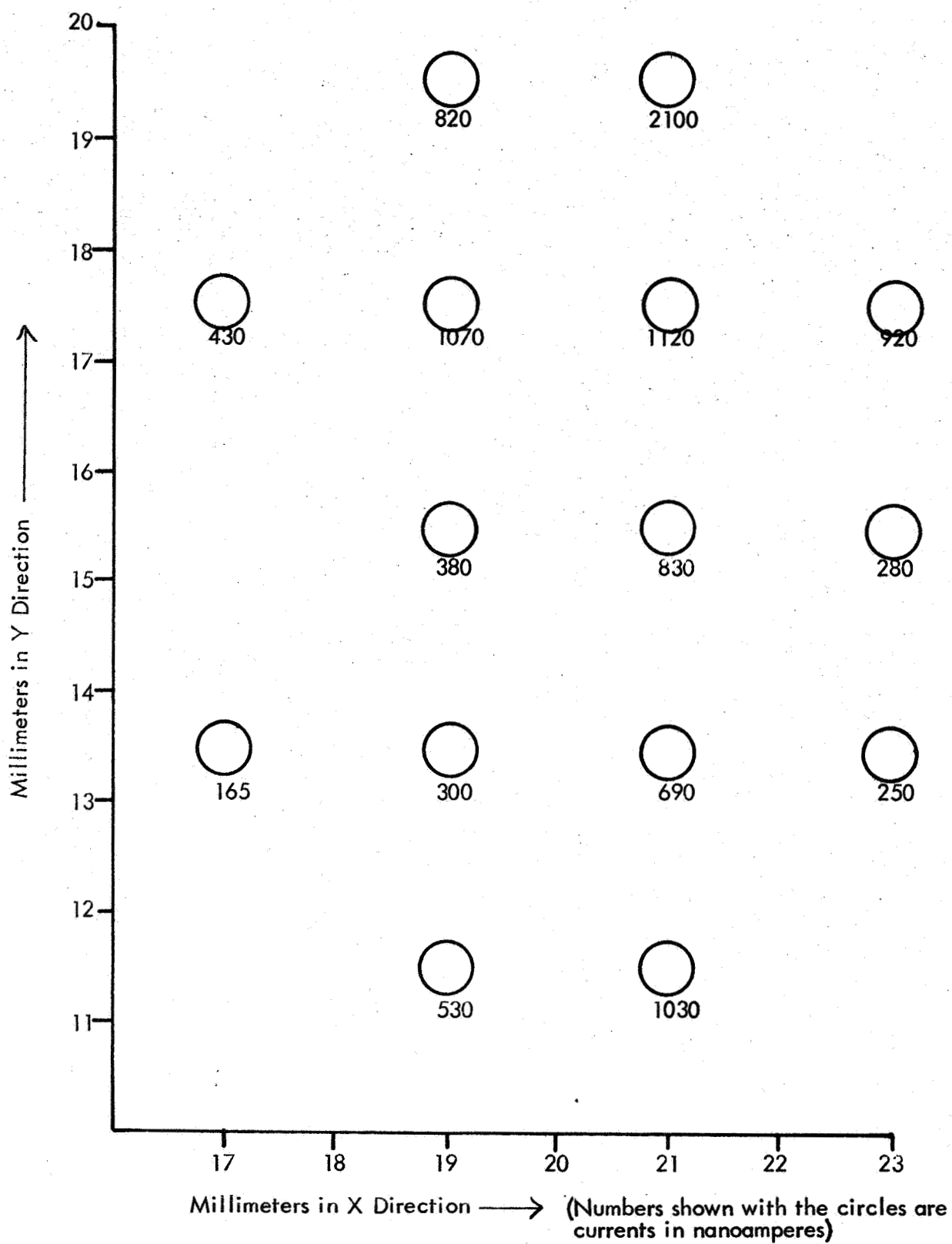


FIGURE A-6. $I_{\text{(both sides)}}$ in Nanoamperes, as a Function of Position on Cell #A-D.

A. A-Type

The data were obtained with two collinear beams which produced exactly opposite illuminated spots of no greater than 0.5 mm diameter on the faces of cell #A-D. The cell was then displaced to various positions in an X-Y plane perpendicular to the beam axis without change in the light beams. Measurements of output currents and calculations of M_{static} were made at the fifteen points shown, on the CdS surface. In this experiment a very weak green-green light combination was used. This gave extremely large M values which, however, were not very reliable since they were calculated from very small currents, mostly in the nanoampere range.

For such a case where the enhancement effect is being used as a powerful magnifier of small phenomena, minute variations in the cell materials might well be expected to have an accentuated effect. Despite so much variation, however, this area of this cell was the one used successfully with rather weak green-green beams to demonstrate the breadboard model of a beam tracker, as described in Section VI.

8. Multiple Spot-Pairs

In order to round out the picture on spot positions and to provide a better base for applications analysis, an experiment will be described here as a matter of information which was not a part of the contract effort. The main point of the experiment was to illuminate two or more pairs of opposite holes at once, as might be required in some kinds of star chart matching applications, for example.

A. A-Type

The results were somewhat complex. The total current from simultaneous illumination of a spot-pair group was always less than the sum of the output currents from individual spot-pairs. Perhaps some sort of saturation phenomenon is involved.

Cell # A-C was fitted with masks having four pairs of opposite holes. One mask is illustrated to scale in Figure A-7. The four pairs of holes at the top, middle, bottom, and side of the cell face area, indicated by T, M, B, and S, were of 0.36 mm diameter.

When each of these four pairs of holes was illuminated separately at the same intensity combination, from two monochromators with a green-green wavelength combination, the values of $I_{(both\ sides)}$ shown in Figure A-7 were found. The amount of variation in properties of the cell materials between these four spot-pair positions is about the same as Figure A-6 showed for cell # A-D.

The data obtained with illumination of several spot-pairs at once are listed in Table A-II. The results are non-additive. The last column shows that on an average the current arising from illumination of a group of several spot-pairs is only 73% of the sum of the currents from illuminating each spot-pair of the group individually. An even more important point, from the standpoint of a pattern matching application, is that some of the values of I in the second column would not serve to uniquely distinguish one from another among the various spot-pair combinations.

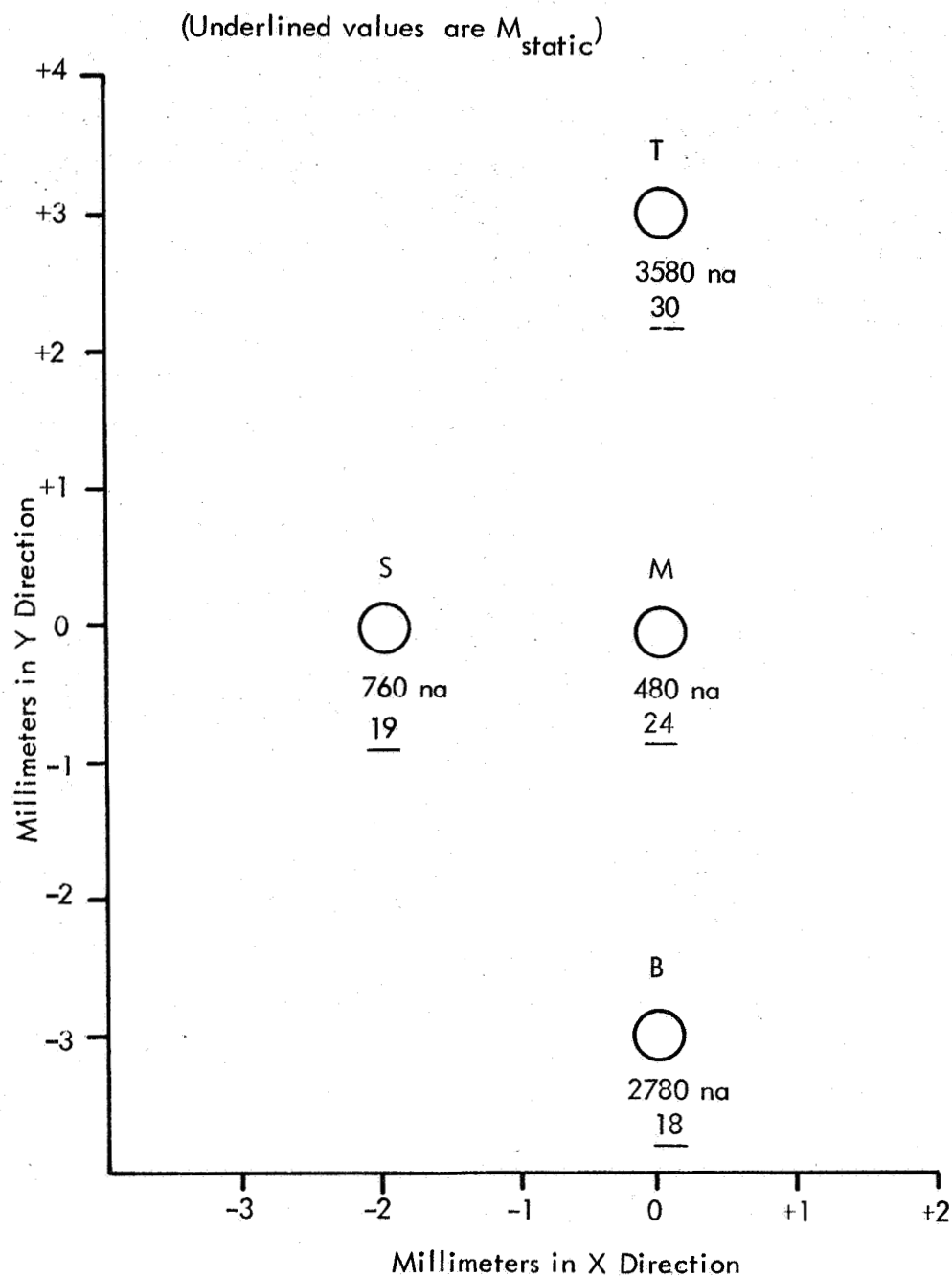


FIGURE A-7. $I_{(both\ sides)}$ and M_{static} as Function of Position on Cell #A-C.

TABLE A - II

I AND M WITH MULTIPLE ILLUMINATED SPOT-PAIRS

<u>Spot-pairs illuminated</u>	<u>I_(both sides) in nanoamperes</u>	<u>M_{static}</u>	<u>Sum of separate pairs, nanoamperes</u>	<u>Current-ratio of multiple pairs to sum of separate pairs</u>
T	3580	30		
B	2780	18		
S	760	19		
M	480	24		
<hr/>				
M+S	1080	22	1240	87 %
M+B	1580	16	3260	48 %
M+T	1980	28	4060	49 %
T+B	4670	27	6360	73 %
T+S	3080	16	4340	71 %
B+S	2380	21	3540	67 %
M+S+T	4780	21	4820	99 %
M+B+T	5280	31	6840	77 %
M+S+B+T	6380	20	7600	84 %
Average =				73 %

Note: Largest value of I_(one side only) for either side, for any one spot or combination of spots, is 200 nanoamp.

A. A-Type

The limitation on matching shown by these data arises partly from non-uniformity of the polycrystalline material, and partly from the non-additivity aspect of the phenomena involved. No basic barrier is appreciated at present which would prevent a considerable degree of improvement of the materials uniformity factor.

An auxiliary experiment was performed to explore the effect of extraneous light sources added to one of the patterns being matched. As listed in Table A-III, in addition to the illumination of various combinations of spot-pairs, certain other single spots were simultaneously illuminated on one cell face only. The output currents shown in the Table are seen to provide even less discrimination among the various combinations than before. Only one or two of the multiple pair cases in Table A-II, give a markedly greater I than all of the single pair cases. A further saturation or quenching phenomenon seems to be present here.

TABLE A-III

RESPONSE FROM MULTIPLE ILLUMINATED SPOT-PAIRS, WITH ADDITIONAL SPOTS
ILLUMINATED FROM ONE SIDE

<u>Spot-pairs illuminated</u>	<u>Additional single spots illuminated on glass side only</u>	<u>I_(both sides) in nanoamperes</u>	<u>M_{static}</u>
T	B, S, M	1940	13
B	T, S, M	1290	9
S	T, B, M	420	3
M	T, B, S	230	2
<hr/>			
M+S	T, B	390	3
M+B	T, S	800	6
M+T	B, S	1590	11
T+B	S, M	2390	15
T+S	B, M	1740	12
B+S	T, M	1090	9
M+S+B	T	1140	8
T+B+S	M	2270	14
M+B+T	S	1890	12
M+S+B+T	None	2090	13

Note A: $I_{(\text{glass side only})} \approx 137$ nanoamp with all four spots illuminated.

Note B: $I_{(\text{one side only})} \leq 20$ nanoamp in all cases.

APPENDIX B. THEORETICAL TREATMENTS *

Attempts were made to formulate a theoretical model which would account for a photo-current enhancement effect in CdS cells. These attempts are documented in Refs. I, II, and III, but primarily in Ref. II.

Mathematical treatments were formulated which included the effects of rate of generation of majority charge carriers, their mobility, motion in the field, and disappearance due to trapping and recombination reactions. Several computer programs were written to handle the complex differential equations which were generated.

The literature was searched for appropriate values of physical parameters which were assumed in the analysis to govern the behavior of the system. Several of the material parameters were not known and had to be estimated. Others were allowed to vary freely. These models did indeed yield significant predictions of photocurrent enhancement for several combinations of parameters. However, the material parameters could not be related to the real properties of the materials.

The models were also applied, after certain similar assumptions, to germanium. A small enhancement effect was predicted for germanium. However, as is discussed elsewhere, no such enhancement effect was observed. In fact, a new phenomenon, not predicted by the model, was observed in germanium. Perhaps the best that can be said about the theoretical treatment is that it showed that an enhancement type phenomenon can be derived and is a natural consequence of the consideration of dynamic interaction of the processes of charge carrier generation, motion, and disappearance.

* This Appendix prepared by Dr. Daniel Grafstein.

APPENDIX C. APPLICATIONS SIGNIFICANCE*

There are numerous potential applications of the enhancement phenomena and there are several different ways in which these could be grouped for discussion. There are the cases which use the cell in the static mode, and those which use it in the dynamic mode. However, let us now classify the uses by the fields of simple detectors, optical communication, navigation and tracking, pattern recognition, and others. Following the remarks on these various fields, a short survey of competing sensors is presented.

1. Simple Detectors

Of course, the foremost features of the enhancement effect as a simple detector are that it does not require high voltage, that it has no moving parts, that it is entirely a solid-state device and so not particularly fragile, and that without physical motion of the detector it will cover a very broad angular field of view (of the sky for instance) simultaneously, without picking up noise from all of that field. Also, the detector can be set at a certain intensity threshold level and so "see" only, for example, stars of a certain magnitude out of a very mixed field — again without including noise from any of the rejected sources.

However, the best feature probably is the fact that an arrangement for very high sensitivity has been found (Section III) which, at least in the static mode of operation, yields no detectable noise whatever at a level of amplification entirely suitable for operating various output devices.

* This Appendix is based partially on material prepared by Mr. Jesse Kaufman, of GPL Division, General Precision Systems Inc.

C. Applications2. Communication

An optical communication system requires a band width of 3500 cps for good voice transmission, and usually about 10^6 cps for real-time transmission of television pictures.

"Slow" television and some forms of telemetering do not need such high speeds.

Another requirement is that the detector be sensitive at a wavelength for which an efficient transmitter is available. If security of information is important, one way of assuring this is to use a wavelength and a beam intensity which can not be successfully intercepted by others. Another desirable characteristic would be a reasonable degree of linearity of the detector.

The experiment described in Section VI demonstrated that the photovoltaic enhancement effect in CdS has adequate speed for voice transmission. It can probably be made to operate in this fashion satisfactorily at 10^{-9} watts average radiant power input. If the photoconductive "de-enhancement" effect in Ge turns out to have response times in the μsec range, it should be able to handle real-time television signals from not too distant sources.

The photoconductive enhancement effect in CdS could be used in slow television systems, and it has the advantage of operating well on as little as 10^{-12} watts. The power receivable from a 25 watt argon laser source ($\lambda = 5150 \text{ \AA}$) at a range of 10^{11} cm (approximately 10^8 miles), when a receiving aperture of 1 meter diameter is used, would be about 2.5×10^{-11} watts. Narrow-beam communication could thus be maintained with a vehicle at about the distance of the planet Mars which carried a fairly low-power source.

C. Applications

Of course, all long range applications involving seeing through the earth's atmosphere will have to cope with the dynamic refractive effects caused by short term variations of temperature and pressure within the atmospheric path. These cause the image of the source to blur and to fluctuate in position and intensity. The various fluctuations have frequency components between 1 and 10^3 cps. The largest displacements, however, generally fall into the frequency range below 10 cps. The maximum angular displacement is usually about 10 seconds of arc.

Such speeds and displacements are within the compensation capability of a CdS enhancement cell attached to a tracking system, so as to remain on the beam continuously.

As to transmitter wavelengths, the experiments described have shown that all the enhancement effects (except for the B-type cell) have good sensitivities over more than one hundred Ångstroms. Either conventional light sources, or numerous laser types, will suffice for adequate transmission.

As to security of communications, the A-type cells will show a photoconductive $M > 1$ for an incoming signal too weak to be recorded at all by any single-sided photoconductive cell — and in many circumstances it could not even be seen by a vacuum photoemissive cell because of noise in other parts of the field of view.

Special classes of communication applications would involve employing a local-oscillator laser shining simultaneously on the same spot as the incoming laser beam signal. This would permit use of various phase modulated and frequency modulated arrangements, for code purposes for example. Because of the negligible sensitivity to angle of incidence observed with the CdS enhancement effect, it should be easier to keep such systems in angular adjustment than with ordinary detectors.

C. Applications3. Navigation and Tracking

The tracking accuracy of present-day transducers is of the order of 15 seconds of arc. A reduction of this figure would be highly desirable. In tracking, sensors for present day space applications fall into three main categories: sun sensors, star sensors, and planet sensors. Since the sun is of high intensity and subtends a relatively large angle, sun sensors generally employ rather unsophisticated designs - either a single detecting element with a reticle, or a mosaic of individual elements, such as are used by shadow mask sensors, digital sensors, and critical angle sensors. The critical angle sensor has the best null accuracy of the group. Sun sensors have a basic limitation on null accuracy caused by shifting of the center of the radiance of the sun by as much as 0.75 sec of arc, due to solar activity.

Stars are essentially point sources, since they subtend angles of under 0.1 second, and thus could be used with sensors of high accuracy. Present sensors for this purpose include the photomultiplier, the quadrant multiplier, the image dissector, and the vidicon. However, these are not capable of anything of like 0.1 second.

Since planets subtend relatively large angles for most missions (greater than 0.25°), the null accuracy is generally limited by target irregularities such as oblateness, variations in the altitudes of the emitting radiation sources, irregular cloud cover, and variations in the temperature of the emitting sources. Current horizon and edge trackers employ infrared sensors with fields of view narrower than that subtended by the planet, since the thermal gradient at the edge of the planet's disk generates the signal.

Further details on the above competing sensors are given in Subsection 6, below.

C. Applications

In the navigation category, single-spot signals may be stars, satellites, or lighthouses. Multiple-spot signals may be constellations or more complex patterns, such as a photograph which must be matched against a ground view. In the multiple-spot applications, the enhancement detector has not yet been shown very successful. However, with future improvement in uniformity of the cell materials the capability in this field might become high.

It may be noted that existing lensless optical correlators can convert such complex optical pattern pairs into a single spot which indicates the match. The appearance of a small black spot in the center of the detector plane indicates the match position, while any displacement or change in size of the spot indicates an error in the match position due to one or more of the six angle and position variables. The enhancement cell could well be used as a precision detector of this spot, which would avoid its present problems with multiple-spot pairs.

In general, the most important questions about a tracking application are the resolving power of the cell, its sensitivity, and the speed of response. The experiments on the A-type cells show adequate speed of response in the photoconductive mode for tracking, although it might be slow for acquisition if a large field of view had to be searched. The resolution of the cell has not yet been tested for spots smaller than $50\ \mu$ diameter. Perhaps $5\ \mu$ resolution would be desirable for a sensor to greatly surpass present day equipment. As to sensitivity, the 10^{-12} watts figure indicates the ability to track a small laser beacon at interplanetary distances. For nearer or stronger sources the cells in the photovoltaic mode would permit faster acquisition.

One strong advantage of the enhancement detector for navigation as well as for other

C. Applications

purposes, is that a small area of temporary interest within a large field of view can be selected for study, without disturbance from noise arising in the rest of the field not under study. (Although very close and intense extraneous sources might sometimes cause false alarms in pattern matching.)

It should also be noted that star tracking, for example, does not have to be based only on the magnitude of the photosignal. Experiments were mentioned which show that the cells have a faster time response wherever $M > 1$. This feature can also be made the basis for a tracker, and in fact such an apparatus has already been demonstrated by General Precision in work not connected with the present contract.

However, all of the tracking applications require a moving scanner beam on one side of the cell. Since the rest of the system would have no mechanical moving parts, it would be highly desirable to avoid mechanical motions for the scanning beam. Electrical means of deflecting a light spot have been used in a preliminary fashion with the enhancement cells. These include imaging either a multiple-array luminescent panel, or the face of a flying-spot cathode ray tube, onto one face of the cell. Both methods were successful in demonstrating M_{dynamic} with no moving mechanical parts. However, this art is still in a state of intense development — as in the current quest for a really good way to deflect laser beams electrically — and future improvements can be expected from various groups now active.

4. Pattern Recognition

In the field of pattern recognition, the enhancement device could perform an optical correlation process directly on the two surfaces of the photoconductive material. The two images being matched might be derived from two external scenes, or from one external scene and a star map on film. One of the two images would then be

C. Applications

adjusted in three linear directions and three rotational planes until the highest photo-current output occurred. The degree of response of the detector would depend, among other parameters, on the necessary rate of "dithering" one of the images, and on the number of resolution elements in the scene. A typical frequency figure would be $10^3 - 10^4$ cps. Image resolution would probably not have to be smaller than 100μ .

Such an arrangement has the effect of producing opposite illuminated spot pairs corresponding to each bright point of the images, whenever they have been correlated properly. As already mentioned, it will require improvement in materials uniformity beyond the level of the existing cells in order to accomplish this type of matching — but this could well be anticipated.

In addition to the more obvious pattern recognition applications such as star map matching, there are other pattern problems worth considering. For example, the retrieval of information stored in some intricate pattern on a surface, the use of optical cipher codes, or the matching of positive and negative images to show a single outstanding discrepancy, are good possibilities.

In the pattern matching field, certain spots of light could easily be put on one surface of the cell by a set of optical fibers coming from a common light source. Or, spots of different colors could be formed by fibers leading to different sources.

In general, the various pattern recognition uses could well afford to employ 100 ft-candles of local illumination for one side of the cell. In the experiments described it was shown that a bright light spot on one side of the cell will, under many circumstances, greatly increase the speed of response of the cell to a weak spot illumination on the other side.

C. Applications

5. Other Applications

Another major type of application is a TV camera system. The various arrangements today which require arrays are quite complex. This is particularly so in the infrared, where no TV camera is very satisfactory today. The needed resolution of about 300 lines per inch corresponds to about 80 microns between lines. This is a range already validated by the A-type cell experiments, which found good values of M with $50\ \mu$ spots.

The quoted sensitivity figure of 10^{-12} watts, with no noise detected, implies the possibility of an ultra low light level TV camera which would be capable of operating at light levels that are impossible to utilize today.

Another type of use is for spectrum discrimination. The enhancement phenomenon is at a maximum for certain general wavelength combinations. If the output amplifier is set at a proper discrimination level other wavelengths in a mixed group of sources can be ignored. Although, as already mentioned, the wavelength sensitivity is not sharper than some hundreds of Angstroms, except in the case of the B-type cell. This cell showed a strong decrease in M at $\pm 50\ \text{\AA}$ from its best wavelength.

There is also the field of positioning and control, with possible applications to a micro-lathe, an autocollimator, dimensional inspection, and microscopic positioning. However, a laser is the most obvious tool in this field.

C. Applications6. Competing Sensors

The various sensors employed in optical systems with which the coincidence detector may be compared are divided into two categories: those with internal signal gain and those which provide information on the position of a remote source. These categories correspond to the static and dynamic modes, respectively.

6.1 Devices with signal gain.

PHOTOCONDUCTORS - have a photoconductive gain factor, G , equal to the number of electrons passing through the device per excitation or absorbed photon. Gain factors as large as 10^4 have been reported for CdSe. The gain depends upon the electrode spacing and applied field, which are parameters which also affect the photoconductive enhancement factor, M . Photoconductors which simultaneously exhibit gain factor, G , and enhancement factor, M , offer a potentially attractive device with over-all gain comparable to other techniques.

MULTIPLIER PHOTOTUBES - make use of the external photoelectron effect, and the subsequent amplification of the electron current by means of a number of secondary emitting stages. Typically, commercial photomultipliers are constructed with nine to fourteen stages, have gains of $10^5 - 10^7$, and are generally bandwidth limited to $10^8 - 10^9$ cps due to electron transit time spread between cathode and anode. The output current is nearly a linear function of the input light over a large dynamic range. The spectral response is limited to the visible and near infrared with a long wave cut-off at $\lambda = 1.2 \mu$.

C. Applications

AVALANCHE DIODES - are photodiodes which are biased against the direction of easy current flow, i.e. the positive voltage is applied to the n region. Absorption of a photon initially generates an electron-hole pair. The applied field accelerates the electron which may jar loose a valence electron from a neighboring atom, generating an additional electron-hole pair. The number of times this process repeats itself is dependent upon the magnitude of the applied field. The net result of this chain reaction is the generation of an avalanche of carriers producing internal gain. A recent technical advance has been elimination of localized, unstable avalanche regions (microplasmas) which were undesirable due to their introduction of limited and fluctuating gain. Materials presently include Si and Ge, which offer wide modulation bandwidth capability and spectral response in the visible and near infrared. If used in applications where thermal or amplifier noise dominates over signal-related noise (i.e. shot noise), the internal signal gain improves the signal-to-noise ratio. Theoretical expressions have been developed for gain, signal response, noise and bandwidth. It is shown that for the shot-noise-limited condition, the avalanche photodiode operating at a high avalanche multiplication (gain) condition provides nearly the solid-state analog of the photomultiplier tube. Experimental results for the shot-noise-dominant case indicate that the SNR is improved at low bias levels, since noise increases slightly faster (with respect to bias voltage) than does the signal, and is optimized when the shot and thermal noise are equal. However, the device gain is then not maximized. In the 1 - 10 GHz modulation frequency region, the gain-bandwidth product for Si avalanche photodiodes is 10^{11} Hz, while gains up to 10^6 have been measured in the audio modulation frequency region. Due to the small size, modest power supply requirements, general simplicity of construction and large modulation bandwidth, the avalanche photodiode will most likely be the device with which the enhancement detector (in the static mode) must compete.

C. Applications

OPTICAL HETERODYNE - detection of laser radiation may be accomplished with any square-law detector, provided that certain spatial coherence requirements between the two inputs are met at the photosurface. The incoming carrier (signal) is mixed with the reference signal (local oscillator), providing sum and difference frequencies. The difference frequency (or intermediate frequency) is passed through an electrical filter to the load. The application of the local oscillator provides gain for both the signal and other optical noise inputs. By providing a strong local oscillator, heterodyne detectors (with their inherent optical spatial filtering) can suppress all of the noise sources except the quantum noise associated with the input signal and local oscillator, and that portion of background noise which falls within the bandwidth of the intermediate frequency (IF) filter. For signal and local oscillator power, P_s and P_{lo} , respectively, the voltage signal gain is

$$G = (P_{lo}/P_s)^{1/2}$$

when the post-detection IF bandwidth is adjusted to include the significant lower and upper sidebands associated with the modulation spectrum. Note that this detection technique is applicable to phase or frequency modulated light as well as intensity modulated light, whereas video detection (no local oscillator) responds only to intensity modulation.

CHANNEL ELECTRON MULTIPLIER - in its simplest form, the channel multiplier is a straight glass capillary, the inner surface of which contains a layer of special semi-conducting material having secondary electron emission characteristics suitable for an electron multiplication process. When a potential difference is applied between the ends of the tube, an axial electric field is established down its length and any electron

C. Applications

ejected from the surface is accelerated down the tube. Simultaneously, the electrons drift across the cavity of the tube with whatever lateral velocity was acquired in the ejection process. Electron multiplication occurs when the potential difference and the tube dimensions are such that these free electrons gain enough energy from the electric field between encounters with the surface that, on the average, more than one secondary electron is generated at each encounter. Typical length to inner diameter ratios are from 50 to 100. Current gains up to 10^8 have been reported. SNR data are unavailable.

6.2 Point position indicators

IMAGE TUBES - include the vidicon, image orthicon, and image intensifier orthicon (listed in order of increasing sensitivity), available for operation from the near ultraviolet to the near infrared. Special vidicon tube geometries combined with liquid hydrogen cooling of the thin film photoconductive "target" material enables operation to be extended out to $\lambda = 20\mu$. Although there are fundamental differences between the three devices, they may be lumped together in that each has an image transducing section where a light image is transformed into an electrical image (voltage pattern), and each has a readout section consisting of a scanning electron beam. Another common feature is that they possess an image storing capability. Because of its extreme sensitivity (10^{-8} ft-c) and larger size and weight, the image intensifier orthicon is not considered applicable to daylight startracking. The resolution of vidicons and image orthicons appears to be limited by the size of the electron readout beam (a minimum of 12μ) and by image "graininess" resulting from the appearance of an image of the retinal mesh (which has a maximum density of $\sim 10^3$ lines/inch, or $\sim 25\mu$ between lines).

C. Applications

MULTIPLIER PHOTOTUBES - are often used in conjunction with a mechanical scanning system in star tracking applications. They have already been discussed above.

IMAGE DISSECTORS - are identical in function to the multiplier phototube with the exception that a small area of the photocathode can be sampled electronically, rather than mechanically. It has a fast rise time and good resolution, approaching 10^3 lines/inch. As with the multiplier phototube and image (camera) tubes, the principal trade-offs are size, weight and electronic complexity.

LATERAL PHOTOEFFECT - semiconductors consisting of a broad, thin photovoltaic pin junction having two pairs of connections on the n-layer. These connections are arranged in an orthogonal manner and thus define four quadrants. The position of a spot of light incident on the p-layer of the cell, relative to the center of the cell, is indicated by the magnitude and polarity of the generated photocurrents from the four quadrants. These devices are attractive in that they are relatively simple, compact, and require neither a power supply nor a scanning means to obtain position information. The equivalent of mechanical rotation of the cell can be obtained by application of sweep voltages. Electronic chopping of the light signal can also be performed. Cells have been fabricated using Si (visible response, $0.5 \mu - 1.1 \mu$) and InSb (infrared response, $1.5 \mu - 6 \mu$). Data on the Si lateral effect cell indicates it has poor detectivity ($10^9 \text{ cm} - \text{Hz}^{1/2} - \text{watt}^{-1}$), as compared to that of a photovoltaic Si detector ($10^{12} \text{ cm} - \text{Hz}^{1/2} - \text{watt}^{-1}$) used as a two terminal device. The detector sensitivity is thus heavily compromised to provide positional information. For the case in which the dominant noise is thermal noise, it has been shown that the SNR varies with spot displacement, and naturally goes to zero at the null point. Data on Si cells of different resistivity indicate the usual gain bandwidth trade-offs, with a time constant

C. Applications

as small as 6μ sec. The null position accuracy is about 13 microns.

MOSAICS - of multiple individual elements, are available in numerous configurations and are generally arranged in a symmetrical fashion. From one to ninety (or more) elements may make up one quadrant of the total array. The outputs of corresponding detectors in each group (or sub-group) are sampled and compared simultaneously to indicate if the image is centered on the 0,0 axis. If a large number of elements are employed, formidable logistics, cross-coupling, reliability and uniformity problems arise. Four-element "quad-cells" are available in both multiplier phototube and solid state types. They require that all four elements be illuminated simultaneously if complete magnitude and phase information is to be obtained. As with the lateral photo-effect detector, they tend to become confused when more than one image appears on the photosurface. The minimum cell size of an individual element is about 40μ , with a separation between cells of 25μ . Additional problems are related to the need for individual preamplifiers for each element, and to the readout techniques. If fine resolution is not a prime requirement, then an array of individual channel electron multipliers (the individual capillaries have inside diameters ranging from a tenth of a millimeter to more than a millimeter) would provide individual outputs each having high gain.

APPENDIX D. NEW TECHNOLOGY

The following points of new technology have been developed in the course of this contract.

	<u>Subject</u>	<u>Page</u>
1.	Determination that a noise-free signal which was large enough, fast enough and spatially well defined enough for close servo tracking, could be obtained in a CdS cell with only 10^{-12} watts of red light input.	22
2.	Current enhancement obtained with sintered powder CdS layers merely pressed between plates of conducting glass for electrodes , up to 1.6 mm thick.	44
3.	Strong quenching in single crystal CdS photoconductivity for dual illumination of opposite spots with one beam at 8000 Å and the opposite beam of shorter wavelength and 5850 Å; values of M as small as 0.1; slow response time.	46
4.	The new phenomenon of photovoltaic enhancement in CdS found with faster response than in photoconductive enhancement.	49
5.	B-type CdS cells found to have a wavelength sensitivity for M as small as about ± 50 Å in the photovoltaic mode.	61
6.	The new "de-enhancement" phenomenon with single crystal germanium, predominantly in the near infrared.	62

D. New Technology

	<u>Subject</u>	<u>Page</u>
7.	A low-light level TV camera employing a light beam readout instead of electron-beam scanning.	71
8.	A photoconductive beam tracker based on the value of M at the signal spot location, with an A-type cell.	77
9.	Transmission of voice on a spatially locatable light beam by means of the new photovoltaic enhancement effect with an A-type cell.	78
10.	The photoconductive enhancement phenomenon in A-type cells is insensitive to the angle of incidence of the light beams, at least to 27° - contrary to most light-mixing detectors, where two coherent beams must be closely aligned in angle in order to mix properly.	85
11.	The time of response to a weak signal light spot on one face of an A-type cell can be greatly decreased by applying a strong light to the opposite spot on the other face.	97